From the Department of Oncology-Pathology
Karolinska Institutet, Stockholm, Sweden

ADVANCING ANTIVIRAL STRATEGIES AGAINST EMERGING RNA VIRUSES BY PHENOTYPIC DRUG DISCOVERY

Marianna Tampere

Karolinska Institutet

Stockholm 2021

Marianna Tampere

marianna.tampere@gmail.com

MSc: Biomedicine
University of Tartu
BSc: Gene technology
University of Tartu

All previously published papers were reproduced with permission from the publisher.
Published by Karolinska Institutet.
Printed by Universitetsservice US-AB, 2021

ISBN 978-91-8016-148-0
Cover illustration: Inspired by the Cell Painting project. By Marianna Tampere.

Advancing antiviral strategies against emerging RNA viruses by phenotypic drug discovery
THESIS FOR DOCTORAL DEGREE (Ph.D.)

By

Marianna Tampere

The thesis will be defended in public at Science for Life Laboratory, Stockholm, 21st May 2021 at 09.00 am.

Principal Supervisor:
Prof. Ali Mirazimi
Karolinska Institutet
Department of Laboratory Medicine

Co-supervisors:
Dr. Marjo-Riitta Puumalainen
Karolinska Institutet
Department of Oncology-Pathology

Prof. Thomas Helleday
Karolinska Institutet
Department of Oncology-Pathology

Opponent:
Dr. Leen Delang
KU Leuven
Department of Microbiology, Immunology and Transplantation
Laboratory of Virology and Chemotherapy

Examination Board:
Dr. Gerald McInerney
Karolinska Institutet
Department of Microbiology, Tumor and Cell Biology

Dr. Annika Karlsson
Karolinska Institutet
Department of Laboratory Medicine
Division of Clinical Microbiology

Prof. Magnus Evander
Umeå University
Department of Clinical Microbiology

Science, my lad, is made up of mistakes,
but they are mistakes which it is useful to make,
because they lead little by little to the truth.

– Jules Verne

To my beloved family, for their infinite support and love

DOKTORITÖÖ POPULAARTEADUSLIK KOKKUVÕTE

Viirused on silmale nähtamatud patogeenid kes ei kuulu elusolendite hulka, kuid kes pole ka eluta. Nagu on näidanud COVID-19 pandeemia, levivad viirused globaalselt ja nende poolt põhjustatud haigused mõjutavad suuresti meie tervist ning majanduslikku käekäiku. Vaatamata sadadele haigustekitajatele leidub täna viirusevastast ravi ainult ligikaudu kümne vastu. Viiruste eripäraks on nende ülepääsmatu sõltuvus rakkudest, näiteks inimese, kuid ka teiste loomade, lindude, taimede ja isegi bakterite rakkudest. Viirused kasutavad kavalalt ära rakumehhanisme, et toota uusi viirusosakesi. Varasemalt on näidatud, et eri perekondadesse kuuluvad viirused kaaperdavad sarnaseid raku signaaliradu, mis pakub võimalust luua laiahaardelise toimega ravimikandidaate. Käesoleva doktoritöö eesmärk oli uurida viiruse- ja rakuvahelist suhtlust, avastada uusi viirusevastaseid molekule ning laiendada ravimiarenduse metoodikat.

Esmalt arendasime me uuendusliku mikroskoopial põhineva meetodi eesmärgiga testida neljasaja molekuli viirusevastast toimet. Need molekulid inhibeerisid rakulisi protsesse, mis meie hüpoteesi kohaselt võiksid viiruste paljunemist toetada. Me tuvastasime kaks eri molekuli TH3289 ja TH6744 mille toimel patogeensete viiruste nagu näiteks Ebola, COVID-19 põhjustava SARS-CoV-2, Krimmi-Kongo hemorraagilise palaviku ning Zika viiruse nakatuvus pidurdus märgatavalt, kuid peremeesrakkude elutegevus ei olnud häiritud. Need tulemused kinnitasid meie molekulide laiahaardelist toimet. Veelgi enam, oma töös näitasime, et meie molekulidel on lai terapeutiline aken ning molekul TH6744 päästis rakud ja ka inimese aju mini-organoidid Zika viiruse poolt põhjustatud surmast.

Järgnevalt täiustasime viirusevastaste raviainete avastamise metoodikat, keskendudes peremeesrakkude morfoloogilistele muutustele nakatumise ja molekulitöötluse käigus. Me kombineerisime meie mikroskoopial põhineva ja eelnevalt kirjeldatud “rakkude värvimise” (ingl. Cell Painting) meetodi, mille käigus rakud maalitakse erinevate helendavate värvidega, mis võimaldavad rakkude ja organellide kuju, suurust ning heledust mõõta. Võrreldes nakatunud ja mittenakatunud rakke, me avastasime, et nakatunud rakkude morfoloogia oli märgatavalt erinev tervetest rakkudest. Eriti põnev oli avastus, et viirusevastased ravimid ja ka meie avastatud molekul muutsid nakatunud rakkude morfoloogia tagasi mittenakatunud rakkude sarnaseks, jäljendades justkui viirusnakkuse ravimist rakulisel tasandil. Rakkude värvimise meetod võimaldab uurida viiruste mõju peremeesrakkudele ning ka ravimite toimet nakatunud rakkudele veelgi põhjalikumalt.

Viimaks me uurisime milliseid raku protsesse TH6744 mõjutab ning kuidas antud molekul viiruseid inhibeerib. Nimelt toimivad ravimid enamasti seondudes oma rakulistele märklaudadele. Rakendades termodünaamilisi printsiipe ja mass-spektromeetria meetodeid, uurisime TH6744 rakulisi märklaudu proteoomi tasandil ja avastasime, et saperonid ehk tugivalgud, mis toetavad teiste valkude kokkuvoltumist, kerkisid esile kui võimalikud märklaudvalgud. Eelnevalt avaldatud uurimuste kohaselt on viirused tugivalkude suhtes hüpertundlikud oma suuremahulise valgutootmise tõttu ning TH6744 võib viirusevastast toimet omada just tugivalke inhibeerides.

Kokkuvõtteks avastasin enda doktoritöö käigus kaks uudset molekuli, millel on laiaspektriline toime erinevate patogeensete viiruste vastu. Selline toimemehhanism on hädavajalik, et võidelda olemasolevate viirustega, nagu SARS-CoV-2 ja Zika viirus, kuid ka tulevikus esilekerkivate uute patogeenidega. Lisaks ma arendasin ka uudseid meetodeid viirusevastaste ravikandidaatide avastamiseks rakendades mikroskoopia ja proteoomi uuringuid.

POPULAR SCIENCE SUMMARY OF THE THESIS

Viruses are microscopic parasites – they are not living organisms, but they are not dead either. Diseases caused by viruses influence our well-being across the globe and unfortunately there is no cure to treat the majority of human viral pathogens. What makes them so unique is their insurmountable dependency on other organisms such as us, humans, but also other animals, birds, various plants and even bacteria. Viruses depend on us to copy and paste new viruses. Virologists have found out that viruses from very different origin can hijack the host cell by similar principles, presenting an opportunity to develop treatments that hit multiple viruses at once, named broad-spectrum antivirals, a useful strategy to prepare for new viruses that may unexpectedly appear in the future.

Investigating viruses as small as 50 nanometers in diameter can be very abstract, but luckily specific antibody molecules that shine under microscope come in very handy. As a part of my thesis work, we developed a method to visualize virus-infected human cells and leveraged it to find new antiviral molecules. We tested a collection of molecules that inhibit cellular processes and found two, TH3289 and TH6744 that inhibited multiple pathogenic viruses such as Ebola virus, Zika virus, severe acute respiratory syndrome coronavirus 2 (SARS-CoV-2) and Crimean-Congo hemorrhagic fever virus. These encouraging results confirmed that our new molecules tick the criteria boxes to qualify as a broad-spectrum antiviral. Additionally, TH3289 and TH6744 were not toxic to the host cells at concentrations where they inhibited virus, but TH6744 rescued the cells and even organoids, a collection of cells growing three dimensionally, from dying due to the virus infection.

After identifying TH3289 and TH6744, we were curious what the molecules do within the cells and how do they inhibit viruses. Drugs usually perform their therapeutic action by binding to proteins within cells. With the help from thermodynamic principles and mass spectrometry, we revealed how TH6744 binds to a group of proteins called chaperones that are responsible for correct structure of cellular proteins. Importantly, viruses also rely on cellular chaperones to ensure correct structure and we suggest that our molecules inhibit viruses by interrupting chaperone functions.

Our method based on antibodies is rather simplistic and only measures the number of infected cells, therefore we aimed to further explore how the infection also influences host cells. We implemented a popular method to paint infected cells with different dyes and examined their morphological changes. We noticed how the shape and size of virus-infected cells was very distinct from the non-infected cells. Even more exciting, some antiviral inhibitors transformed the infected cell morphology back to being non-infected. We propose this method as an advancement for discovering novel antiviral therapies.

To summarize, this thesis discovered new antiviral molecules, characterized their function in host cells and activity across different pathogenic human viruses. Additionally, we implemented new microscopy and mass-spectrometry based methods to boost finding novel antivirals.

ABSTRACT

Pathogenic RNA viruses can emerge from unexpected sources at unexpected times and cause severe disease in humans, as exemplified by the ongoing coronavirus disease 19 (COVID-19) pandemic caused by severe acute respiratory syndrome coronavirus 2 (SARS-CoV-2) and Ebola virus (EBOV), Crimean-Congo hemorrhagic fever virus (CCHFV) and Zika virus (ZIKV) outbreaks from the past decade. Despite the increasing impact of emerging viruses to health and economy worldwide, our preparedness to stand against these diseases is hampered by the lack of approved and effective antiviral therapies. Thus, the development of novel antivirals is of urgent need.

To date, antiviral drug discovery has primarily focused on targeting specific viral proteins, but these treatments often suffer from viral resistance and are limited to only one or few viruses. Instead, phenotypic drug discovery enables the identification of drug candidates that are active in the disease-relevant model and not restricted to previously characterized biological processes. As RNA viruses are highly dependent on the host cell pathways due to their relatively small genome, targeting virus vulnerabilities within the host cell has been a promising antiviral strategy for broad spectrum antivirals, but is relatively unexplored so far. In fact, phenotypic approaches can additionally identify host-directed antivirals due to the unbiased nature.

The focus of this doctoral thesis was to identify novel antiviral compounds with broad spectrum activity and investigate the compound mechanism of action and target pathways from the host cell and virus perspective. To achieve these goals, multiple cutting-edge phenotype-based methodologies were implemented that additionally advanced the antiviral drug discovery landscape.

In **Paper I**, we developed an image-based phenotypic antiviral assay and screened our in-house chemical library targeting cellular oxidative stress and nucleotide metabolism pathways in Hazara virus (HAZV)-infected cells. Screening hit compounds TH3289 and TH6744 activity was validated by their therapeutic window and both compounds were also active beyond HAZV, especially TH3289 that was tested and displayed activity against EBOV, CCHFV, SARS-CoV-2 and a common cold coronavirus 229E (CoV-229E). We also excluded the intended target 8-oxoguanine DNA glycosylase (OGG1) protein to be responsible for TH6744 antiviral activity and characterized host cell chaperone and co-chaperone network as target pathways of TH6744 by implementing thermal proteome profiling methodology.

In **Paper II**, we transferred our image-based phenotypic assay to ZIKV-infected brain cells in order to screen structural analogs of TH3289 and TH6744 against a pathogenic RNA virus. TH3289 and TH6744 again appeared among the screening hits and presented a promising therapeutic window in various cellular models, further confirming their broad activity. Moreover, TH6744 reduced ZIKV infection and progeny release in cerebral organoid model and impressively rescued ZIKV-induced cytotoxicity in organoids. Additionally, treatment

with TH6744 rapidly diminished ZIKV progeny release during late replication cycle stages, elucidating the antiviral mechanism of action.

In **Paper III**, we established an untargeted morphological profiling method to provide in-depth host cell responses during antiviral screening. We combined the Cell Painting protocol with antibody-based virus detection in a single assay followed by automated image analysis pipeline providing segmentation and classification of infected cells and extraction of cell morphological features. We demonstrated how our assay reliably distinguished CoV-229E infected human lung fibroblasts from non-infected controls based on cellular morphological features. Furthermore, our method can be applied in phenotypic drug screening as validated by nine host- and virus-targeting antivirals. Effective antivirals Remdesivir and E-64d treatment reversed the infection-specific signatures in host cells. Thereby, the developed method can be implemented for antiviral phenotypic drug discovery by morphological profiling of drug candidates.

LIST OF SCIENTIFIC PAPERS

Thesis publications:

I. **Novel Broad-Spectrum Antiviral Inhibitors Targeting Host Factors Essential for Replication of Pathogenic RNA Viruses. Tampere, M.,** Pettke, A., Salata, C., Wallner, O., Koolmeister, T., Cazares-Körner, A., Visnes, T., Hesselman, M. C., Kunold, E., Wiita, E., Kalderén, C., Lightowler, M., Jemth, A.-S., Lehtiö, J., Rosenquist, Å., Warpman Berglund, U., Helleday, T., Mirazimi, A., Jafari, R., Puumalainen, M.-R. *Viruses* (2020) 12, 1423.

II. **Broadly Active Antiviral Compounds Disturb Zika Virus Progeny Release Rescuing Virus-Induced Toxicity in Brain Organoids.** Pettke, A.*, **Tampere, M**.*, Pronk, R., Wallner, O., Falk, A., Warpman Berglund, U., Helleday, T., Mirazimi, A., Puumalainen, M.-R. *Viruses* (2021) 13, 37.

III. **A phenomics approach for antiviral drug discovery.** Rietdijk, J., **Tampere M**., Pettke A., Georgieva P., Lapins M., Warpman Berglund, U., Spjuth O., Puumalainen M.-R., Carreras Puigvert J. *Submitted manuscript*.

Scientific publications not included in this thesis:

IV. **Circle-to-circle amplification coupled with microfluidic affinity chromatography enrichment for in vitro molecular diagnostics of Zika fever and analysis of anti-flaviviral drug efficacy.** Soares, R. R. G., Pettke, A., Robles-Remacho, A., Zeebaree, S. Ciftci, S., **Tampere, M.,** Russom, A., Puumalainen, M.-R., Nilsson, M., Madaboosi, N. *Sensors and Actuators: B. Chemical* (2021) 336, 129723.

* - equal contribution

TABLE OF CONTENTS

LIST OF ABBREVIATIONS

Numeric	2D	Two dimensional
	2D-TPP	Two-dimensional thermal proteome profiling
	3D	Three dimensional
A	AI	Artificial intelligence
	APN	Aminopeptidase N
	Arbovirus	Arthropod-borne virus
	ATP	Adenosine triphosphate
B	BSL	Biosafety laboratory
C	C	Capsid protein
	Cas9	CRISPR associated protein 9
	CCHFV	Crimean-Congo hemorrhagic fever virus
	CD13	Cluster of differentiation 13
	CETSA	Cellular thermal shift assay
	Co-IP	Co-immunoprecipitation
	CoV-229E	Coronavirus 229E
	COVID-19	Coronavirus disease 2019
	CPE	Cytopathic effects
	CRISPR	Clustered regularly interspaced short palindromic repeats
D	DAA	Direct-acting antivirals
	DAPI	4′,6-diamidino-2-phenylindole
	DENV	Dengue virus
	dGTP	Deoxyguanosine triphosphate
	DMSO	Dimethylsulfoxide
	DNAJB11	DNAJ homolog subfamily B member 11
	DNAJC3	DNAJ homolog subfamily C member 3
	Dpi	Days post infection
	DRC	Democratic Republic of Congo
	DSF	Differential scanning fluorimetry
E	E	Envelope protein

	EC_{50}	Half maximal effective concentration
	ER	Endoplasmic reticulum
	EBOV	Ebola virus
	EDEM3	ER degradation-enhancing alpha-mannosidase-like protein 3
F	FBS	Fetal bovine serum
	FDA	Food and drug administration
G	GBS	Guillain-Barré syndrome
	GO	Gene ontology
	GTP	Guanosine triphosphate
H	HAZV	Hazara virus
	HBV	Hepatitis B virus
	HIV	Human immunodeficiency virus
	HCV	Hepatitis C virus
	Hpi	Hours post infection
	HSP70	Heat shock protein 70
	HSP90	Heat shock protein 90
	HSV	Herpes Simplex virus
I	IMPDH	Inosine monophosphate dehydrogenase
	iPS cells	Induced pluripotent stem cells
	ITDR-CETSA	Isothermal dose response CETSA
J	JEV	Japanese encephalitis virus
L	LASV	Lassa virus
	LC-MS/MS	Liquid chromatography tandem mass spectrometry
M	MERS-CoV	Middle east respiratory syndrome coronavirus
	MoA	Mechanism of action
	MOI	Multiplicity of infection
	mRNA	Messenger RNA
	mTOR	Mechanistic target of rapamycin
N	NCAM1	Neural cell adhesion molecule 1
	NP	Nucleoprotein

	NS-1	Non-structural protein 1
O	OGG1	8-oxoguanine DNA glycosylase
	ORF	Open reading frame
P	PBS	Phosphate buffered saline
	PCA	Principal component analysis
	PCR	Polymerase chain reaction
	PFA	Paraformaldehyde
	PI3K	Phosphoinositide 3-kinase
	PLS-DA	Partial least-squares discriminant analysis
	prM	Precursor membrane protein
	PS	Penicillin-streptomycin
R	RdRP	RNA-dependent RNA polymerase
	RNA	Ribonucleic acid
	RNAi	RNA interference
S	SARS-CoV	Severe acute respiratory syndrome coronavirus
	SARS-CoV-2	Severe acute respiratory syndrome coronavirus 2
	SDS	Sodium dodecyl sulfate
	shRNA	Small hairpin RNA
	siRNA	Small interfering RNA
	SOD1	Superoxide dismutase 1
	ssRNA	Single-stranded RNA
T	T_h1	T helper cells 1
	T_h2	T helper cells 2
	T_m	Melting temperature
	TPP	Thermal proteome profiling
	TPP-TR	Temperature range TPP
	VHF	Viral hemorrhagic fever
	vRNA	Viral RNA
W	WHO	World health organization
Z	ZIKV	Zika virus
Symbol	ΔT_m	Melting temperature shift

1 LITERATURE REVIEW

1.1 INTRODUCTION

Natural epidemics and outbreaks of emerging infectious diseases impose a continuous and major public health burden worldwide. Not only the currently ongoing unprecedented coronavirus disease 19 (COVID-19) pandemic caused by Severe Acute Respiratory Syndrome Coronavirus 2 (SARS-CoV-2), but recent examples from the last decade such as the Zika virus (ZIKV) epidemic during 2016, Ebola virus (EBOV) outbreak during 2014-2016, regional Crimean-Congo hemorrhagic fever virus (CCHFV) and seasonal Influenza virus outbreaks underline the increasing impact of emerging ribonucleic acid (RNA) viruses to human health (**Figure 1**). To date, hundreds of viral pathogens are known to cause a wide spectrum of human disease ranging from neurological conditions, respiratory infections to life-threatening hemorrhagic fevers. Nonetheless, specific and effective antiviral therapies have been developed and approved only for ten viral pathogens[1,2], highlighting the urgency to discover novel pharmaceutical treatments and the importance of exploring the underlying biology of viral infections.

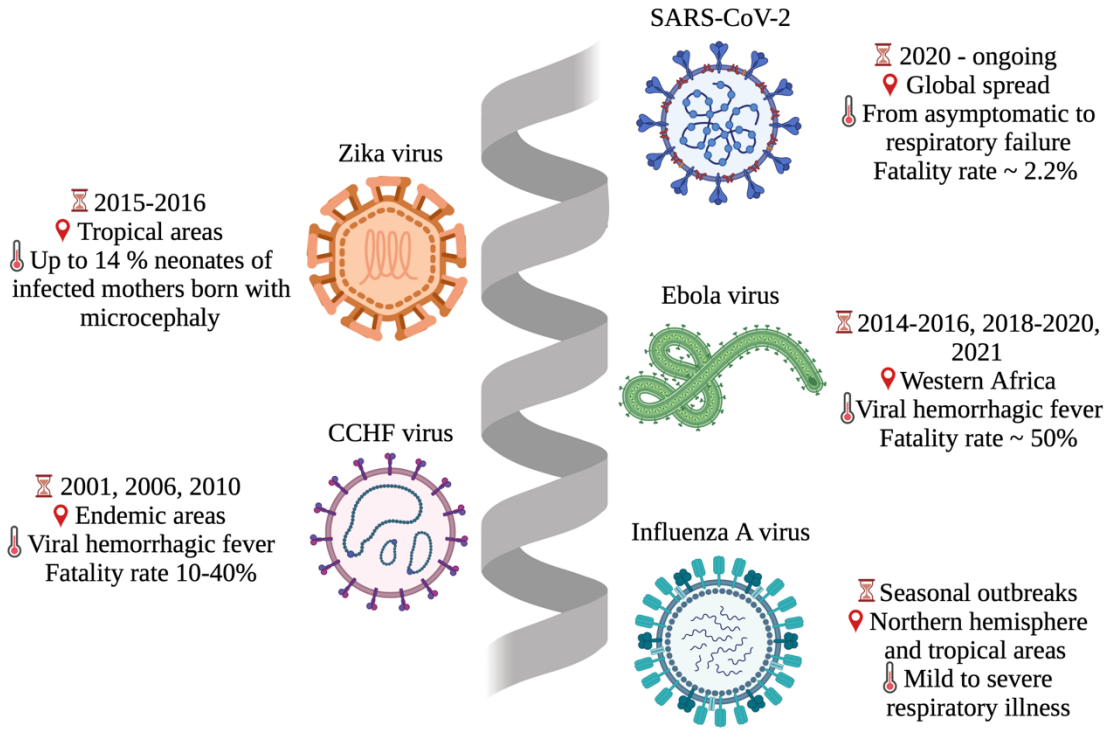

Figure 1. **An overview of emerging RNA viruses from the past and present**. Summarized are time and duration, geographic distribution and main clinical outcomes of the outbreaks.

1.2 EMERGING RNA VIRUSES

1.2.1 Zika virus

ZIKV is an enveloped virus belonging to the *Flaviviridae* family and was first isolated from an infected Rhesus monkey in the Zika forest (Uganda) in 1947 (ref.[3]). ZIKV infectious particle is approximately 50 nm in diameter, consists of positive sense single-stranded RNA ((+) ssRNA)) genome encapsulated inside viral structural proteins and a lipid bilayer. ZIKV is an arthropod-borne virus (arbovirus) primarily transmitted to humans by the bite of infected *Aedes aegypty*[4] and *Aedes albopictus*[5] mosquitos, but ZIKV can also be transmitted sexually[6,7], by blood transfusion[8], breast milk[9], and from infected mother to the fetus[10,11]. Overall, ZIKV infection can be asymptomatic, clinically mild and non-specific or cause severe complications to adults and fetuses. To date, no approved vaccines or antivirals exist against ZIKV infection.

1.2.1.1 ZIKV epidemiology

ZIKV epidemiology illustrates the transition of a neglected tropical disease to the cause of a major global health threat. For many decades, ZIKV was not considered an important human pathogen. Within 60 years after isolation, a negligible number of ZIKV cases were documented. The first reported outbreak occurred in Yap Island in the Pacific Ocean in 2007 and 49 patients having mild illness were confirmed to be infected with ZIKV[12]. In 2013, ZIKV was detected in French Polynesia in 30'000 patients with unique and, in few cases, more severe neurological symptoms[13]. Thereafter, ZIKV was initially introduced into Brazil in late 2013 (ref.[14]) while explosive spread in the Americas was detected during late 2015, establishing a serious international outbreak. As of 2017 at the end of the epidemic, more than 220'000 confirmed and 580'000 suspected cases were reported and provided definitive evidence for unforeseen consequences[15].

1.2.1.2 Zika virus disease symptoms and clinical complications

Large proportion of all ZIKV infections are asymptomatic. When present in approximately 20% of the cases, symptoms are generally mild, clinically non-specific and most commonly summarized as Zika virus disease or Zika fever[16]. Most common symptoms include fever, headache, maculopapular rash, conjunctivitis, arthralgia, myalgia and fatigue[16]. Before the French Polynesia outbreak in 2013, ZIKV was considered as self-limiting disease without any severe complications[17], but as the outbreak evolved, it became apparent that ZIKV infection can cause severe complications in adults and fetuses. First evidence of causality between ZIKV and increased incidents of Guillain-Barré syndrome (GBS) in adults were confirmed by two case-control studies in French Polynesia[18,19]. GBS is a rare but severe autoimmune disease accompanied with damage of the myelin insulation of peripheral nerves. The disease develops rapidly during few weeks and may lead to severe consequences such as respiratory failure and paralysis which can be life-threatening in 4-15% cases[20,21]. The exact mechanism of GBS pathogenesis is unknown, but majority the of cases occur 1-2 weeks after *Campylobacter jejuni,* Cytomegalovirus, Influenza virus and, as recently shown, ZIKV infections[21].

In addition to GBS in adults, ZIKV causes microcephaly in neonates, a condition in which newborn babies are born with an abnormally small head. Local researchers and physicians in Brazil reported an unusual increase of microcephaly cases in 2015 (ref.[22]). In comparison to annual 150-200 cases between 2010-2014, Brazil reported 3530 microcephaly cases in 2015 (ref.[15]). Such alarming reports prompted World Health Organization (WHO) to declare an international public health emergency. A causal relationship between ZIKV and microcephaly has been strongly demonstrated by several case studies[11,22–25].

According to a meta-analysis of eight studies, microcephaly appears between 0.3-14% of the babies born to ZIKV-infected mothers, depending on factors such as gestational age at infection, region and outbreak investigated as well as study design[26]. A large-scale retrospective analysis covering over 4 million births across Brazil during 2015-2017 reported that ZIKV infection during pregnancy is associated with 15-75-fold increased risk of neonatal microcephaly and infection during the first two trimesters confers a greater risk[27]. Importantly, not all mothers who experience ZIKV symptoms during pregnancy develop microcephalic fetus and an asymptomatic infection does not account that the fetus will not develop microcephaly[26]. Accumulating evidence also present a link between ZIKV and other congenital malformations[28] as well as a spectrum of neurodevelopmental[29], visual[30], hearing[31] and cognitive function[28] complications in adults and neonates. ZIKV infection was thereby declared neurotropic and teratogenic.

1.2.1.3 ZIKV infection molecular complications

Within the human body, ZIKV infects a unique subset of cell and tissue types. Establishment of ZIKV infection models such as neural stem cells, human brain organoids and mice have provided valuable insights on ZIKV target cells. In these models, ZIKV infects neural progenitor cells in the fetal brain cortex area leading to attenuated neural growth, disrupted cortical development and increasing cell death as a consequence[32–34]. Additional studies report how ZIKV infects microglia and astrocytes in the fetal brain, thereby modulating host immune response[35–37]. Besides damaging developing human brain directly, ZIKV persists and successfully replicates in human eyes and causes visual impairment[38,39]. Another significant site of ZIKV persistence in adults is the male reproductive tract. Infectious ZIKV was found in semen during first weeks after disease onset, while ZIKV RNA persisted in semen for longer than 6 months[40]. Two independent studies in mice report that ZIKV significantly disrupts testicular tissue by replicating in spermatogonia, Sertoli and Leydig cells, reduces sex hormone levels and male fertility[41,42]. Importantly, ZIKV infects dendritic cells[43,44] and monocytes[45] which are considered to act as “Trojan horses” to deliver ZIKV to immune-protected tissues such as placenta, brain, eyes and testes. Aforementioned studies reveal merely the tip of the iceberg of complex molecular events caused by ZIKV in the developing human brain and other target tissues.

1.2.1.4 Zika virus genome and replication cycle

General principles of ZIKV intracellular replication cycle can be inferred from widely studied members of the *Flaviviridae* family such as Dengue virus (DENV), but ZIKV-specific molecular events have also been recently uncovered. Similar to any other virus, ZIKV is an intracellular pathogen with an encoded aim to find suitable host cell, replicate and release new progeny virus particles into the surrounding environment. Infectious ZIKV virion is 50 nm in diameter and enveloped, meaning it is surrounded by a lipid bilayer membrane and surface proteins arranged by icosahedral symmetry (**Figure 2a**). ZIKV particles consist of non-segmented (+) ssRNA genome of approximately 11'000 bases in length[16,46]. ZIKV genome carries a single open-reading frame (ORF) that encodes ten proteins, including three structural proteins such as capsid (C), envelope (E) and precursor membrane (prM), which are crucial for ZIKV pathogenesis and structure, and seven non-structural proteins such as NS1, NS2A, NS2B, NS3, NS4A, NS4B and NS5 (**Figure 2b**). Non-structural proteins have distinct roles and are involved in viral pathogenesis, immune evasion and supporting different stages of the replication cycle[47].

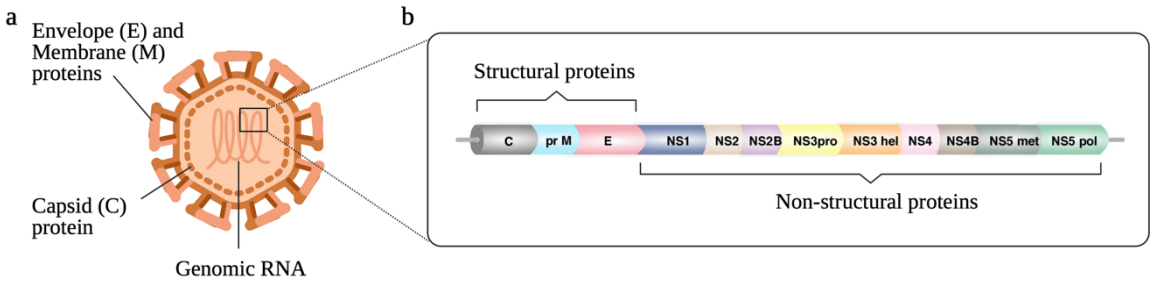

Figure 2. ZIKV virion structure and genome organization. a) ZIKV virion is round and consisting of genomic RNA that is surrounded by lipid bilayer membrane and envelope (E), membrane (M) and capsid (C) proteins. **b)** ZIKV genome is non-segmented (+) ssRNA consisting of a single ORF that encodes three structural and seven non-structural proteins. ZIKV genome organization is reprinted with permission from Elsevier from Mottin *et al.*[48].

ZIKV replication cycle is initiated when infectious viral particle reaches a permissive target cell and attaches onto cell surface receptor(s) (**Figure 3a**). Initial studies using cellular models implicated Axl protein, a receptor tyrosine kinase, to serve as the entry receptor for ZIKV[35,49]. However, Axl gene editing using the clustered regularly interspaced short palindromic repeats (CRISPR) -CRISPR associated protein 9 (Cas9) knock-out technology did not impact ZIKV infectivity in human neural progenitor cells, cerebral organoids or mice[50,51]. Therefore, current understanding is that Axl is not an indispensable factor for ZIKV infection and rather has an immune-modulatory role. Recent study employing chemical proteomic techniques described Neural Cell Adhesion Molecule 1 (NCAM1) as a new ZIKV receptor[52]. Additional ZIKV receptors, with probable redundancies, are yet to be discovered.

Upon binding to the cell receptor, ZIKV internalizes via clathrin-mediated endocytosis and traffics to endosomes (**Figure 3b**)[35,53]. Acidic environment inside the endosome triggers conformational changes in E protein, thereby inducing viral and host endosome membrane fusion and viral genome release into the cytoplasm (**Figure 3c**)[53–56]. Due to ZIKV RNA

genome (+) polarity, viral genome serves as a messenger RNA (mRNA) template and is translated into single polyprotein by host protein synthesis machinery, processed co- and post-translationally by viral and host enzymes, resulting in ten functional viral proteins, including NS5 protein, the RNA-dependent RNA polymerase (RdRP) (**Figure 3d**). RdRP then generates a complementary (-) RNA strand of ZIKV genome, which then serves as a template for replicating new (+) RNA genomes (**Figure 3e**)[57]. Flaviviruses, including ZIKV, remarkably rearrange the host endoplasmic reticulum (ER) membrane structures to form replication factories within the ER lumen[58]. It is believed that such formations enable spatial concentration of host and viral metabolites, but also protect the viral ssRNA genome from cellular nucleases and innate immunity triggers[59]. Newly generated ZIKV (+) RNA genome copies have two functions – they may serve as a template for new translation cycle or assemble into new virus particles.

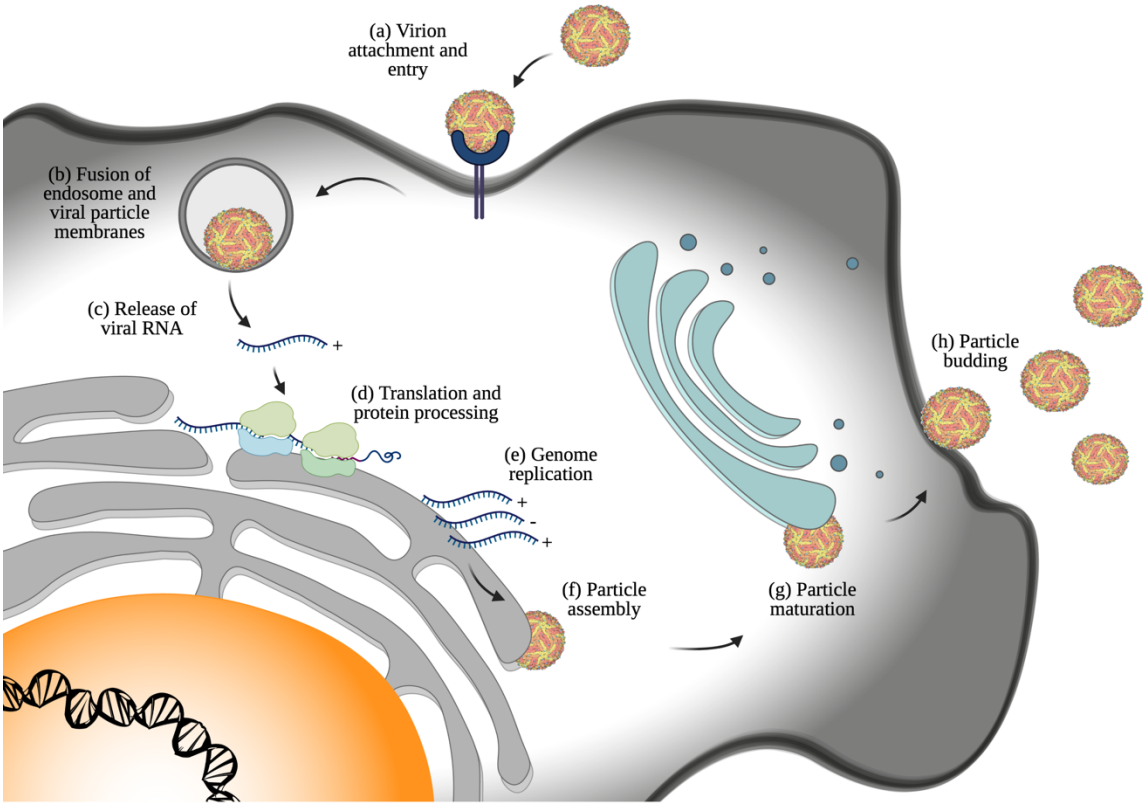

Figure 3. Schematic illustration of ZIKV replication cycle. a) ZIKV attaches to its cellular receptor(s) and enters the cell via endocytosis. b) ZIKV virion and endosome membrane fusion is triggered by the low pH in the endosome. c) Upon membrane fusion, vRNA is released into the cytoplasm. d) vRNA is translated by the host translation machinery and ZIKV polyprotein processed into functional proteins. e) vRNA genome is replicated by viral RdRP in ER. f) When sufficient quantity of vRNA genome and viral proteins have been produced, ZIKV particle assembly is initiated in the ER lumen. g) Immature particles are transported and maturated via Golgi apparatus network. h) ZIKV particles are budded out from the cell via exocytosis. Cellular organelles and virions are not on scale.

ZIKV particle assembly takes place in ER lumen (**Figure 3f**) and is initiated by NS2A recruitment of ZIKV genomic RNA, NS2B/NS3 protease and the structural C-prM-E polyprotein to the virion assembly site[60]. When the C-prM-E polyprotein has been processed, NS2A presents genomic RNA to the structural proteins[60]. Cleaved C protein and viral RNA

genome form a nucleoprotein complex which is subsequently packaged into lipid bilayer containing E and prM proteins[60]. These intracellular viral particles are immature, non-infectious and must undergo maturation process[61–63]. At this stage, prM protein functions as a platform protein preventing premature fusion of membranes as virus moves out of the cell[64]. Subsequently, particles are transported through trans-Golgi network (**Figure 3g**) where prM undergoes Furin protease-mediated cleavage[64]. Lastly, particles are released to the extracellular environment by exocytosis (**Figure 3h**).

1.2.2 Human coronaviruses

Coronaviruses are a diverse group of enveloped viruses carrying a (+) ssRNA genome. Besides infecting human populations, coronaviruses can infect and cause disease in various avian species, pets, poultry and livestock animals and thereby pose a medical and veterinary threat to the "one health" principles. Diseases accompanied with coronavirus infections in humans range from self-limiting upper respiratory tract infection or "common cold" to highly pathogenic life-threatening conditions. The global spread of SARS-CoV-2 and the unprecedented medical, economic and social impact of the COVID-19 pandemic marks as the third transfer of zoonotic coronavirus to humans. Previously spreading SARS-CoV-1 and Middle East Respiratory Syndrome Coronavirus (MERS-CoV) alarmed society for the impact of coronaviruses and for the urgent need of countermeasures.

1.2.2.1 Sever Acute Respiratory Syndrome Coronavirus 2 (SARS-CoV-2)

The first reported cases of patients experiencing respiratory disease with unknown cause originated from late December 2019 and were epidemiologically linked to live animal market in Wuhan, in Hubei province in China[65,66]. Within two weeks, etiological identification revealed previously unseen betacoronavirus as the causative agent and was thereafter named Severe Acute Respiratory Syndrome Coronavirus 2 that causes COVID-19 (ref[66–69]). Although less deadly compared to SARS-CoV-1 and MERS-CoV, the confirmation of human-to-human transmission[70,71] and the rapid global spread of SARS-CoV-2 during the following months prompted WHO to declare pandemic on March 11th in 2020 (ref.[72]). Although some genetic evidence suggest bats as the most probable SARS-CoV-2 natural hosts, there is currently no consensus on when and where the virus first entered human population[68,73]. An international mission coordinated by WHO was carried out in China to investigate the zoonotic origin of SARS-CoV-2 and the researchers are soon due to publish their initial report[74].

The clinical features of SARS-CoV-2 infection in humans vary from mild self-limiting disease to severe respiratory failure, affecting all ages of population. Importantly, virus also transmits from asymptomatic individuals which poses an additional challenge to break the transmission chain. To date, the true extent of asymptomatic infections remains unclear due to inadequate characterization of persistently asymptomatic cases[75]. The most vulnerable sub-population to SARS-CoV-2 infection appear to be older (>60 years old) men with underlying co-morbidities that have an increased risk to develop respiratory failure, require hospitalization or die[76]. Most common symptoms are fever, cough, fatigue and shortness of breath, while less frequently

occurring symptoms include sputum production, headache, diarrhoea and olfactory and taste disorders based on the studies of patients in China and Italy[71,76–79]. Additionally, increasing number of studies report persistent and heterogeneous long-term impact of SARS-CoV-2 infection to patients who experienced either mild or severe acute infection, so called "long COVID". A plethora of long-lasting symptoms have been reported, such as fatigue, loss of taste and smell, sleep difficulties, anxiety or depression, to name a few[80,81]. Even though substantial progress has been made to understand and combat the acute phase of SARS-CoV-2 infection, the progress of long COVID symptoms remain poorly characterized and negatively influence many patients.

To date, two monoclonal antibody therapies have received emergency use authorization[82–86] and a repurposed antiviral Remdesivir have received approval[87] from Food and Drug Administration (FDA) to treat COVID-19. As of March 2021, there are nearly five hundred therapeutics in clinical development for COVID-19. As SARS-CoV-2 infection continues to spread, the coordinated efforts of researchers, health care providers, governments and most importantly, the public, are crucial to tackle this pandemic.

1.2.2.2 Human Coronavirus 229E (CoV-229E)

Unlike the aforementioned pathogenic coronaviruses, human Coronavirus 229E (CoV-229E), CoV-OC43, CoV-NL63 and CoV-HKU1 generally cause mild to moderate disease with self-limiting upper respiratory tract infection and contribute to approximately 15-30% of the common cold cases in humans[88,89]. Prior the emergence of SARS-CoV-1 in 2002-2003, alphacoronavirus CoV-229E and betacoronavirus CoV-OC43 were the main subjects of human coronavirus-related research. CoV-229E enters host cells via cellular receptor Aminopeptidase N (APN; also known as cluster of differentiation 13 (CD13)) and mainly targets upper respiratory tract epithelial cells. However, CoV-229E infection has been detected in immunocompromised patients and potentially leading to more severe respiratory illness[90,91]. In some occasions, CoV-229E RNA has been detected in human brain tissues[92] and shown to infect human neural cell lines[93], supporting neurotropic nature of this respiratory virus. However, the impact of CoV-229E presence in neural tissues to human disease remains poorly understood. Overall, studies on CoV-229E have extensively contributed to our in-depth understanding of human coronavirus pathogenesis, replication cycle and host-virus interactions that appear absolutely crucial to shape strategies against the current pandemic.

1.2.3 Viral hemorrhagic fever (VHF) viruses

VHF is caused by members from several different RNA virus families that are all enveloped viruses and carry their genome as ssRNA. Many VHF viruses have restricted geographical distribution such as EBOV and Lassa virus (LASV) in West Africa, but some VHF such as CCHFV, DENV and Hantavirus can spread through larger areas across the globe.

CCHFV is a highly pathogenic tick-borne arbovirus and a member of family *Bunyaviridae* causing severe hemorrhagic disease with case fatality rate between 5-30%. Ticks of the *Hyalomma* genus serve as the main reservoir and vector of CCHFV, yet humans may also

become infected by handling infected livestock, wild animals or through the contact of infected patients. Recently, a DNA-based vaccine candidate showed successful protection against CCHFV in non-human primates[94]. Hazara virus (HAZV) is closely related to CCHFV but does not cause disease in humans, can be handled in the biosafety laboratory level 2 (BSL-2) and has therefore been used as a surrogate virus to study CCHFV pathogenesis[95]. Despite certain differences between HAZV and CCHFV entry mechanisms[96], HAZV has been implemented as a model virus in current thesis work.

EBOV is another highly fatal hemorrhagic fever virus from *Filoviridae* family that gained international attention during 2014-2016 in West-Africa causing one of the most widely spread, fatal and long-lasting EBOV epidemics in history. Second largest outbreak occurred in Democratic Republic of Congo (DRC) during 2018-2020 which received rapid response by safety and efficacy trials of investigational EBOV therapeutics and mass-vaccination. As a sign of re-emergence, Guinea and DRC independently reported a cluster of EBOV cases in February 2021 and immediately declared an outbreak, ramped up surveillance, infection prevention and testing to strengthen the response in the countries that have already enormously suffered from the disease[97,98]. Currently two vaccines[99–101] and two monoclonal antibody treatments Inmazeb (also known as REGN-EB3)[102] and Ebanga (also known as mAb114)[103,104] have been approved by the FDA. Common symptoms to all VHF are bleeding disorders and high fever potentially progressing to life-threatening outcome.

Given the growing impact of aforementioned viruses as emerging pathogens, huge gaps remain in knowledge on molecular events during infection as well as specific therapeutic tools to combat these diseases. Our ongoing vulnerability to viral pathogens underlines the importance to explore basic biology of virus infections and to develop novel therapies.

1.3 EXISTING ANTIVIRAL THERAPIES

Viral diseases can either be prevented by vaccines or treated by small molecule antivirals or antibody-based therapies. Over the past five decades, antiviral drugs have been approved against approximately ten human viral pathogens of which majority are against Human Immunodeficiency virus (HIV), Hepatitis C virus (HCV), Influenza virus, Herpes Simplex virus (HSV) and recently one antiviral against the newcomer SARS-CoV-2 (ref.[1]).

While vaccines act as highly specific for individual viruses, a large proportion of antivirals display activity beyond their originally intended target, presenting broad activity across virus families[105]. In an ideal scenario, at the emergence of a novel virus, existing antivirals with safe clinical profile and proven efficacy against previously circulating viruses would be the basis for rapid *in vitro* and *in vivo* pre-clinical efficacy studies. These results would provide scientific evidence to initiate clinical trials in an epidemic/pandemic setting which, in case of successful outcome, would enable repurposing of the existing antivirals to treat the emerging virus infection. Meanwhile, vaccines would be underway, but patients could benefit from the repurposed broad-spectrum antivirals, bridging the gap during vaccine development.

1.3.1 Clinical candidates against emerging viruses

Generally, antiviral drugs can be classified based on their therapeutic target, originating either from viral named direct acting antivirals (DAAs) or from cellular components called host-directed antivirals. Both alternatives have advantages and disadvantages.

DAAs are designed to be highly specific towards a selected viral enzyme, inhibit it with high potency and minimally interfere with host processes. DAAs therefore heavily suffer from the emergence of drug-resistant viral variants and from therapeutic failure. DAAs account fewer side effects, but are often active only against one specific virus, representing the “one drug, one virus” dogma (**Figure 4**). However, some antivirals targeting RdRP are exceptions because polymerase is an absolutely essential enzyme encoded by all RNA viruses and also conserved to some degree[106]. Antivirals Remdesivir, Ribavirin and Favipiravir have showed broad activity and represent “one drug, multiple viruses” dogma (**Figure 4**). A vast majority of approved antivirals are small-molecule DAAs primarily targeting viral genome replication, proteolytic processing or virus entry[107].

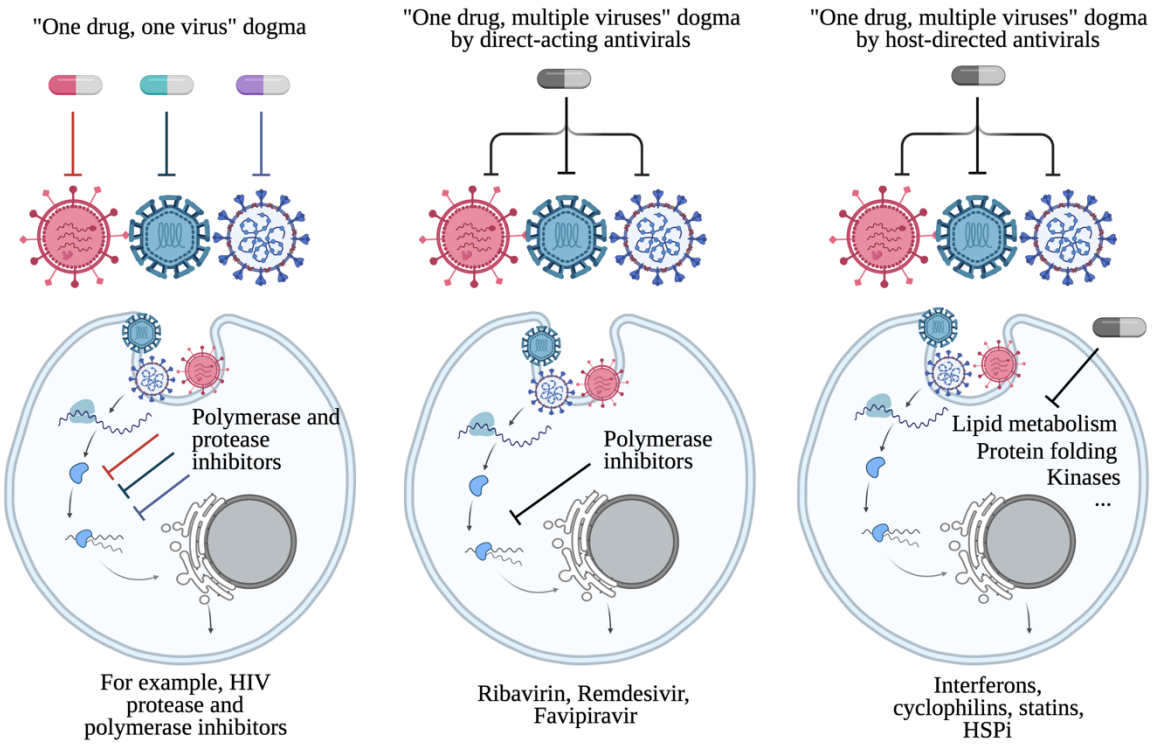

Figure 4. Some DAAs and host-targeting antivirals provide broad-spectrum antiviral. Inhibitors targeting viral enzymes such as polymerase, protease or others generally exhibit narrow yet potent specificity towards one virus, summarized as "one drug, one virus" dogma. Few polymerase inhibitors such as Ribavirin, Remdesivir and Favipiravir have broad spectrum activity and inhibit viral polymerase of different viruses. Host-directed antivirals block cellular processes that are crucial for virus propagation and are thereby antivirally active.

An alternative approach to DAAs are the host-directed antivirals. Because viruses from different families rely on similar cellular pathways[108], host-directed antivirals can inhibit a wide range of viral pathogens and also represent the "one drug, multiple viruses" dogma (**Figure 4**). Host-directed antiviral strategy is less explored in the clinics, however a small number of immunomodulators such as Interferons and antimitotic agents exert their activity by targeting host cell processes and not viral proteins directly[1].

To date, multiple repurposed DAA and host-directed antiviral compounds have been identified against ZIKV infection and some drug repurposing success stories against SARS-CoV-2 have been presented using *in vitro* and *in vivo* models. Selection of clinically available broad-spectrum drug candidates are described below.

1.3.1.1 Ribavirin

One of the most extensively studied small-molecule antiviral, a synthetic guanosine analog Ribavirin has multiple mechanism of actions (MoA) and displays broad activity against several RNA and DNA viruses[109,110]. Ribavirin treatment is extensively used against HCV in combination with Type I Interferon[111–113]. Additionally, Ribavirin is the only available and recommended antiviral medication to treat LASV and CCHFV. Unfortunately, there is insufficient reliable clinical data for Ribavirin treatment efficacy in CCHFV patients[114,115]. Ribavirin has been shown to inhibit ZIKV replication in various cell models[116] as well as to

increase survival of STAT1-deficient mice who exhibit lethal outcome upon ZIKV infection without treatment[117].

Although with not fully understood MoA, Ribavirin is believed to inhibit viral RNA (vRNA) elongation[118], induce viral genome mutagenesis by increasing the error-rate of viral RdRP[119,120] as well as deplete intracellular guanosine triphosphate (GTP) and deoxyguanosine triphosphate (dGTP) pools by inhibiting host protein inosine monophosphate dehydrogenase (IMPDH)[121]. Accumulating evidence show that Ribavirin also modulates host immune system, favoring T helper cell 1 (T_h1) immune response over T_h2 and potentially supporting viral clearance in HCV patients[122]. Ribavirin therefore exhibits properties of both DAA and host-directed antiviral. However, multiple studies report viral resistance[123,124] and adverse side effects[125] as major worrisome drawbacks of Ribavirin treatment. Owing to the FDA approval and broad-spectrum activity, Ribavirin is used as a positive control in this doctoral thesis work.

1.3.1.2 Remdesivir

Remdesivir is structurally an adenosine nucleotide analog acting as a prodrug and disturbing vRNA replication by inhibiting RdRP. Gilead Sciences developed Remdesivir as an antiviral against EBOV and reported therapeutic efficacy in non-human primates during 2015 (ref.[126]). Subsequently, antiviral activity of Remdesivir was confirmed against a wide range of RNA virus families such as coronaviruses, paramyxoviruses and other filoviruses, showing the broad spectrum activity and potential indications against viruses with significant public health impact[127–129].

During the EBOV outbreak in DRC during 2018-2020, Remdesivir treatment was included in a randomized controlled trial aside three other promising investigational treatments ZMapp, MAb114 and REGN-EB3[130]. After initial results, Remdesivir and ZMapp trial arms were terminated based on an interim study analysis concluding that Remdesivir and ZMapp treatments remained inferior to the antibody therapies MAb114 or REGN-EB3 based on the primary end point of death at 28 days[130]. Nonetheless, the favorable clinical safety profile obtained from the EBOV trial and the *in vitro* antiviral activity against SARS-CoV-2 (ref.[131]) prompted physicians and researchers across the world to initiate clinical studies for the use of Remdesivir in COVID-19 patients. Based on clinical efficacy evidence[132–134], FDA ultimately granted an approval for Remdesivir use in hospitalized COVID-19 patients. Meanwhile, WHO included Remdesivir in their large-scale international Solidarity trial with primary goal to repurpose antivirals for reducing SARS-CoV-2 in-hospital mortality[135]. Remdesivir had little or no effect on the hospitalized COVID-19 patients leading WHO to recommendation against the use of it in COVID-19 patients due to lack of evidence of improving patient survival or the need of mechanical ventilation. Still, certain countries continue using Remdesivir in hospitalized COVID-19 patients, but such discouraging conclusions dampened the early hopes that came along with small-scale studies and further highlight the need for more research and drug discovery efforts.

1.3.1.3 Favipiravir

Favipiravir also called as T-705 is clinically approved in Japan to treat severe influenza virus infections. Favipiravir acts as a prodrug, is phosphoribosylated by cellular enzymes to its active form which is structurally a nucleoside-triphosphate analog[136]. Viral RdRP recognizes Favipiravir as a purine nucleotide resulting in disturbed vRNA replication. Importantly, Favipiravir activity reaches beyond influenza and is also able to inhibit flaviviruses, alphaviruses, bunyaviruses and other RNA viruses[136,137]. In the clinic, the treatment has been well-tolerated by healthy volunteers[138] and seems to have a high barrier for resistance development[139–141]. Altogether, Favipiravir has characteristics of a promising broad-spectrum antiviral against emerging viruses.

1.3.2 Viral resistance

Acquired resistance to antivirals, especially to DAAs, represents a major clinical challenge across viral diseases. Viruses, especially those with RNA genome have high capacity to adapt with novel environments such as host immune system or antiviral treatment due to rapid rate of replication, error prone RdRP and large pre-existing genome variation[142]. Antiviral therapies of chronic viral infections such as HIV do not provide cure and patients must undergo life-long treatment, increasing the probabilities for resistance development[143]. With that in mind, research community is driven to explore novel and innovative approaches such as host-directed antivirals, to circumvent resistance mechanisms and identify new targets for treatments.

1.3.3 Host-directed antiviral approach

Targeting host proteins required for virus but not critical for the host survival has been proposed as an alternative and powerful antiviral approach. Recent studies have identified various host cell factors involved in viral infection, confirming active host-pathogen interplay[144,145]. In fact, any life cycle step from viral attachment to budding may serve as a potential target. Host-directed therapies have higher barrier for resistance development, but also entail a higher chance of unwanted side effects. Thus, it remains crucial to characterize host-virus interactions and understand the complex biological processes during infection.

In recent years, numerous studies have defined ZIKV, EBOV and SARS-CoV-2 interactions with host by proteomic or functional genomic analysis, revealing systems-wide understanding of virus-induced host molecular changes. In 2018, Pietro Scaturro and colleagues individually expressed ten ZIKV proteins in a neuroblastoma cell line, performed unbiased proteome analysis and identified 386 host proteins interacting with ZIKV as well as 1216 ZIKV-specific phosphorylation sites in host proteins[146]. Additionally, four independent research groups mapped SARS-CoV-2 and other human coronavirus interactions with host cell networks, providing a rich resource for targeted therapies[147–150]. Collectively, identifying host pathways required for viral life cycle and understanding the molecular biology of virus-host interplay provides a valuable basis for antiviral drug and target discovery.

Only a handful host-directed antivirals are clinically approved. Interferons enhancing the cellular innate antiviral response are used against Hepatitis B virus (HBV)[151] but come with several unwanted side effects. Clinically available corticosteroid immunosuppressant Dexamethasone is currently administered to hospitalized COVID-19 patient receiving respiratory support[152]. Tyrosine kinase inhibitors used to treat cancer patients have shown promise in the repurposing studies[153,154]. Additionally, other cellular targets have been investigated for their supportive role for virus life cycle such as host lipid metabolism[155] targeted by statins[156–159], cyclophilins[160–162], and heat shock proteins[163,164].

1.4 ANTIVIRAL DRUG AND TARGET DISCOVERY

In principle, the screening approaches in early drug discovery can be divided as target-based or phenotypic. In target-based screening, the study design is based on a defined therapeutic target and its known or hypothetical MoA in a disease which thereby leveraged for drug screening, hit identification and eventually validated in disease-relevant models (**Figure 5**). On the contrary, phenotypic screening is investigating a therapeutic effect linked to disease phenotype and do not require underlying molecular understanding of the disease or the target.

In the past three decades, new drug leads were primarily developed towards specific, well-characterized therapeutic targets, but in recent years the screening based on cellular phenotypes have resurged[165]. In fact, phenotype-based approaches delivered more first-in-class medicines between 1999-2008, while target-based approach led to the discovery of follower drugs in a particular drug class, marking a shift in paradigm[166].

Currently, majority of antiviral drug discovery efforts are target-based and directed towards viral proteins with well-characterized function in the replication cycle, resulting in DAAs. Often, high-throughput screening campaign to identify antiviral drug candidates are carried out by monitoring target protein activity by *in vitro* enzymatic assays, such as the polymerase or protease activity assays[167,168]. Additionally, pseudotyped viruses[169,170] and viral replicon systems[171–174] have been valuable surrogate tools for pathogens that require high-containment laboratories and enable feasible screening cascades, but are limited to certain steps of the virus replication cycle. However, target-based approaches focusing on one virus may be insufficient to provide necessary readiness for emerging viruses. Therefore, development of broad-spectrum antivirals is critical and phenotypic drug discovery presents a suitable approach.

1.4.1 Phenotypic drug discovery

Phenotypic drug discovery exploits the incompletely understood disease mechanisms and provides the possibility to identify disease-relevant drug candidates (**Figure 5**). In contrast to the target-based approach, early phenotypic drug discovery assays are performed in disease relevant model systems such as cell lines, patient-derived primary cells[175–177], three dimensional (3D) organoid cultures[178,179] or even whole organisms such as Zebrafish larvae[180].

In antiviral research, phenotypic screening enables the discovery of antiviral compounds with potentially broad-spectrum activity, because screening design is not directed towards one specific protein, but rather towards the infection in a broader sense. Popular antiviral assays measuring cell CPE are phenotypic by nature and capture the entire virus replication cycle. However, CPE assays depend on virus infection causing cell death and not all viruses kill their hosts. In high-throughput CPE screens, compounds are evaluated based on their ability to rescue host cells from virus-induced cell death by quantifying cell viability as a bulk measurement. Compound cytotoxicity and efficacy can be assessed by a wide range of assays measuring cell viability[181], Caspase-3 activity[182], crystal violet uptake[183] or numerous alternatives.

Due to the unbiased nature, target identification has been a bottleneck in phenotypic drug discovery endeavors. Recent advancements in both high-throughput image-based assays as well as proteome-wide target-identification methods have assisted researchers both in academia and industry to venture the phenotypic approach. Identifying novel compounds by phenotypic screening and subsequently investigating the compound's molecular targets by target identification methods illustrates the unconventional way to study new or incompletely understood diseases and find novel therapeutic targets (**Figure 5**)[184].

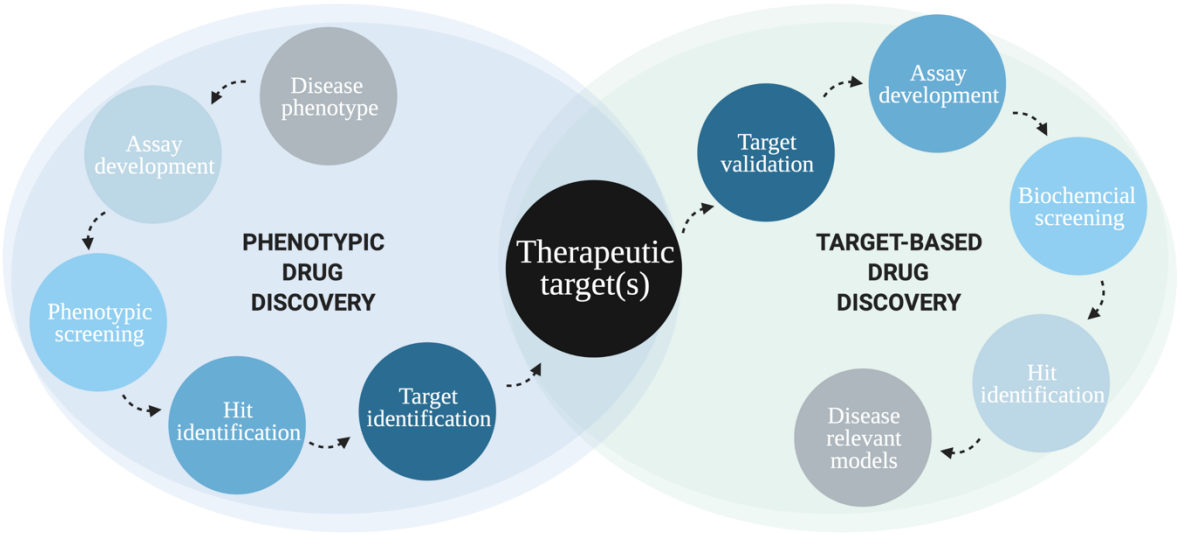

Figure 5. Comparison of target-based and phenotypic drug discovery. Phenotypic drug discovery is initiated by disease phenotype of interest, for instance virus infection or formation of stress granules. The phenotype is developed into high-throughput assay to screen compound libraries and evaluate the effect on the disease phenotype. Screening hits are modifying the disease phenotype and must undergo target identification process to elucidate the molecular mechanisms behind the phenotype. Target-based drug discovery relies on a specific protein and its proven or hypothetical role in a disease. The assay development goal is to measure the function of the protein, generally by purified proteins in a biochemical assay. Hits of the high-throughput screening specifically inhibit or activate the function of the protein. Finally, hit compound(s) are tested on disease relevant models.

1.4.1.1 Image-based phenotypic screening

Image-based phenotypic screening assays have provided success stories across disciplines, especially in tumor biology, and is also being slowly introduced in virology aside classical cell-based phenotypic assays such as the CPE[185]. Access to high-throughput microscopy and automated image analysis tools have boosted the development of image-based antiviral assays. For instance, multiple studies have provided *in vitro* evidence for drug repurposing possibilities by implementing image-based quantification of ZIKV[186,187] , EBOV[188] or SARS-CoV-2 (ref.[189]) infection.

In principle, antiviral image-based assays rely on virus-specific antibodies coupled to fluorescent labels to distinguish infected and non-infected cells, representing a screenable phenotype. Detection of viral factors is usually combined with cellular marker(s) such as nuclei stain and captured by high-throughput or high-content microscopy. Automated image analysis tools facilitate the extraction and quantification of virus- and cell-specific read-outs. Cellular

cytotoxicity can be quantified based on nuclei staining and antiviral efficacy based on virus staining, providing valuable information about the therapeutic window between compound antiviral efficacy and cytotoxicity. To summarize, image-based antiviral assays visualize infected cells and evaluate a specific pre-defined phenotype such as viral antibody staining. However, biological images carry much deeper information about cellular morphology which can be leveraged as indicators of cell health and ongoing processes by advanced morphological profiling techniques.

1.4.1.2 Morphological profiling by the Cell Painting assay

When screening campaigns usually quantify pre-selected parameters, then morphological profiling techniques evaluate large quantities of information about cellular morphology changes in response to biological or chemical perturbations (**Figure 6a**)[190]. The Cell Painting assay is the most popular morphological profiling assay that is based on multiplexed staining of relevant subcellular organelles by fluorescent dyes (**Figure 6b**)[191].

In Cell Painting, images are acquired by high-content microscopy and analyzed by image analysis tools or presented to machine learning strategies (**Figure 6a**). Automated image analysis software such as open-source CellProfiler[192,193] extracts approximately 1200-1500 morphological features per individual cell which can be various measurements from cell size, shape, intensity, granularity, etc. Finally, cellular features are the basis for single-cell analysis or for producing cell population profiles[191].

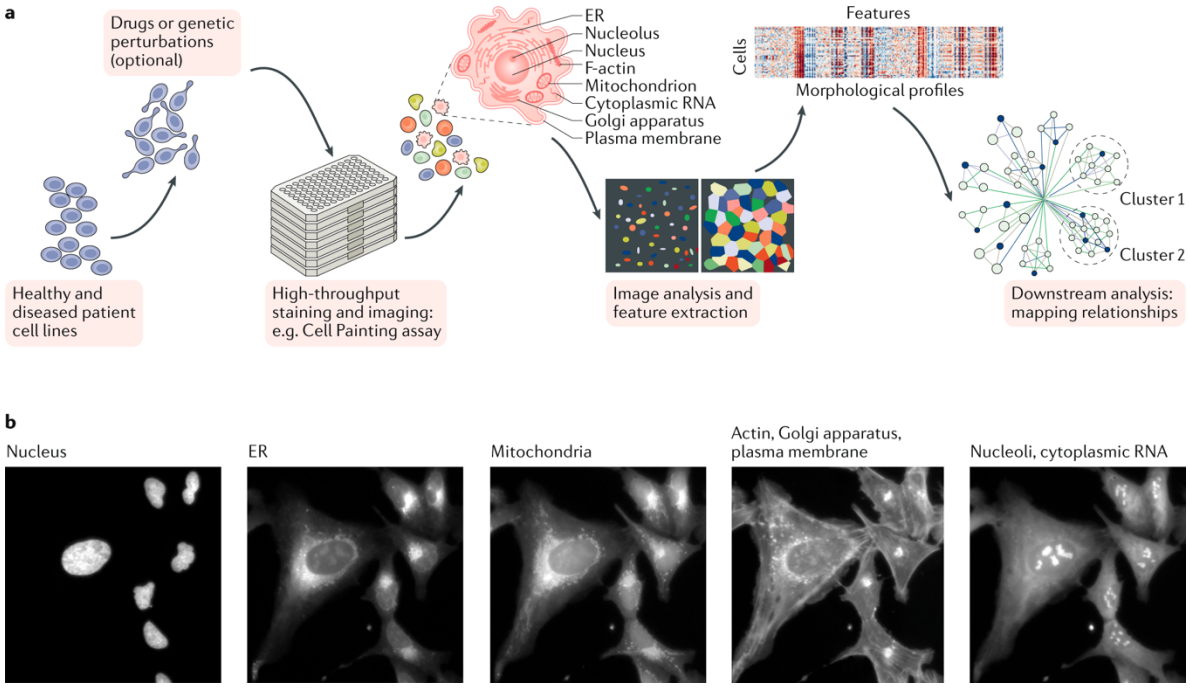

Figure 6. Key steps of the Cell Painting methodology. a) Cell Painting assay examines the morphological signatures of cells treated with drugs, modified genetically or originating from healthy and diseased patients. Assay is performed on multi-well plates and cells are stained with fluorescent dyes to detect relevant subcellular organelles. Images are captured by high-content microscopy and processed by image analysis tools to extract morphological features (cell size, shape and staining intensity, among others). Finally, features are categorized based on their similarities and differences by computational methods. b) Examples images of cells stained with

five different dyes capturing eight different cellular organelles. Reprinted with permission from Springer Nature from Chandrasekaran, *et al*.[194].

Since Anne Carpenter and her team developed the assay in 2016, several Cell Painting applications have been described. For instance, morphological profiling can predict the MoA and indicate the molecular target(s) of novel compounds by comparing the cellular features of uncharacterized compounds with well annotated references[195–198]. The predictions are based on an assumption that compounds with similar MoA result in similar phenotypic signatures[199]. Researchers provided scientific community with a large dataset consisting morphological profiles from cells treated with more than 30'000 individual small molecule compounds, along with raw images, chemical annotations, quality control metadata and CellProfiler pipelines[197]. This work enables the community to readily access Cell Painting generated information and mine the data based on their scientific questions. This is highly valuable as resources needed for the computational algorithms within the Cell Painting workflows are not routinely available for all researchers. In another study, phenotypic clustering identified phosphoinositide 3-kinase (PI3K) and mechanistic target of rapamycin (mTOR) as novel target of a known casein kinase II inhibitor Silmaitasertib[200]. Additionally, Cell Painting assay aided the MoA deconvolution of Autoquin by demonstrating its accumulation in lysosomes and preventing the fusion with autophagosomes[201].

In addition to small molecules, cellular phenotypes may also undergo changes upon disease progression[202–204]. A morphological profiling study was recently published in a pre-print server where the authors performed Cell Painting on primary fibroblasts from 90 Parkinson's disease patients and healthy controls[205]. By using morphological disease phenotypes obtained from machine learning models, the authors were able to distinguish cells between healthy and Parkinson's disease individuals. This study characterizes Parkinson's disease phenotypes that may be implemented in screening campaigns to facilitate finding novel therapeutics for Parkinson's disease. Recently, our group presented a Cell Painting workflow to distinguish phenotypes in virus infected and non-infected cells[206]. Our screenable workflow provided in-depth morphological signatures of the selected compounds in presence and absence of virus infection and presented a proof-of-concept how potent antiviral compounds reversed the infection phenotype that resembled the uninfected state.

Collectively, the vast information present in biological images has been thoroughly leveraged by morphological profiling techniques such as Cell Painting and is readily contributing to the drug discovery as well as the novel understanding of disease-related biology. Overall, morphological profiling further integration with deep learning, novel disease models and drug discovery processes will lead to even broader discoveries.

1.4.2 Target identification: from antiviral phenotype to target

Similar to understanding the MoA, identification of the therapeutic target poses a key challenge after finding a promising drug candidate, especially for those arising from phenotypic screens. But it also presents an opportunity to find new biological phenomena and thereby previously unknown targets in context of the disease of interest. Knowing the MoA and molecular target

may not be absolutely necessary, yet seems to increase the likelihood for drug approval[207]. For instance, a 7-18% fraction of drugs have been approved by the FDA without defined molecular target[208]. As drugs mainly achieve their therapeutic activity by binding to target(s) within cells, information about drug-target interaction *in vitro* and *in vivo* is invaluable for further development of the candidate drug.

A variety of biochemical, genetical or proteomic-based techniques may be implemented for target identification. For instance, CRISPR-induced genetic variation facilitates the selection of mutations that result in drug resistance in cancer cells[209]. This study presents an advancement of a standard method studying drug resistance induced mutations which is also widely used in virology. Affinity-based pulldown of proteins interacting with the drug and different variations of this method have been applied for target identification purposes for decades[210]. Protein thermodynamic principles have been exploited to measure drug-target engagement by differential scanning fluorimetry (DSF)[211] and by the state-of-the-art cellular thermal shift assay (CETSA)[212].

1.4.2.1 Principles and applications of CETSA and Thermal Proteome Profiling

In 2013, a groundbreaking study described a novel method to monitor drug binding to target proteins in living cells[212]. CETSA is based on a biophysical phenomenon of ligands or small molecules that induce changes in thermal stability of their target proteins. When cells and thereby cellular proteins are heated, proteins unfold from their native conformation and denature (**Figure 7a**). When a ligand or a drug is bound to the protein, thermal stability may increase or decrease, indicating drug-target engagement (**Figure 7a**). Native protein levels in the soluble fraction are quantified in order to create a protein melting curve and calculate a protein-specific melting temperature (T_m), the temperature at which 50% of the protein is unfolded[212,213]. Difference in protein T_m between vehicle- and drug-treated samples indicate thermal shift (ΔT_m; either stabilized or destabilized effect) and thereby drug-target engagement (**Figure 7a**). Cellular proteins are detected by endpoint assays such as low-throughput antibody-based read outs such as western blot (**Figure 7b**) or high-throughput AlphaScreen technique[214] enabling the evaluation of drug-target engagement. CETSA can be performed in living cells, providing information about drug penetration, drug metabolism and drug activity in a living system or alternatively in cell lysates, allowing more controlled conditions and distinguishing of primary drug-target binding from indirect downstream effects.

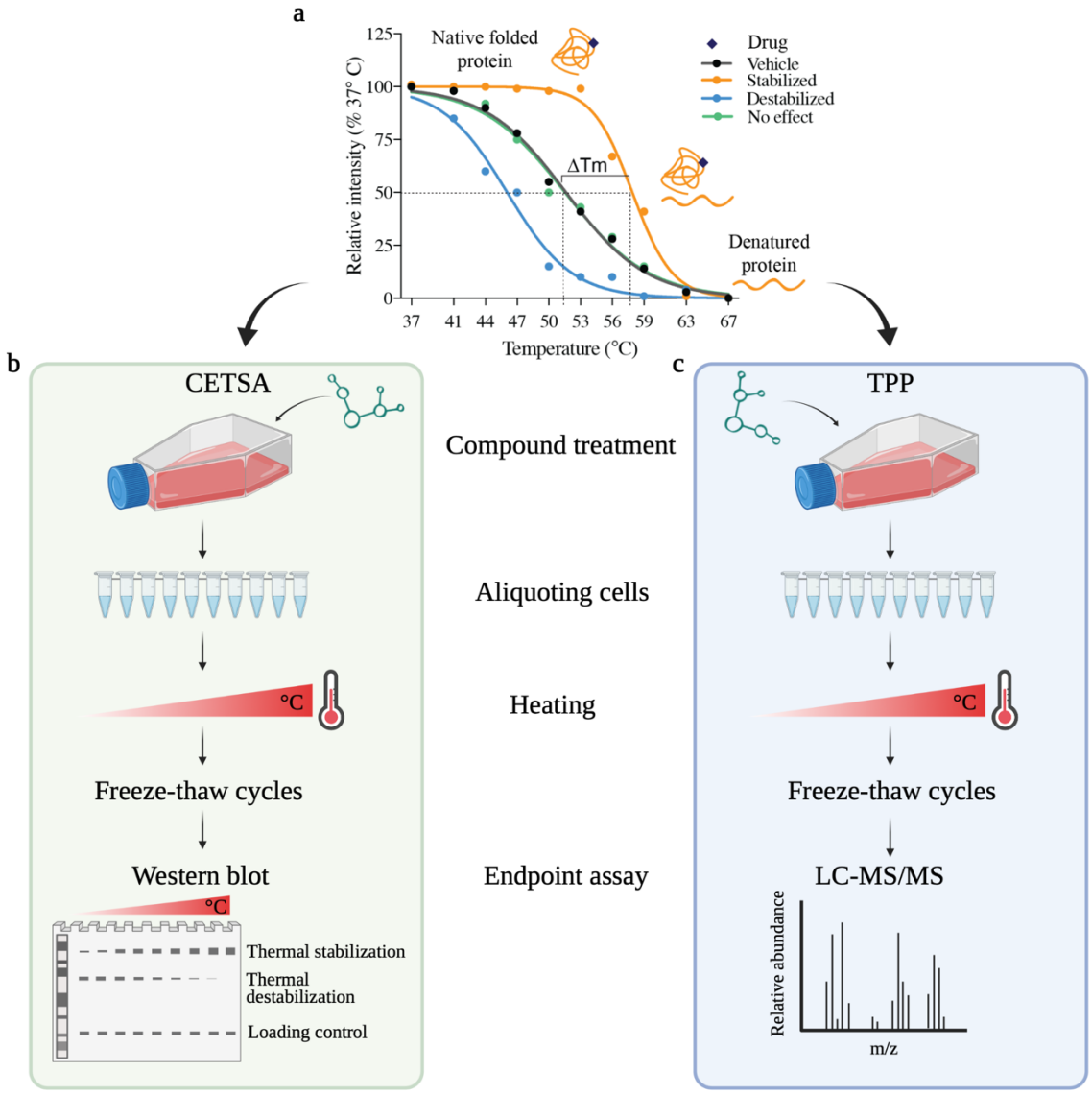

Figure 7. General workflow CETSA and TPP techniques. a) Both CETSA and TPP are based on a thermodynamic principles of protein denaturation when treated with heat. But when a ligand or a small molecule is bound to the protein, its thermal stability increases or decreases, illustrating thermal stabilization or destabilization, respectively. CETSA and TPP measure the difference of protein melting temperature (ΔT_m) between treated and untreated samples. b, c) The general version of CETSA and TPP are performed in cells treated with drug and a vehicle control for a given time. Cells are thereby harvested, aliquoted in individual tubes and each tube is heated at different temperature. Cells are lysed by freeze-thaw cycles and the soluble protein fraction is separated from the insoluble and analyzed by endpoint assay. b) CETSA endpoint assay is usually western blot and evaluates thermal stability of pre-selected protein(s) of interest. c) TPP endpoint assay is LC-MS/MS evaluating thermal stability on the proteome scale.

More recently, an extended approach thermal proteome profiling (TPP) was developed, combining CETSA method with the power of multiplex quantitative mass-spectrometry (MS)[215,216]. TPP is capable of monitoring drug-target engagement across the cellular proteome (**Figure 7c**). While CETSA is well suited for targeted approach for studying protein of interest, then TPP enables monitoring drug targets, off-targets and downstream effects in an unbiased manner. More specifically, indirect drug targets, for instance downstream effects resulting in drug binding to the direct target(s), can be studied by complementary TPP in live cells and in cell lysates. Proteins that engage with the drug in both living cells and cell lysates are generally

considered as drug target candidates. For instance, novel targets were recently discovered by TPP for the pre-clinical anti-parasitic compound ENH1 in *Toxoplasma*[217] and for clinically approved kinase inhibitor vemurafenib[215].

Furthermore, the target profiling technique has been further improved to enable drug affinity assessments by combining thermal and drug concentration gradient measurements in a two-dimensional TPP (2D-TPP) workflow[218]. To date, TPP protocol is well applicable to monitor soluble fraction of the proteome and improvements to capture insoluble fraction are currently being made[219,220]. TPP does not require any modifications of drugs or cells, and thereby presents an accessible and powerful bridge between the drug's phenotypic activity and the therapeutic target.

The modification of protein thermal stability reaches far beyond small molecule inhibitors. In fact, the thermal stability status of a protein may be additionally influenced by other biological factors. TPP toolbox have recently enabled to study protein thermal stability status in relation to posttranslational modifications[221–223], protein mutation status, protein-protein interactions[224–226] or any biological ligand such as nucleic acids[226], metabolites[227] or others. Along these lines, host proteome stability was studied in human epithelial colorectal adenocarcinoma Caco-2 cell line during SARS-CoV-2 infection by TPP and the authors demonstrated substantial changes in protein thermal stability across diverse cellular pathways such as mRNA splicing and protein folding by chaperones[228]. These changes may represent pro-viral modifications induced by SARS-CoV-2 or cellular antiviral defense mechanisms which could be therapeutically targeted. Indeed, the authors shortlisted potentially druggable host targets, provided evidence for cellular chaperone heat shock protein 90 (HSP90) inhibitor tanespimycin as non-toxic antiviral and thereby showcased how monitoring proteome thermal stability may reveal new therapeutic targets against viral diseases. Similar to the SARS-CoV-2 study, host-pathogen interactions have been mapped by TPP in primary human fibroblasts following human cytomegalovirus infection[229].

Recent advances in the proteomic-based target engagement methods help reducing the hurdles of drug target identification process and contribute to the understanding of molecular MoA, novel therapeutic targets and thereby to clinical efficacy. It holds true that all experimental techniques carry limitations and are unable to definitely identify a compound's target. Instead, for a successful pinpointing of the most probable target complementary methods should be applied.

2 PRESENT INVESTIGATION

2.1 THESIS OBJECTIVES

Emerging RNA viruses such as ZIKV, CCHFV, EBOV and SARS-CoV-2 cause serious disease in humans and spread rapidly, thus antiviral therapies are urgently needed. RNA viruses encode only a small number of proteins and are therefore entirely dependent on host cell pathways to produce viral progeny. During infection, well-coordinated interplay between virus and host factors offer a range of specific antiviral targets with potentially broad-spectrum activity and therapeutic benefits.

Virus infections are known to cause enhanced oxidative stress[230,231], yet they must protect their vRNA and proteins from oxidation, degradation and maintain integrity. Cellular oxidative stress response pathways have been reported to activate upon viral infections[232,233], thus posing a possibility that oxidative stress pathways are supporting viral replication cycle.

The Helleday laboratory has developed a small molecule inhibitor library targeting oxidative stress and nucleotide metabolism pathways and presented strategies for the treatment of tumours and inflammatory diseases[234,235]. Based on the activation of host oxidative response during infection, in **Paper I** we hypothesized that modulating cellular oxidative response balance with small molecule compounds can disturb viral replication. We first aimed to establish a phenotypic assay to screen the in-house compound library for their antiviral activity using HAZV as a model virus. We chose HAZV because it does not cause disease to humans and is permitted within BSL-2 setting but belongs in the same serogroup as CCHFV. Next, our goal was to determine the hit compounds activity, or lack of it, against emerging viruses EBOV, CCHFV, SARS-CoV-2 and finally determine the cellular targets that drive the antiviral activity of the identified compounds.

Based on the obtained results in **Paper I** showing broad spectrum activity of the in-house compounds and the evolving ZIKV epidemic in 2016, in **Paper II** we aimed to screen structural analogs from the HAZV screening hits against ZIKV, presenting an emerging pathogenic RNA virus. Additionally, we aimed to study the antiviral MoA within the virus replication cycle.

Screening assays implemented in the antiviral drug discovery process are often constrained to already existing knowledge about the virus and lack the depth of details about host cell responses to drug candidates. Morphological profiling techniques such as Cell Painting provide the possibility to assess the in-depth features of host cells. In **Paper III** we aimed to apply the Cell Painting protocol to identify virus-induced cellular phenotypes that could be leveraged for drug screening, repurposing as well as to profile host cell responses to viral infections.

The above-described objectives are addressed in the constituent thesis papers by answering following research questions:

Paper I

- Can antibody-based detection of HAZV-infected cells be leveraged for automated high-throughput phenotypic antiviral screening capturing the whole virus replication cycle?
- Does the in-house small-molecule compounds designed to target 8-oxoguanine DNA glycosylase (OGG1) possess antiviral activity against HAZV?
- Does the series of compounds efficiently inhibit a broad range of emerging viral pathogens, namely EBOV, CCHFV and SARS-CoV-2?
- What is the therapeutic window of the compound screening hits TH3289 and TH6744 in HAZV-infected human cells?
- Does depletion of OGG1 expression by RNAi in human cells phenocopy the antiviral effect by the compounds?
- What are the molecular target pathways of the small-molecule antiviral compound TH6744?

Paper II

- Can the high-throughput phenotypic screening assay be transferred to ZIKV-infected cells?
- Does the structural analogs of TH3289 exhibit antiviral activity against ZIKV in human glioblastoma cells and how does it compare to their activity against HAZV?
- What is the therapeutic window of the screening hit compounds in ZIKV-infected human cells compared to the reference drug Ribavirin?
- Can TH6744 rescue ZIKV-induced cytopathic effects in human glioblastoma cells?
- Can 3D cerebral brain organoids originating from induced pluripotent stem cells support ZIKV infection and progeny production?
- Does ZIKV infection induce cell death in the brain organoids and if so, does antiviral compounds TH6744 and TH5487 rescue or enhance the virus-induced toxicity?
- Does TH6744 and TH5487 entail antiviral activity against ZIKV in the brain organoid model?
- At which ZIKV replication cycle steps TH6744 exhibits the antiviral activity in comparison to Ribavirin with characterized MoA?

Paper III

- Can Cell Painting protocol be combined with virus-specific antibody staining?
- Does CoV-229E infection induce measurable morphological changes in human lung fibroblast cells?
- Which phenotypic features have the largest differences between CoV-229E and non-infected cells?

- Can CoV-229E-infected and non-infected cells be distinguished solely based on the Cell Painting morphological features while excluding information from the virus-specific antibody staining?
- Does the novel Cell Painting workflow identify antiviral compounds based on the morphological profiles from cells treated with +/- CoV-229E and +/- antiviral drug?

2.2 RESEARCH APPROACH

The approaches to address the doctoral thesis objectives were multidisciplinary and comprised of various molecular and cell biology, virology, proteomics and image-based methodologies, including the image-based phenotypic assay as a key method in all publications.

Generally, addressing the research questions were initiated by employing an image-based phenotypic antiviral screening of small-molecule compound library from the Helleday Laboratory. The image-based assay was thereby adapted to several small-scale assays to characterize the screening hits across virus families in two dimensional (2D) and 3D cell models and also combined with Cell Painting workflow for unbiased morphological profiling of virus infected and compound-treated cells. The antiviral activity of screening hit compound was related to cellular target pathways by cell-based target engagement assays.

The outline of the research approach:

1. Evaluating the antiviral spectrum of novel in-house and previously characterized compounds
    a. Investigate HAZV and ZIKV infectivity and cell proliferation after treatment with in-house compounds by high-throughput phenotypic screening assay (Paper I and II; see chapter “Key Methodology”)
    b. Evaluate the screening hit compound activity against several emerging RNA viruses such as EBOV, CCHFV and SARS-CoV-2 (Paper I)
    c. Explore morphological features of infected and compound-treated cells by Cell Painting phenomics workflow (Paper III)
    d. Confirm the antiviral activity and cell proliferation after the treatment with screening hit and selected reference compounds by dose-response regime (Paper I and II)
    e. Unravel the antiviral MoA during ZIKV replication cycle by time-of-addition, infection kinetics and viral budding assays (Paper II)
    f. Establish 3D organoids as an antiviral model for ZIKV by quantifying the progeny virus release by the image-based assay and analyzing organoid viability
2. Study the role of OGG1 (originally intended target of the screening hit compounds) mediating the antiviral activity of screening hits
    a. RNAi-mediated depletion of OGG1 in cells to investigate the effects on HAZV infection (Paper I)
    b. Correlate antiviral screening data to *in vitro* OGG1 activity (Paper I)

3. Monitor TH6744 cellular target pathways (Paper I)
    a. Analysis of screening hit TH6744 cellular target engagement by monitoring protein-compound interactions on a proteome scale by two alternative TPP's (see chapter "Key Methodology")
    b. Determine the most enriched cellular pathways and gene ontology (GO) term clusters from TPP analysis by gene set enrichment analysis
    c. Validation of target engagement by CETSA
    d. Validation of virus and host protein-protein interaction by co-immunoprecipitation (co-IP)

2.3 KEY METHODOLOGY

2.3.1 Image-based phenotypic antiviral assay

2.3.1.1 General protocol

The image-based phenotypic antiviral assay was easily adjusted to high-throughput screening as well as to small scale follow-up validation studies. Some differences occurred in the detailed protocol of high- and low-throughput assay set-up, as well as ZIKV and HAZV screens, but two assay steps were generally constant: 1) measuring infected cells during compound treatment and 2) quantifying virus progeny release by re-infecting new cells with the supernatant.

In the high-throughput antiviral screening using HAZV, prior the work with cells and infectious material, compounds were dispersed in 384-well assay plates at the final concentration of 10 µM with final dimethylsulfoxide (DMSO) concentration being maximum 0.1% and plates were stored at 4 °C. At the beginning of the screening cascade, SW13 cells were inoculated with HAZV at multiplicity of infection (MOI) 10 on cell culture flasks in presence of 10% fetal bovine serum (FBS) and 1% penicillin-streptomycin (PS) for 1 h. Cells without virus inoculation served as the non-infected control. Virus-containing inoculum was removed, cells were washed with phosphate buffered saline (PBS) and harvested by trypsinization. Infected and non-infected cells were thereby seeded on the 384-multiwell plates containing the compound library at the density of 3000 cells/well in 30 µL culture medium. Cells and viruses were allowed to replicate during 24 h. Supernatants were collected, and infected cells were then fixed in 4% paraformaldehyde (PFA) for 20 min and subsequently in methanol-acetone (1:1) solution at -20 °C for additional 20 min.

In the ZIKV screen and follow-up hit validation studies such as dose-response treatment or viral kinetics, cells were seeded on the 96-well plates one day prior the experiment (**Figure 8**). Cells were thereby inoculated with virus (ZIKV or HAZV) in 50 µL culture medium for 1 hour. Compounds were pre-diluted on a separate multi-well plate reaching desired final concentration and added on top of the cells. Cells and viruses were allowed to replicate between 24-72 h, depending on the scientific question. Supernatants were collected, and infected cells

were then fixed in 4% PFA for 20 min and subsequently in methanol-acetone (1:1) solution at -20 °C for additional 20 min.

To quantify virus progeny release, new cells were seeded on multi-well plates and were infected with supernatants from the primary infection screen for 24 h (**Figure 8**). Cells were thereby fixed in 4% PFA for 20 min and subsequently in methanol-acetone (1:1) solution at -20 °C for additional 20 min.

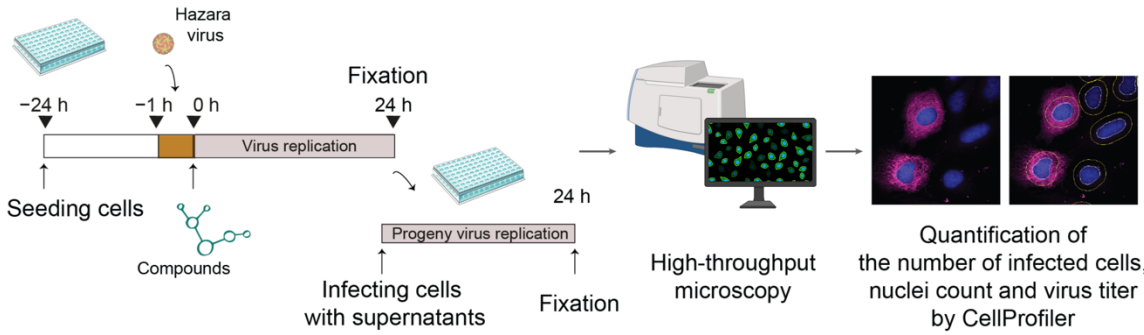

Figure 8. Schematic overview of the antiviral phenotypic assay. Cells are seeded on multi-well plates, inoculated with virus for 1 h and incubated with compounds generally for 24-72 h. Supernatant containing progeny virus is collected and added on new cells to measure progeny production. Both assay plates from infected cells and progeny measurement are fixed, stained for virus-specific antibody and DAPI. Images are captured by high-throughput microscope and analyzed automatically by CellProfiler software.

Immunostaining, image acquisition and analysis was similar in both primary infection and progeny virus evaluation. Infected cells and non-infected controls were incubated with primary virus-specific antibody, either ZIKV Non-structural protein 1 (NS-1; ab218546, Abcam) or HAZV Nucleoprotein (NP; produced in-house), overnight at 4 °C. Primary antibody was removed, cells were washed 3 times for 10 min with PBS and incubated with secondary antibody coupled to fluorophore and 4′,6-diamidino-2-phenylindole (DAPI) for 1 h at room-temperature. Secondary antibody solution was removed, and cells were washed 3 times for 10 min with PBS.

ImageXpress Micro XLS high-throughput analysis system from Molecular Devices was used to automatically acquire images in two fluorescent channels using ×10 Plan Fluor 0.3 NA objective. Subsequent image analysis was carried out by open-access software CellProfiler[192]. In brief, CellProfiler pipeline begun by identifying individual cells based on the DAPI signal intensity threshold between foreground and background. Identified objects were named primary objects. Secondary objects were identified by expanding the nucleus area by 15 pixels and measuring intensity in the virus antibody staining channel. Such secondary object classification by nuclei expansion is possible for viruses with perinuclear staining. Finally, cells were classified within two custom-defined bins based on the virus antibody staining intensity, infected or non-infected. Assay quality was evaluated by Z-factor[236] where uninfected DMSO-treated cells were negative control and infected DMSO-treated cells were positive control.

2.3.1.2 Issues and limitations

Even though this assay provides phenotypic evaluation and quantification of infected cells without prior knowledge of the virus, current assay design comes with certain limitations. The foremost, the assay robustness heavily relies on the accessibility of specific, high-affinity and high-quality antibody towards the viral protein(s). Upon emergence of a new and unforeseen virus, obtaining specific tools may take months to be readily available for use. Additionally, the assay set-up requires access to high-throughput microscope.

2.3.2 CETSA and Thermal Proteome Profiling

2.3.2.1 General protocol

The key steps in CETSA and TPP methodologies include 1) heating cell samples in the presence and absence of compound treatment to thermally denature proteins that are not stabilized by the compound and 2) separation of the soluble fraction containing native folded proteins from the insoluble fraction containing denatured proteins by centrifugation.

The simplest version of this method monitors target engagement across a range of temperatures at a single compound concentration, named temperature range CETSA (CETSA-TR)[212] and temperature range TPP (TPP-TR)[215]. As a follow-up, compound affinity and potency towards the target protein can be evaluated by isothermal dose-response experiment, called ITDR-CETSA[212]. In 2D-TPP, concentration- and temperature-dependent measurements are combined in a comprehensive assay[218]. In current study, CETSA-TR and ITDR-CETSA were performed during the optimization of TPP assay conditions to find suitable conditions for compound treatment concentration, duration and validate compound uptake into cells, and to validate findings from TPP experiment by western blot.

The TPP-TR was performed in living SW13 cells, infected with HAZV for 16 h and subsequently treated with 20 µM TH6744 or DMSO for 4 hours (**Figure 9**). This experimental design ensured active virus replication at the time of compound treatment. Upon compound treatment, cells were harvested and re-suspended in PBS supplemented with the respective treatment to maintain drug-target interactions throughout the cell harvesting process. Cells from both treatment conditions were divided in ten aliquots in polymerase chain reaction (PCR) tubes and each aliquot was heated at a given temperature (37, 41, 44, 47, 50, 53, 56, 59, 63 or 67 °C) for 3 minutes followed by 3-minute cooling step at room temperature using a gradient PCR machine. Following snap-freezing step of cell samples in dry-ice in absolute ethanol and the subsequent freeze-thaw cycles initiated rapid cell lysis (**Figure 9**). Then, cell lysates were clarified by centrifugation at 20'000 ×g for 40 minutes to separate the soluble and insoluble fractions. The soluble fraction was thereby transferred to new PCR tubes, supplemented with 0.1% sodium dodecyl sulfate (SDS) for virus inactivation and processed for liquid chromatography tandem mass spectrometry (LC-MS/MS) sample preparation. CETSA-TR protocol followed the same principles, but the resulting soluble fraction was analyzed by western blot using antibodies specific for OGG1 and HSP70. Highly thermostable superoxide dismutase 1 (SOD1) detection was used as a protein loading control in western blot.

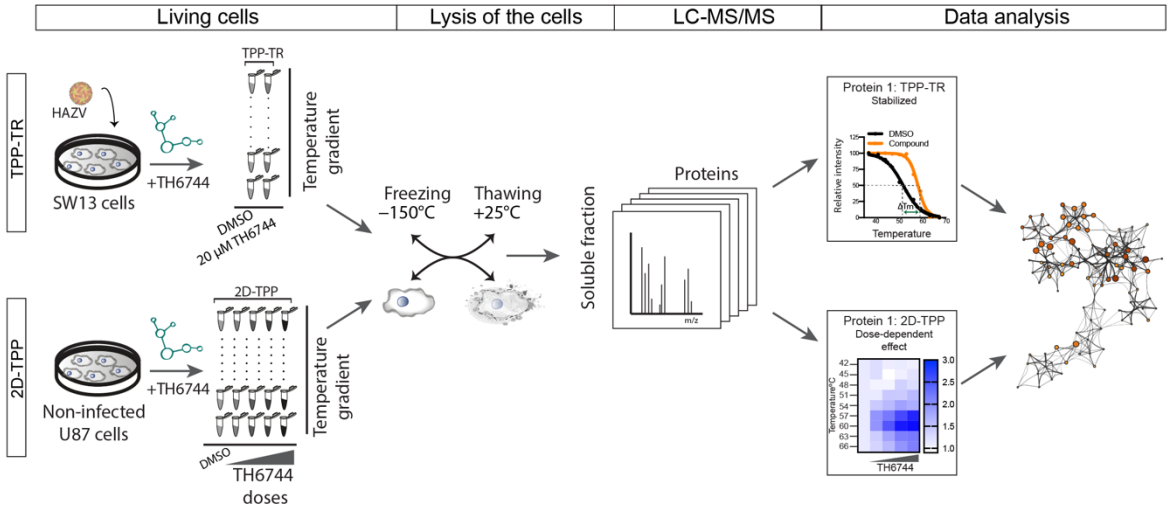

Figure 9. Similarities and differences in the TPP-TR and 2D-TPP workflow. TPP-TR experiment was carried out in SW13 cells infected with HAZV. Cells were infected with HAZV for 16 h and treated with 20 µM TH6744 or DMSO for 4 h. Cells were harvested, aliquoted and subjected to gradient heat treatment. Cells were lysed by freeze-thaw cycles and soluble fraction was analyzed by LC-MS/MS. Data analysis yielded melt curves from DMSO- and TH6744-treatment for individual proteins across the proteome. 2D-TPP experiment was performed in uninfected U87 cells. Cells were treated with DMSO, 1 µM, 3 µM, 10 µM or 30 µM TH6744 for 1.5 h. Cells were harvested, aliquoted and subjected to gradient heat treatment, thereby resulting in dose- and temperature gradient. Cells were lysed by freeze-thaw cycles and soluble fraction was analyzed by LC-MS/MS. Data analysis yielded heat maps with TH6744 dose on the X-axis and temperature on the Y-axis for individual proteins across the proteome. Protein-protein interactions and pathway enrichments were studied on the overlapping significant hits of TPP-TR and 2D-TPP analyses.

Experimental details of the 2D-TPP followed similar steps as described above, but 2D-TPP was performed in uninfected U87 cells due to the change of main model system in the project and our focus on the host targets. In fact, we perceived the change of cell line as a strength to validate TPP-TR findings in another model cell system. Additionally, compared to TPP-TR, 2D-TPP-specific differences occurred in the dose-response compound treatment step including 1 µM, 3 µM, 10 µM and 30 µM TH6744 concentrations (**Figure 9**). Cells were harvested in PBS supplemented with DMSO or compound as previously described, but aliquoted in nine PCR tubes and subjected to nine different temperatures (42, 45, 48, 51, 54, 57, 60, 63 or 67 °C). Again, cells were freeze-thawed, soluble fraction was separated from the insoluble by centrifugation and the soluble fraction was processed further for LC-MS/MS analysis.

2.3.2.2 Issues and limitations

One of the drawbacks of the TPP methodology is the limited detection of membrane-bound proteins, because the assay separates and discards the insoluble fraction containing membrane proteins. Efforts have been made to modify the protocols by introducing mild detergents at the cell lysis step which facilitate investigating target engagement of the chromatin- or membrane-bound proteins.

Additionally, TPP in living cells do not distinguish between direct drug target and the downstream effects on cellular pathways that represent the secondary responses. TPP study in

cell lysates would capture compound direct targets and the comparison with live cell TPP results would thereby distinguish the downstream responses.

2.3.3 Biosafety and ethical considerations

The doctoral thesis involves work with pathogens of risk class 2 (HAZV, ZIKV and CoV-229E), risk class 3 (SARS-CoV-2) and risk class 4 (EBOV and CCHFV). The Public Health Agency of Sweden and Karolinska Institutet have all required approvals for working safely with pathogens involved in current doctoral thesis. I, Marianna Tampere have obtained an extensive training to work safely with ZIKV in BSL-2 laboratories of Public Health Agency organized by Prof. Mirazimi, with HAZV and CoV-229E in SciLifeLab premises organized by Dr. Puumalainen and with SARS-CoV-2 in BSL-3 Core Facility in Biomedicum, Karolinska Institutet. Laboratory work involving EBOV and CCHFV was performed by experienced members of Prof. Mirazimi group.

The human cerebral organoid experiments in Paper II are performed in accordance with the ethical permits.

2.4 SUMMARY OF RESEARCH PAPERS

2.4.1 Paper I: Novel Broad-Spectrum Antiviral Inhibitors Targeting Host Factors Essential for Replication of Pathogenic RNA Viruses

The large number of host factors and signaling pathways associated to virus infections as well as how different viruses hijack similar cellular pathways for their advantage prompted us to explore the antiviral potential of our in-house small-molecule library targeting cellular oxidative stress and nucleotide metabolism pathways. In this study, we report a broad-spectrum activity of a novel series of compounds with promising therapeutic window on cell models. We declare the antiviral activity independent from the compound's original intended target OGG1 and describe host chaperone/co-chaperone network members as putative antiviral targets.

First, we established an image-based phenotypic assay to screen the library of 425 in-house developed small molecule compounds targeting cellular oxidative stress and nucleotide metabolism pathways. The assay evaluates the HAZV viral infectivity and SW13 cellular toxicity based on high-throughput image acquisition followed by automated image analysis pipeline using CellProfiler and KNIME software. Importantly, the compound treatments were scheduled at post-inoculation step to investigate the therapeutic rather than prophylactic treatment possibilities. Among all screened compounds, 14 inhibited virus infectivity by 90% while showing viability higher than 80%, illustrating a hit rate of 3.3%. Next, we performed a follow-up screening on selected compounds with varying activity from the primary screening rounds aiming to identify compounds reducing the viral progeny release. We identified eight compounds reducing viral titer by 1-log-unit with negligible toxicity and selected two, TH3289 and TH6744 for further characterization based on their potency on progeny release (**Figure 10a**). Screening validation by dose-response treatments demonstrated TH6744 to have a wider

therapeutic window (**Figure 10b**) compared to TH3289 (**Figure 10c**) based on the half maximal effective concentration (EC_{50}) of antiviral and cell toxicity.

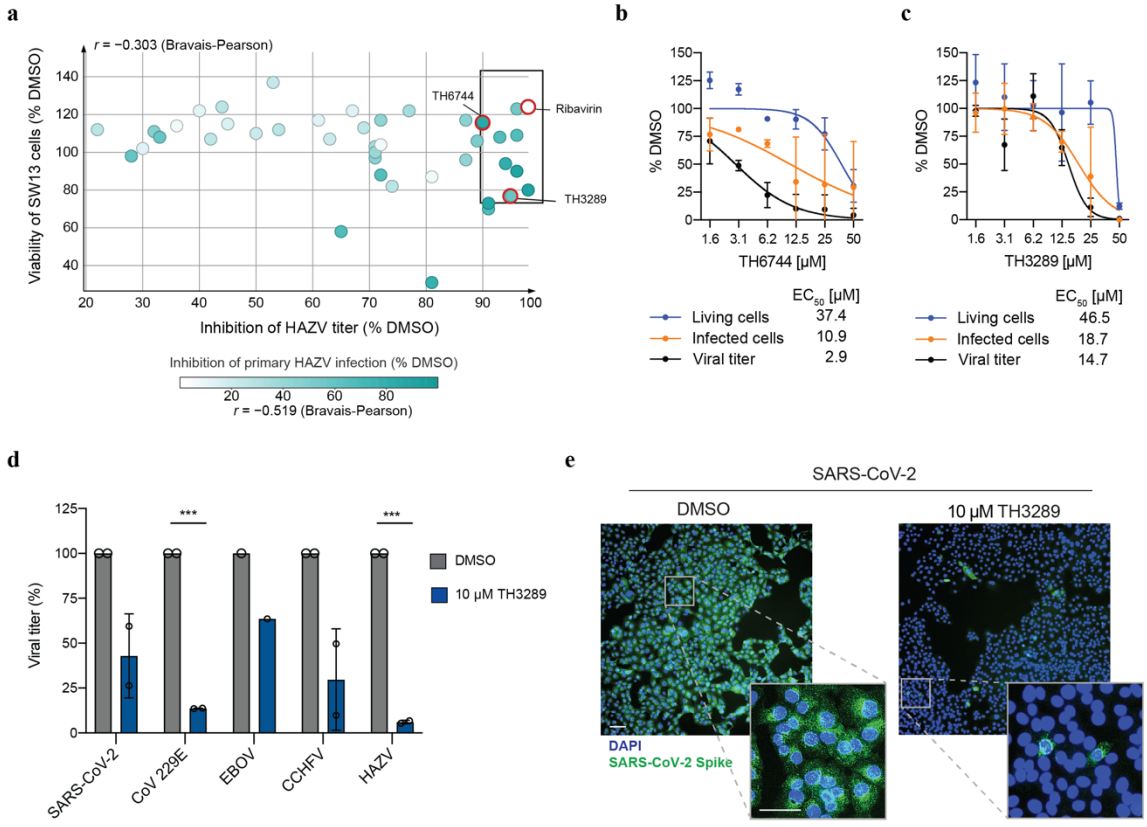

Figure 10. Discovery of a series of novel broad-spectrum antiviral compounds by image-based phenotypic screening using HAZV as a model virus. a) SW13 cells were treated with compounds at 10 µM dose for 24 h and virus-containing supernatant was added on new Vero cells. Virus titer was evaluated by endpoint dilution assay. Cell viability was evaluated based on nuclei count and HAZV titer based on HAZV NP antibody staining by automated image analysis. b,c) SW13 cells were infected with HAZV (MOI 1) and treated with increasing TH6744 or TH3289 doses. Cell viability was evaluated based on nuclei count (in blue), infected cells by HAZV NP antibody staining (in orange) and viral titer by endpoint dilution assay (in black). Data is presented as mean ± SD from n=2 independent experiments. d) Vero E6 cells were infected with SARS-CoV-2 (MOI 0.05), Huh7 cells were infected with CoV-229E (MOI 5), Vero cells were infected with EBOV (MOI 0.5), CCHFV (MOI 1) and SW13 cells were infected with HAZV (MOI 1). Cells were incubated with virus and 10 µM TH3289 treatment for 24 h (SARS-CoV-2, CoV-229E, HAZV) or 48 h (EBOV, CCHFV). Endpoint dilution assay was performed on Vero E6 (SARS-CoV-2), Vero (EBOV, CCHFV, HAZV) or Huh7 (CoV-229E) cells. Data is presented as mean ± SD from n=2 (SARS-CoV-2, CoV-229E, CCHFV, HAZV) or n=1 (EBOV) independent experiments. e) Representative images of Vero E6 cells infected with SARS-CoV-2 and treated with DMSO or 10 µM TH3289 from d. DAPI in blue, SARS-CoV-2 Spike protein in green.

To investigate whether the compounds display activity against viruses from different families, we tested TH3289 and TH6744 activity on various RNA viruses. Both TH3289 and TH6744 were tested against CoV-229E, while only TH3289 was tested against SARS-CoV-2, EBOV and CCHFV, due to limited resources in the high-containment laboratories. Both compounds potently reduced CoV-229E titer, and TH3289 exhibited around 50%, 40% and 70% activity against SARS-CoV-2, EBOV and CCHFV, respectively, illustrating broad antiviral activity across virus families (**Figure 10d, e**).

Given that TH3289 and TH6744 belong to a series of compounds designed to target human OGG1, we next investigated OGG1 role in HAZV infection. OGG1 is a DNA base excision repair enzyme responsible for detecting and removing 8-oxo-guanine damage in the DNA[237–239]. Compounds from the primary screening were evaluated by *in vitro* OGG1 activity assay and correlated to the inhibition of HAZV infection. No correlation between HAZV inhibition and OGG1 activity was observed (**Figure 11a**). Furthermore, we depleted OGG1 by small interfering RNA (siRNA)-mediated approach by using either individual or pooled siRNA sequences. After confirming complete OGG1 protein depletion by western blot, we did not observe any reduction of HAZV infectivity or progeny release upon OGG1 depletion (**Figure 11b, c**), suggesting that OGG1 is dispensable for HAZV and does not mediate the antiviral activity of TH6744 and TH3289.

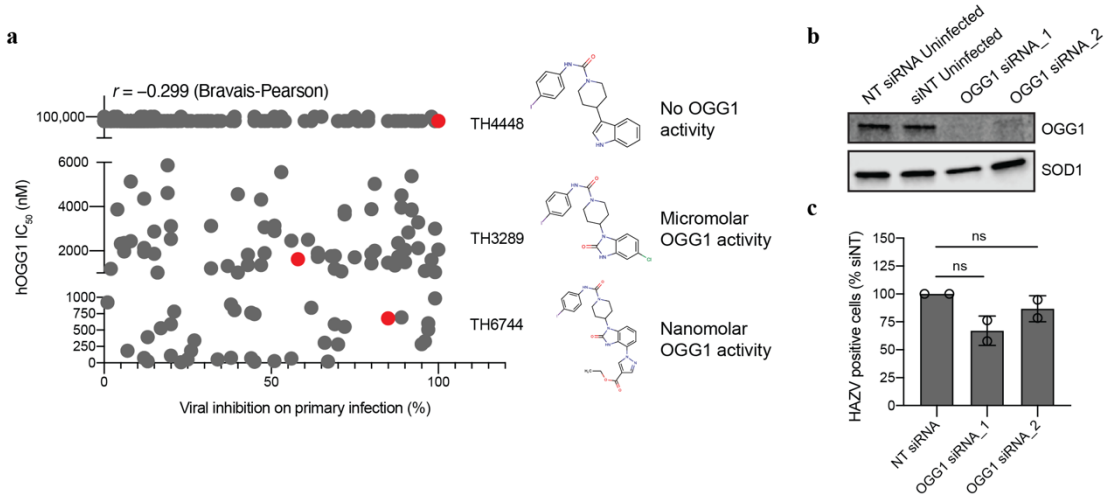

Figure 11. OGG1 inhibition and depletion does not impair HAZV replication. a) Correlation between compounds' effect on *in vitro* OGG1 activity and antiviral activity on HAZV infection. b) Representative image of OGG1 depletion by two individual siRNA sequences. NT – non-targeting siRNA sequence. c) U2OS were reverse transfected with individual siRNA sequences targeting OGG1 mRNA for 48 h. Cells were thereby infected with HAZV for 24 h. Percentage of HAZV positive cells was determined by image-based antiviral assay. Data is expressed as mean ± SD from n=2 independent experiments.

Next, we decided to determine the cellular target proteins and pathways of TH6744 by implementing a proteome-wide target identification technique TPP. We performed two complementary TPP approaches and monitored changes in protein thermal stability, which directly indicates drug-target interactions. TPP-TR was performed in HAZV-infected SW13 cells across a wide temperature range at a single TH6744 concentration and identified regulators of protein folding and mitochondrial matrix as enriched GO terms. Moreover, top hits of TPP-TR included DNAJ homolog subfamily B member 11 (DNAJB11), ER degradation-enhancing alpha-mannosidase-like protein 3 (EDEM3) and DNAJ homolog subfamily C member 3 (DNAJC3), all involved in protein chaperone and co-chaperone networks. We then performed more comprehensive 2D-TPP in uninfected human glioblastoma U87 cells at increasing TH6744 concentrations and identified 220 proteins that were interacting dose-dependently with TH6744. Majority of the 220 proteins were annotated as nucleotide binding, ER-residents or chaperones according to Uniprot annotations. Studying the significant

target candidates from TPP-TR and 2D-TPP revealed 79 common proteins among which a large fraction was involved in chaperone-mediated protein folding, ER unfolded protein response and ER lumen processes (**Figure 12a**). Thus, based on the thermal stability changes we concluded that TH6744 affects multiple components of host chaperone network and may exhibit a multifactorial MoA.

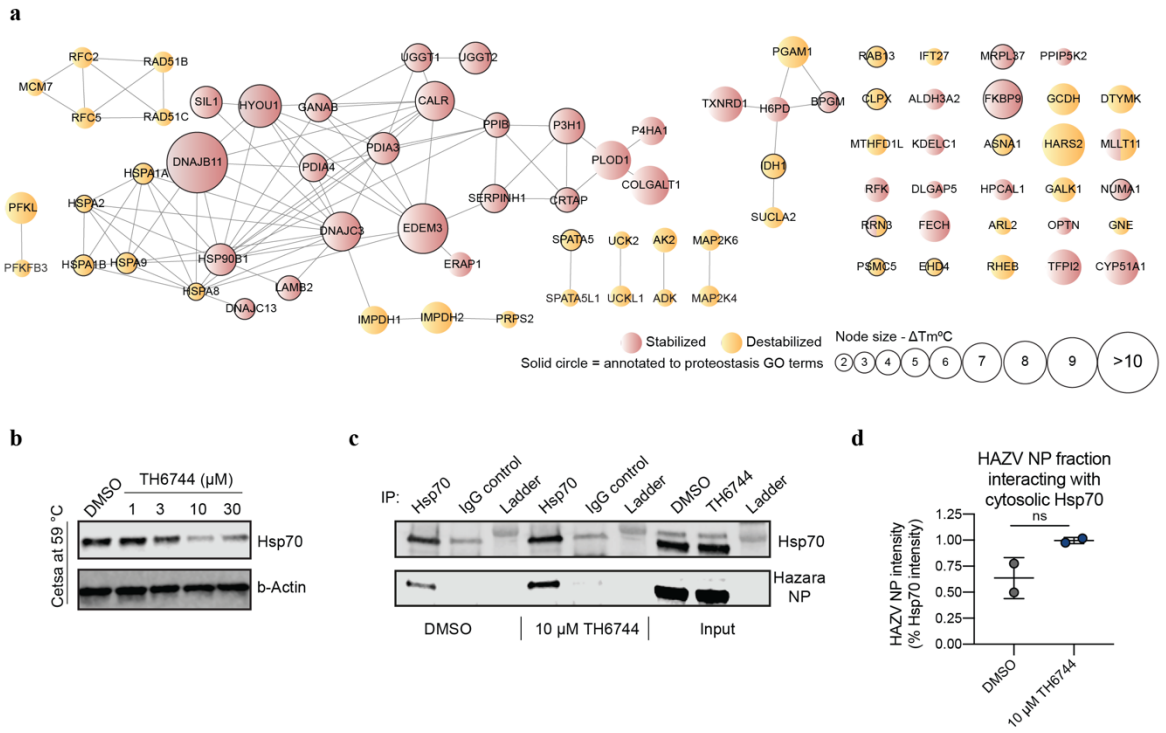

Figure 12. Treatment with TH6744 influences thermal stability and protein-protein interactions of the host chaperone and co-chaperone network. a) Network of validated and predicted protein-protein interactions between 79 overlapping hits from TPP-TR and 2D-TPP analysis. Network was created by STRING database and Cytoscape tool. Nodes represent proteins, lines represent predicted or experimentally proven interactions between proteins, node diameter represents the ΔTm between DMSO and TH6744 treatment and node color represents stabilization (red) or destabilization (yellow) in TPP-TR experiment. b) ITDR-CETSA upon 1 µM, 3 µM, 10 µM and 30 µM TH6744 treatment at 59 °C in U87 cells. c) Immunoprecipitation of endogenous HSP70 in HAZV-infected Hek293T cells. Cells were infected with HAZV (MOI 1) for 24 h, treated with 20 µM TH6744 for 1 h and processed for co-IP. Data is representative of n=2 independent experiments. d) Quantification of HAZV NP signal from c. HAZV NP signal is relative to HSP70 signal.

Viruses are critically dependent on complex cellular processes[108], including protein folding machineries to meet the high demand accompanied with viral protein production. Chaperones and co-chaperones of the cellular heat shock protein network has been described to orchestrate distinct steps in DENV and ZIKV life cycle[145,240] and chaperones HSP70 and GRP78 have been characterized as antiviral targets[145,240,241]. We thereby chose to further investigate HSP70 role within TH6744 antiviral activity and validated HSP70 thermal destabilization by CETSA in U87 cell lines (**Figure 12b**). Moreover, we detected protein-protein interaction between HAZV NP and HSP70 by co-IP (**Figure 12c**). Interestingly, the interaction between HSP70 and HAZV NP increased 2-fold during TH6744 treatment (**Figure 12c, d**). Therefore, TH6744 appears to destabilize HSP70 protein and modify the interaction with HAZV NP.

Altogether, this work characterized a series of novel antiviral compounds and their putative cellular targets from the host chaperone pathways. Additionally, the development of the phenotypic antiviral assay and complementing with target identification provides a novel framework to identify novel antiviral compounds, their cellular targets but also discovery novel viral dependency factors.

2.4.2 Paper II: Broadly Active Antiviral Compounds Disturb Zika Virus Progeny Release Rescuing Virus-Induced Toxicity in Brain Organoids

In **Paper I** we screened a new class of compounds with antiviral activity against HAZV and in **Paper II** we aimed to screen against ZIKV due to its emergence during 2016, implement more advanced infection models and investigate the antiviral mode of action on the virus replication cycle. Because of the ZIKV emergence during 2016, we ought to investigate the activity of our antiviral compounds against ZIKV and selected it as a model virus.

First, we transferred the image-based phenotypic assay to ZIKV-infected human glioblastoma U87 cells to screen the in-house structural analogs of TH3289. We selected 110 compounds and screened antiviral activity by quantifying viral infectivity, cellular toxicity and viral progeny production (**Figure 13a**). Seven compounds, including TH3289 and TH6744 reduced ZIKV progeny release >90% with limited or no cellular toxicity (>80%) (**Figure 13a**; highlighted box). Furthermore, we compared inhibition of ZIKV and HAZV progeny release and identified five hits with >90% activity on both viruses. Interestingly, all five compounds are structurally similar benzimidazolones, among which TH3289 and TH5264 as well as TH6744, TH6545 and TH8283T group together as very close structural analogs, forming two distinct groups. One to two members from both groups were selected for validation studies. Based on this data we concluded the robustness of the image-based assay and the broad-spectrum activity of this compound class against *Flaviviridae* family member.

Next, screening results were validated by dose-response treatments of TH3289, TH6744 and TH5264 on ZIKV-infected U87 (**Figure 13b-d**). Additionally, another in-house developed analog TH5487 was included due to its anti-inflammatory properties[235] (**Figure 13e**). As expected, antiviral activity and cellular toxicity EC_{50} of the selected compounds illustrated a wide therapeutic window comparable to positive control Ribavirin (**Figure 13f**). Additional toxicity studies on uninfected U87 and Vero cells of all four aforementioned compounds revealed TH6744 and TH5487 with the most favorable toxicity profile. Furthermore, we observed how ZIKV-infected U87 cells displayed a distinct CPE phenotype with rounded cells at 72 hours post infection (hpi), while uninfected cells had axon-like protrusions spreading outwards from the cell. Addition of TH6744 remarkably reversed this CPE phenotype in U87 and also Vero cells (**Figure 13g**).

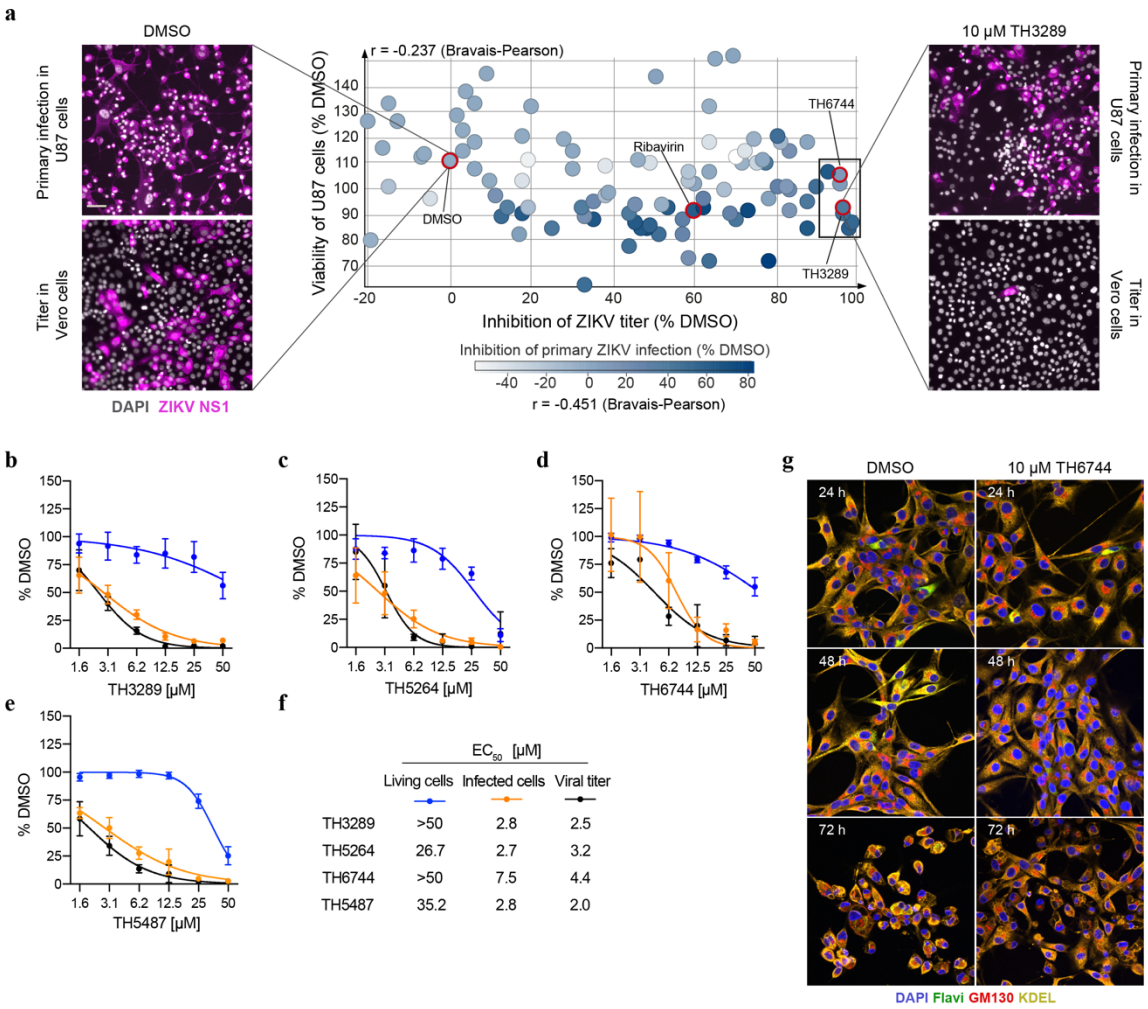

Figure 13. Phenotypic antiviral screening identifies the activity of TH3289 and TH6744 against ZIKV. a) U87 cells were infected with ZIKV (MOI 10) and treated with structural analogs of TH3289 at 10 µM concentration for 48 h. Infected cells were stained for DAPI and ZIKV NS1 and analyzed by high-throughput microscopy. Virus titers from supernatants were determined by endpoint dilution assay and inhibition of viral titer was calculated relative to DMSO. Data is presented as a mean of two technical replicates per compound. Representative images from ZIKV-infected U87 cells treated with DMSO or 10 µM TH3289 (upper image panels; scale bar equals 100 µm) and corresponding example of titrated ZIKV from the endpoint dilution assay (lower image panels). DAPI in grey, ZIKV NS1 in magenta. b-f) Evaluation of compound therapeutic window. U87 cells were infected with ZIKV (MOI 1) and treated with indicated doses of b) TH3289, c) TH5264, d) TH6744 or e) TH5487 for 48 h. Cell viability was evaluated based on nuclei count (in blue), infected cells by ZIKV NS1 staining (in orange) and ZIKV titer by endpoint dilution assay (in black). Data is presented as mean ± SD from n=3 independent experiments. f) Curve fitting was performed in GraphPad Prism to calculate EC_{50} values for living cells, infected cells and viral titer. g) U87 cells were infected with ZIKV (MOI 1) and treated with 10 µM TH6744 or DMSO for 24 h, 48 h or 72 h. Cells were stained for pan-flavivirus (in green), Golgi marker GM130 (in red), ER marker KDEL (in yellow) and DAPI (in blue). Scale bar equals 50 µm.

Encouraged by the phenotypic rescue and the therapeutic window, we next established an induced pluripotent stem (iPS) cell-derived 3D brain organoid model for ZIKV infection to narrow the large gap between cellular and *in vivo* studies in drug discovery. The brain organoids supported active ZIKV replication cycle measured by increasing ZIKV titers over time. Moreover, ZIKV infection reduced organoid viability by 10-50% depending on the time-point and virus dose and induced aberrant changes in organoid structure. Based on this data we concluded the organoids as excellent models to study ZIKV infection, in agreement with

findings from the literature[33,242,243]. Next, we assessed the activity of TH6744 and TH5487 on brain organoids in the presence or absence of ZIKV. Importantly, neither TH6744 nor TH5487 reduced the viability of uninfected organoids, but both compounds phenotypically rescued the organoid structure upon ZIKV infection (**Figure 14a**) and reduced ZIKV progeny production by 70-80% at 3-, 7- and 10-days post infection (dpi) (**Figure 14b**). Treatment with TH5487 increased the mean organoid viability by 35% compared to DMSO-treated ZIKV-infected organoids. Moreover, TH6744 treatment remarkably reduced the the intensity of ZIKV NS-1 staining on cryo-sectioned organoids (**Figure 14c, d**). Collectively, these findings support a strong proof-of-concept of the antiviral activity of TH6744 and TH5487 in brain organoid model.

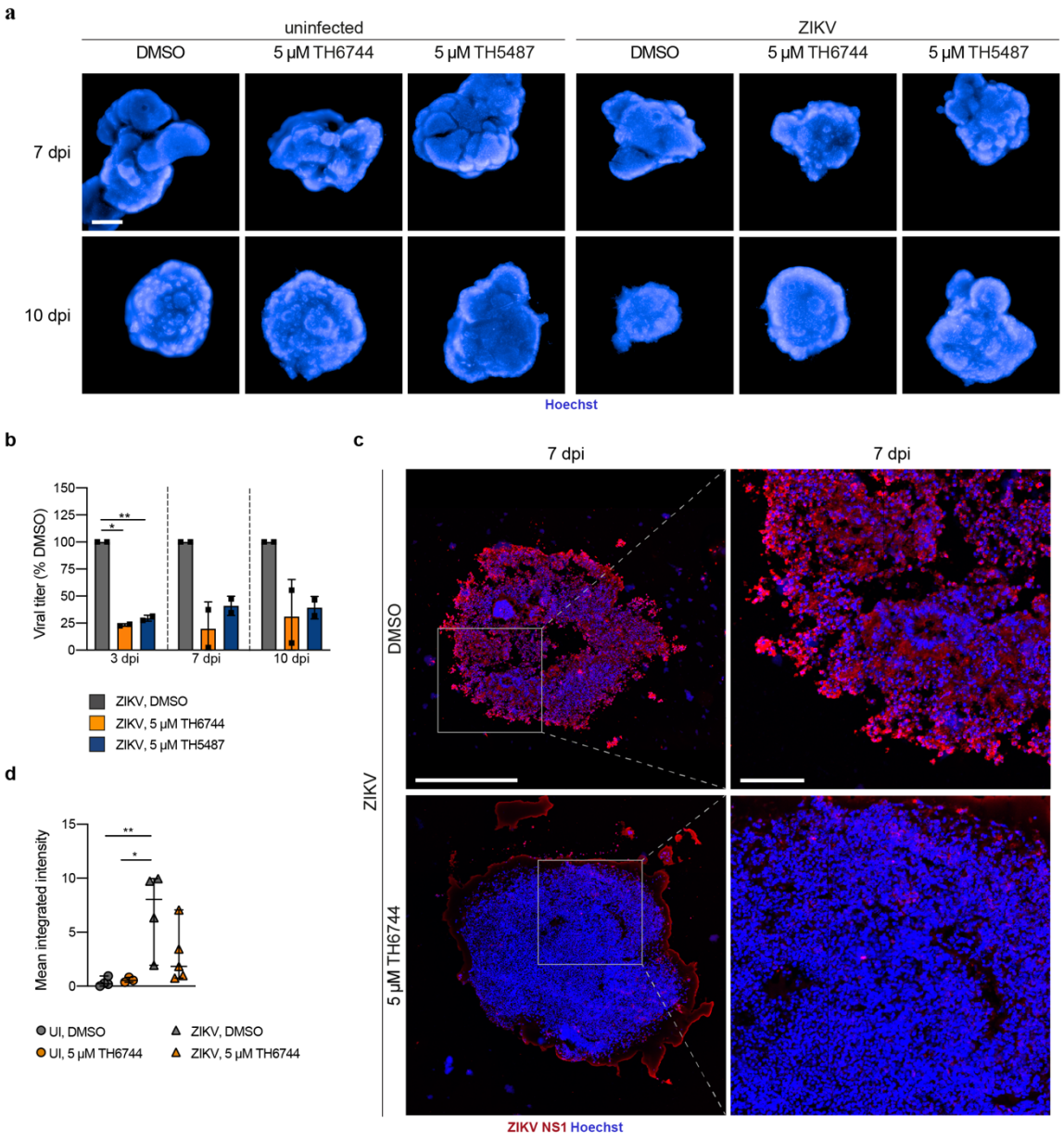

Figure 14. TH6744 and TH5487 treatment rescues ZIKV-induced cytotoxicity and reduces ZIKV progeny production in brain organoids. a-d) Brain organoids were infected with ZIKV (2×10^4 particles/organoid) for 24 h and treated with 5 µM TH6744, 5 µM TH5487 or DMSO. a) ZIKV-infected and uninfected non-sectioned brain organoids were stained with Hoechst and imaged by high-content confocal microscopy. Representative images of

n=2 independent experiments. Scale bar equals 500 µm. b) Viral titer from ZIKV-infected organoids treated with indicated compounds at indicated timepoints was evaluated by endpoint dilution assay. Viral titer is presented as relative to ZIKV-infected DMSO-treated control at respective timepoints. Data is presented as a mean ± SD from n=2 independent experiments. Statistical significance was determined using two-way ANOVA with Sidak's multiple comparison analysis. *$p < 0.05$, **$p < 0.01$. c) ZIKV-infected and treated organoids were cryosectioned, stained with Hoechst and ZIKV NS1 antibody and images were captured by confocal microscopy. Representative images of n=2 independent experiments. Scale bar equals 500 µm in the overview image and 100 µm in the close-up image. Hoechst is in blue and ZIKV NS1 in red. d) ZIKV NS1 staining intensity from c, was quantified by CellProfiler. Data is presented as mean ± SD from n=2 independent experiments. Statistical significance was determined using one-way ANOVA with Dunnett's multiple comparison analysis. *$p < 0.05$, **$p < 0.01$.

With our limited knowledge on the compounds' effect on the life cycle of studied viruses, we quantified the kinetics of ZIKV genome replication and progeny production and utilized time-of-addition approach to identify ZIKV replication cycle steps that remain most sensitive to TH6744 treatment in comparison to Ribavirin. We showed how TH6744 treatment decreases ZIKV progeny production and extracellular vRNA, but do not affect intracellular vRNA replication during 24 h. This was in contrast to Ribavirin treatment that clearly diminished intracellular vRNA levels, as expected. Furthermore, we demonstrated approximately 50% reduction in progeny production during viral entry and viral budding steps by a 2 h pulse treatment with TH6744 (**Figure 15a**). Intrigued by the rapid antiviral effect on ZIKV budding, we next quantified intracellular and extracellular infectious ZIKV virions upon 2 h treatment during budding and observed a reduction within both fractions inside and outside of the cells (**Figure 15b, c**). Based on this data, we concluded that TH6744 targets ZIKV replication cycle during viral entry and especially rapidly after vRNA replication during later in the life cycle.

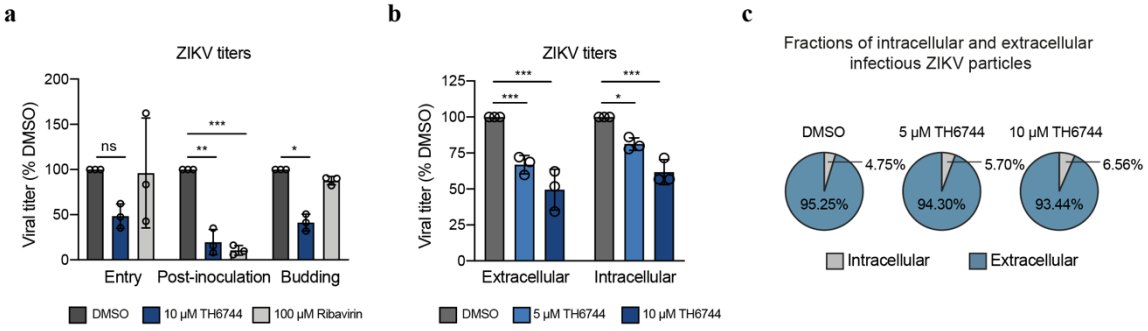

Figure 15. TH6744 treatment rapidly reduces ZIKV progeny release and is distinct from Ribavirin MoA. a) U87 cells are treated with indicated compounds during ZIKV entry, budding or during the whole replication cycle (post-inoculation). ZIKV titer was quantified by endpoint dilution assay. b) U87 cells were infected with ZIKV (MOI 10) for 24 h and treated with indicated compounds for 2 h. Intracellular infectious particles were harvested by mechanical cell lysis and extracellular particles were taken from the supernatant. ZIKV titer was quantified by endpoint dilution assay. c) Average fractions of the intra- and extracellular infectious ZIKV particles relative to total ZIKV particles quantified in b. a-c) Data are expressed as mean ± SD from at least n=3 independent experiments. Statistical significance was determined using one-way ANOVA with Dunnett's multiple comparison analysis. *$p < 0.05$, **$p < 0.01$, *** $p < 0.001$.

Overall, we demonstrated how our phenotypic image-based assay can successfully be transferred from HAZV to ZIKV and further confirmed the broad activity of TH6744 and its analogs. Moreover, we illustrated how the series of in-house compounds rescue ZIKV-induced

toxicity in 3D brain organoids and dampen ZIKV infection and progeny production. Finally, we linked TH6744 antiviral activity to the MoA at viral entry and especially at late viral replication cycle steps after vRNA replication.

2.4.3 Paper III: A phenomics approach for antiviral drug discovery

Encouraged by the robustness of our image-based phenotypic assay in HAZV and ZIKV infection models, in **Paper III** we additionally transferred the assay to human CoV-229E upon the emergence of COVID-19 pandemic. Thereafter, we aimed to combine the principles of our image-based phenotypic assay with unbiased morphological profiling to enable screening antiviral compounds, identification of infected cell properties as well as uncovering host responses to antiviral drug treatments.

Inspired by the recent advancements of morphological profiling methods such as the Cell Painting capturing in-depth quantitative information about cell morphology, rather than only providing the yes/no answer, we modified the original Cell Painting protocol and combined it with CoV-229E antibody-based staining. Precisely, we stained cells with fluorescent Cell Painting dyes such as Hoechst (stains for cell nuclei), SYTO 14 (nucleoli and cytoplasmic RNA), Concanavalin A (mannose residues of glycoproteins, predominantly in the ER), wheat germ agglutinin (plasma membrane and Golgi complex), phalloidin (F-actin) and the CoV-229E antibody in one single assay.

The staining protocol and high-content microscopy enabled us to detect seven individual subcellular organelles or compartments and compare their morphology in infected and non-infected cells on a single cell level. In fact, automated image analysis pipeline from the CellProfiler software segmented individual cells (**Figure 16a**) and extracted 1441 cellular features providing quantitative details about cell/organelle size, staining intensity, granularity, etc. Using this pipeline and clustering the cellular features, we detected distinct phenotypes between infected and non-infected MRC5 cells (**Figure 16b**). Moreover, by applying the principal component analysis (PCA) to reduce feature redundancy and ease the interpretation, we could clearly separate the infected population from the non-infected merely based on the cellular features and without antibody detection (**Figure 16c**).

Next, we explored the specific cellular features that contributed the most to the separation of the infected phenotype. A partial least-squares discriminant analysis (PLS-DA) model was used to identify feature classes linked to the infected cells. We detected ER staining by Concanavalin A and nucleoli and cytoplasmic RNA staining intensity by SYTO 14 as the features most prominently changed upon the infection. Interestingly, Concanavalin A intensity features were particularly discriminant in the nucleus compartment. In sum, the customized Cell Painting protocol and our analysis exemplified how phenomics profiling can specifically discern phenotypes of virus-infected cells.

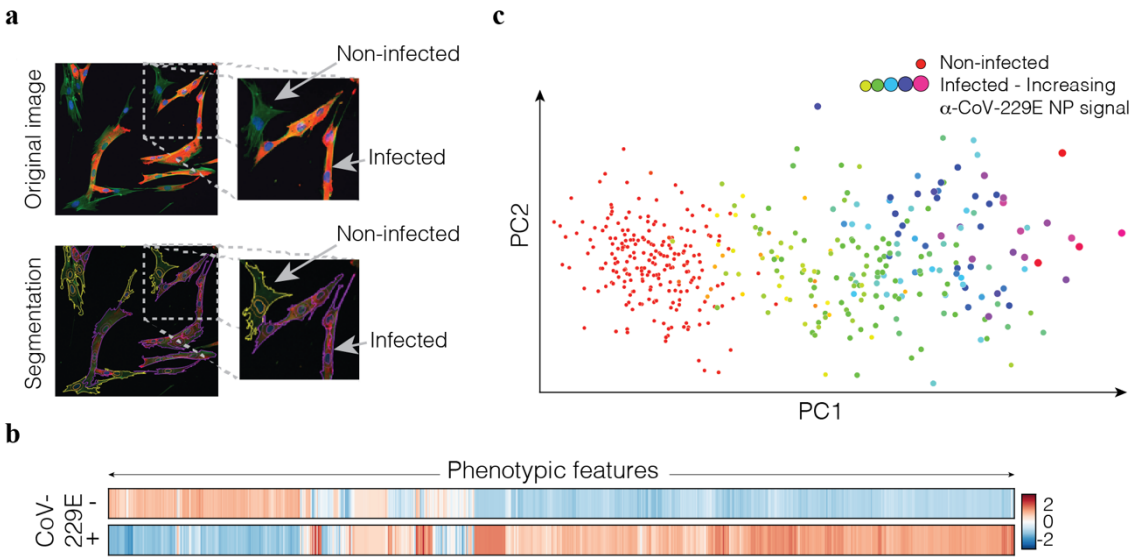

Figure 16. A modified Cell Painting protocol captures virus-specific morphological signatures. a) A representative composite image of infected cells with F-actin in green, nuclei in blue and anti-coronavirus NP antibody in red. Segmentation and classification of individual cells visualized with an outline with infected cells in purple and non-infected cells in yellow. b) Morphological profiles of non-infected and infected cells. c) Dimensionality reduction using PCA applied to the extracted Cell Profiler features per image, coloured according to their infected or non-infected classification based on NP-specific antibody staining.

Next, we aimed to apply our method for antiviral compound screening and therefore established a workflow including CoV-229E infection in MRC5 cells, compound treatment, Cell Painting and virus-specific antibody staining protocol, high-content imaging, automated image analysis and lastly, data analysis and visualization. The workflow enables capturing host cell morphological profiles upon virus-infection, compound treatment or both combined. To put our phenomics workflow to the test in a screening, we selected nine antiviral compounds including two targeting viral RdRp (Remdesivir and Favipiravir), four being host-directed antivirals (E64d, Camostat, Cathepsin L inhibitor and Bafilomycin A) and three novel broadly active antiviral compounds (TH3289, TH6744 and TH5487). All compounds were initially tested for their antiviral activity at three different concentrations using the phenotypic assay with same principles as described in **Paper I**. Evaluating cellular toxicity by nuclei count and antiviral activity by the virus-specific antibody staining, we observed potent antiviral activity with no cellular toxicity upon Remdesivir and E64d treatment, demonstrating wide therapeutic window (**Figure 17**). Treatment with TH3289, TH6744 and TH5487 showed narrow therapeutic window while Bafilomycin A treatment was cytotoxic (**Figure 17**). Neither clinically approved Favipiravir or pre-clinical compounds Camostat and Cathepsin L inhibitors had any antiviral activity at selected concentrations (**Figure 17**).

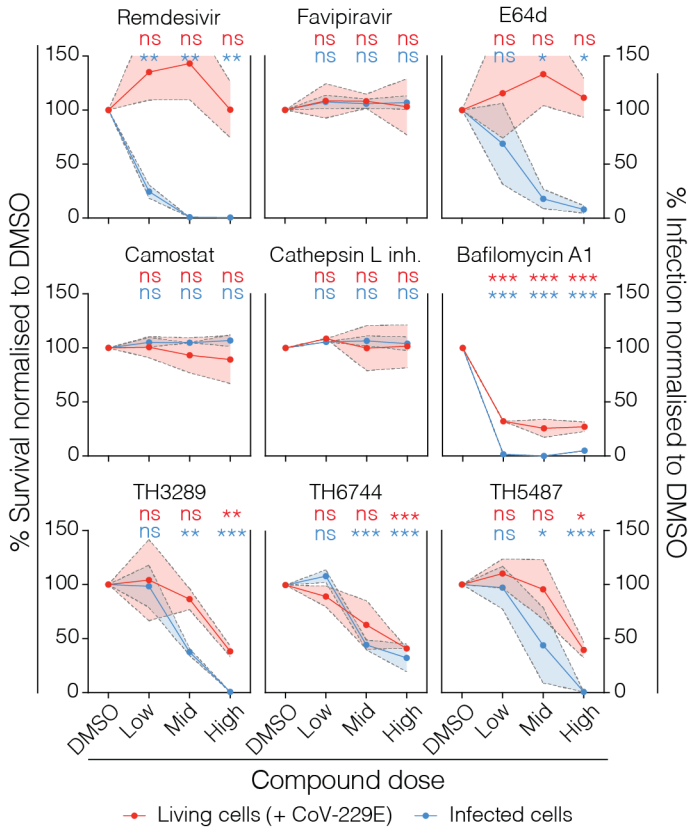

Figure 17. The effect of nine pre-selected compounds on antiviral activity and cellular survival. Percentage of survival (red) and percentage of infected cells (blue) normalized to DMSO (infected) control. Colored intervals indicate the standard deviation of two biological replicates. Two-way ANOVA was performed to assess the statistical significance of each condition (*p<0.05, **p<0.005, ***p<0.0005).

Finally, we selected treatment conditions with cellular survival over 80% and performed unsupervised hierarchical clustering on the morphological profiles. Clustering process mapped the similarities between morphological profiles and resulted in two main clusters including either effective or ineffective antiviral compounds (**Figure 18a**). The first cluster containing ineffective treatments such as Favipiravir, Camostat and Cathepsin L inhibitor also included infected DMSO-treated cells, confirming the lack of activity from the ineffective compounds by morphological profiling. The second larger cluster included conditions from infected and non-infected cells upon Remdesivir, E64d and the TH-compound treatments and additionally non-infected phenotypes from ineffective compounds (**Figure 18a**). Importantly, non-infected DMSO-treated condition also belong to the second cluster, illustrating a rescue of virus-induced phenotype by the effective compounds Remdesivir, E64d, TH3289, TH6744 and TH5487. In addition, the hierarchical clustering also provides information about the compound influence on the host cell in the absence of virus. For instance, structural analogs TH3289, TH6744 and TH5487 cluster closely together meaning they induce similar morphological changes to the host cell.

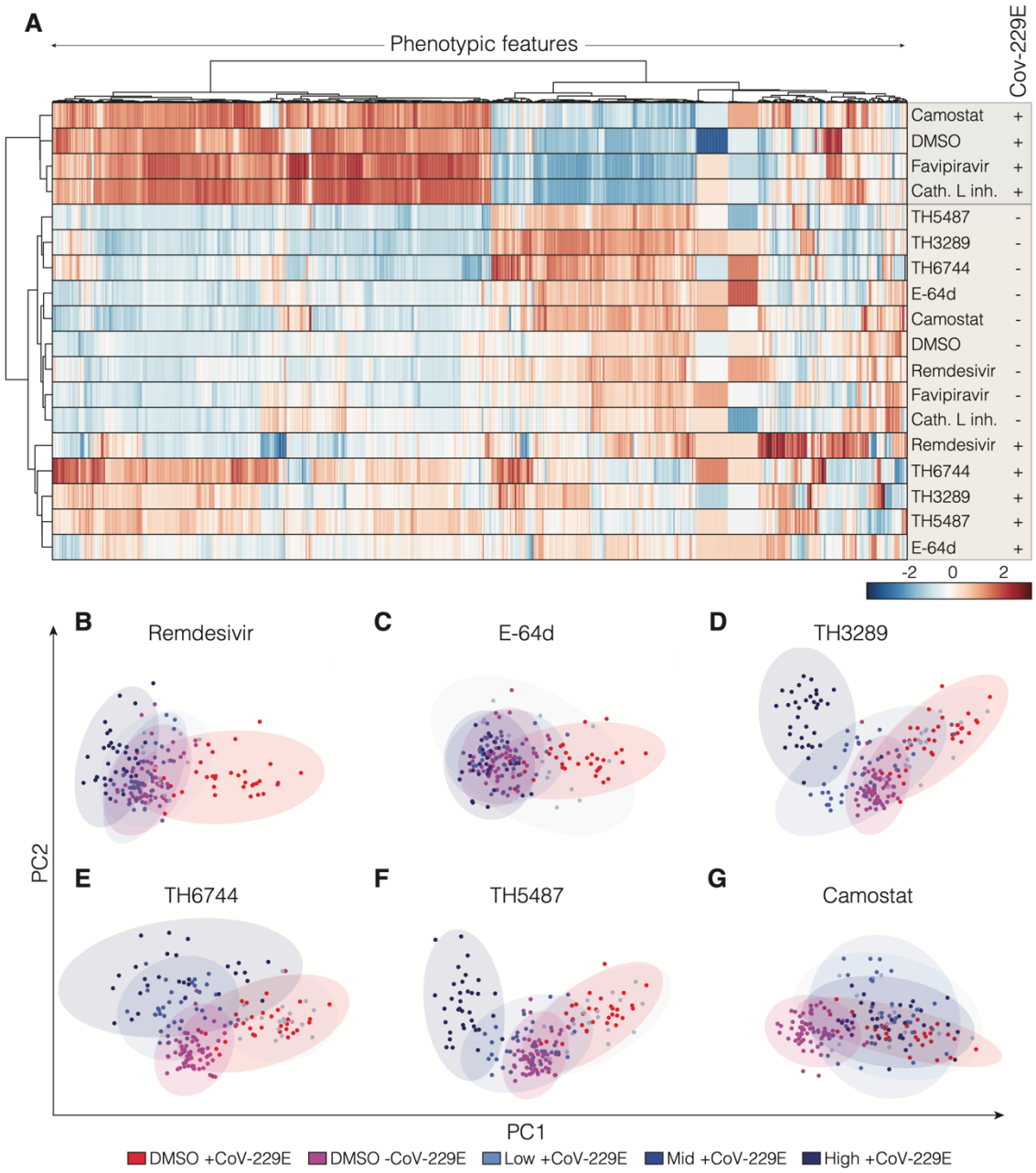

Figure 18. Identification of phenomics profiles of antiviral drugs efficient against CoV-229E. a) Unsupervised hierarchical clustering of morphological profiles of the indicated samples based on their proximity in feature space. Two main groups are shown, non-infected (-CoV-229E) and infected (+CoV-229E), in the presence or absence of Remdesivir, E-64d, TH6477, Camostat or DMSO (vehicle) at the indicated concentrations. b-g) PCA analysis of morphological features upon treatment with Remdesivir, E-64d, TH3289, TH6477, TH5487, and Camostat in non-infected (-CoV-229E) and infected (+CoV-229E) conditions compared to DMSO control. Each dot in the PCA represents one image by taking the mean of all objects in the image.

As next, we implemented PCA to study the effects of each compound in more detail. Morphological profiles from CoV-229E infected cells treated with all Remdesivir or E64d doses remarkably overlapped with the profile from non-infected DMSO-treated cells, supporting the phenotypic rescue observed in the cluster analysis (**Figure 18b, c**). TH3289, TH6744 and TH5487, on the other hand, showed dose-dependent effect where middle dose (10 µM) treatments overlapped with the non-infected phenotype, low dose (1 µM) overlapped with the infected phenotype and the high dose (30 µM) treatment formed a separate cluster along

the second principal component axis (**Figure 18d, e, f**). All conditions from the ineffective compounds such as Camostat fully overlapped with the infected phenotype (**Figure 18g**). Collectively, these results exemplify our phenomics workflow utility as a screening and profiling approach to identify antiviral compounds and the underlying effects on the host cell morphology.

2.5 DISCUSSION

To pave the way for the development of antiviral therapies, it is, on the one hand, crucial to understand molecular events during virus replication cycle and the interactions with the host cell. On the other hand, research should also seek for innovative advancements to boost the antiviral drug discovery process. At the beginning of this thesis work, EBOV and ZIKV epidemics reminded the world how the lack of countermeasures and detailed understanding of the viruses limit our readiness to emerging viral outbreaks. Even more so, the ongoing COVID-19 pandemic stretches health systems to their limits worldwide and once again has brought the urgent need for effective antiviral therapies into sharp focus. It was this gap in knowledge and countermeasures that led me to explore virus dependency on the host oxidative stress and nucleotide metabolism pathways, an avenue the Helleday lab had thoroughly contributed to in the context of tumor biology and inflammatory diseases. In this study we developed two image-based antiviral phenotypic screening approaches with high-throughput capacity and identified a series of novel broad-spectrum antiviral compounds. We shed light on the broad activity across virus families and investigated the antiviral mechanism of action and host cell target pathways of the screening hit compounds.

Antiviral phenotypic screening and hit validation

Paper I and **Paper II** present the discovery of novel broad-spectrum antiviral compounds and highlight the value of phenotypic image-based screening. By implementing our image-based phenotypic screening assay, TH3289 was initially classified as a hit compound reducing HAZV progeny production. After conducting the second screening event, TH6744, a structural analog of TH3289 was discovered and reduced HAZV progeny production to a similar extent. Both compounds exhibited anti-HAZV activity at 10-fold lower dose compared to Ribavirin, an approved antiviral drug with proven *in vitro* activity against SARS-CoV-2[131], ZIKV[244], CCHFV[245] and in clinical trial setting in combination treatment in COVID-19 patients[246]. Shortly after the discovery of TH3289, its antiviral activity was measured against a panel of different viruses. Treatment with TH3289 had higher activity against CCHFV, HAZV, CoV-229E and lower activity against EBOV and SARS-CoV-2. We could thereby conclude TH3289 as a broad-spectrum antiviral, but the varying activity also appoints to virus-specific responses which could be explained by differential dependencies between, for example EBOV and CoV-229E towards TH3289 target pathway(s). Subsequently, we transferred the phenotypic assay to emerging virus ZIKV and selected structural analogs of TH3289 and TH6744 for screening. Again, TH3289 and TH6744 ranked among the classified hits having comparable activity against ZIKV and HAZV, confirming the broad activity of both compounds. By adapting the assay to dose-response regime in both HAZV and ZIKV infection models, we determined >10-fold therapeutic window of TH3289 and TH6744 treatment based on cellular toxicity and antiviral activity EC_{50} in ZIKV models. Slightly wider therapeutic window and more favorable toxicity profile across cell types prompted us to choose TH6744 as the primary tool compound for further studies. It should be noted that I fully acknowledge how the potency characteristics of TH3289 and TH6744 are not sufficient for preclinical antiviral drug development and I take

these compounds as chemical starting scaffolds for further development and as probe tools to explore and advance virology.

In addition to validating the screening hit activity by determining their therapeutic window, we also established 3D cerebral brain organoids to study ZIKV infection and the antiviral compound treatments in collaboration with Dr. Robin Pronk and Dr. Anna Falk. Brain organoids derived from induced pluripotent stem cells have proven to reliably model molecular and cellular consequences accompanied with ZIKV infection[242,243,247]. Implementing 3D organoid models to study ZIKV antivirals was among the main objectives of another thesis from our research group by Aleksandra Pettke. Overall, TH6744 treatment reduced ZIKV progeny release in brain organoids at non-toxic doses, rescued ZIKV-induced cell death phenotype and nearly eliminated ZIKV infection within the brain organoid tissue. Therefore, in spite of cellular toxicity at high micromolar doses in Vero and U87 cells, TH6744 and analogs seem to exhibit substantial double benefits for the brain organoids in the low micromolar range. As TH6744 antiviral activity was validated in several cell lines and 3D brain organoids, we therefore conclude that the phenotypic antiviral screening assay has the potential to capture true-positive antivirals (**Figure 19**).

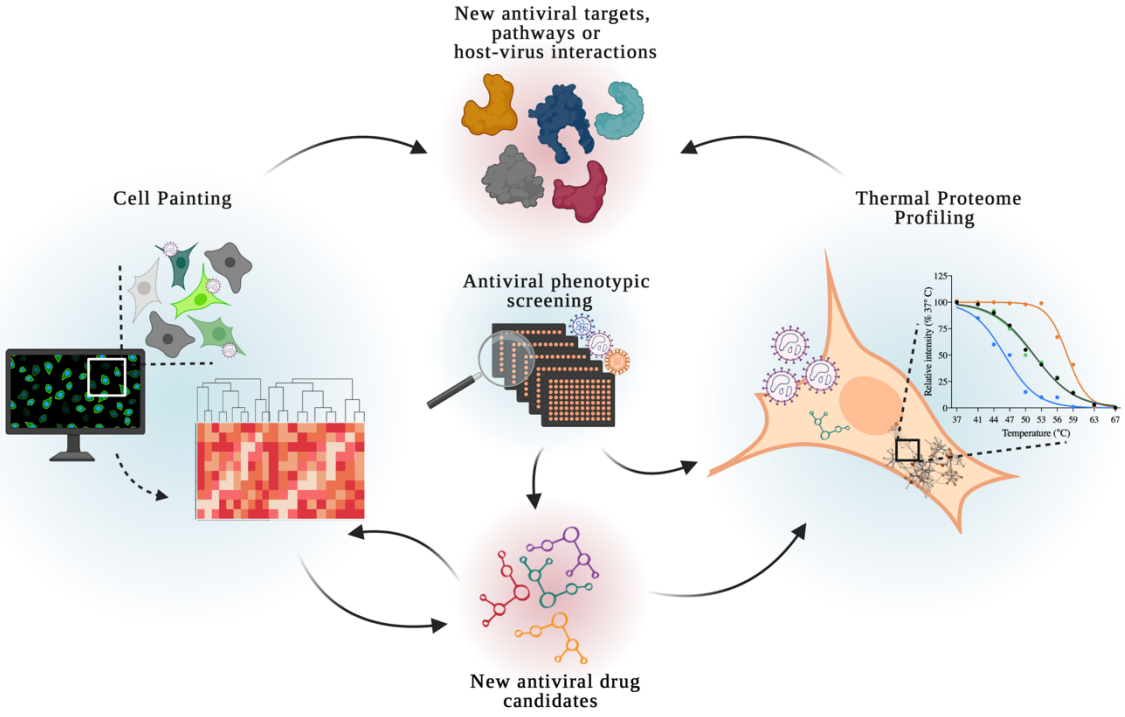

Figure 19. Phenotypic drug discovery toolbox to discover new antiviral candidates and drug targets. Antiviral phenotypic screening identifies new drug candidates with broad-spectrum activity. Candidate compound MoA, target proteins or pathways can be predicted by Cell Painting and/or TPP methodologies. At the same time, Cell Painting can be used to profile and screen new antiviral drug candidates.

Our phenotypic screening approach was in line with previous research efforts to replace labor-intensive gold standard antiviral assays such as CPE[181,183] and plaque-forming assay[248] with more advanced and automated image-based technologies[186,249–251]. We chose a screening approach with unbiased readout that captures the complete replication cycle of the infectious

BSL-2 viruses and is independent from compound library intended target(s). Because we monitored compound antiviral activity both on the infected cells and on the virus progeny production, our assay is not limited to certain replication cycle steps, which is often the drawback of replicon-based systems[172–174], but enables identification of inhibitors across the virus replication cycle. Important to mention, we chose to exclude compound pre-treatment regime, but the assay design can easily be adapted to include detection of viral entry inhibitors by pre-treating the cells prior virus inoculation. Also, the assay is adaptable to custom-specific needs for example evaluating smaller libraries using dose-response treatment or even combination treatments, among others. Moreover, as exemplified by all **three constituent papers**, the assay is also transferrable between different viruses with the pre-requisite of existing specific antibodies enabling the immunofluorescence-based imaging.

The image-based approach of our assay provides a single-cell resolution and a broad overview of the infected cell population. Commonly used antiviral screening assays evaluating CPE reduction are also phenotypic by nature but judge compound activity by averaged values of cell population viability[181–183]. As opposed to CPE, our image-based assay enables quantification of infected cells and cell survival rate on a single-cell level and thereby provides an in-depth analysis of the heterogeneous cell behaviors owing to the possibilities of automated image analysis softwares. We applied open-source software CellProfiler to automatically quantify cellular phenotypes from large image datasets[192], but other tools such as deep-learning platform ImJoy[252] and several "acquisition to analysis" solutions within high-content screening systems also offer versatile image analysis. Even though our phenotypic screening assay presents multiple advancements to the antiviral drug discovery landscape and proved to be absolutely instrumental throughout this thesis work, we continuously noted the unemployed potential by providing only binary yes/no read-outs on the infection status of the cells. We therefore further explored the area of advanced imaging methodologies.

Cell morphology profiling

Consequently, in **Paper III** we combined the phenotypic screening assay with morphological profiling for the evaluation of virus and drug-induced cellular phenotypes in collaboration with Cell Painting experts from Prof. Ola Spjuth research group. Owing to Anne Carpenter's team pioneering work[191,197,198], Cell Painting method has rapidly been implemented across pharmacology and toxicology disciplines[253–255], but its use in the infectious disease field has so far been limited. We adapted the Cell Painting protocol to coronavirus-infected cells and demonstrated how it reliably distinguished infected and non-infected cell populations upon CoV-229E infection solely based on cellular features such as organelle shapes, size, staining intensities, textural patterns, among others, without using the information from CoV-229E-specific antibody staining. Not to our big surprise, increased intensity of ER and cytoplasmic RNA stain signals accounted as the most prominent differences between infected and non-infected cells. Concanavalin A, the Cell Painting dye staining for the host ER, has been previously shown to bind Coronavirus envelope and viral glycoproteins[256–258]. However, the stark increase of Concanavalin A intensity in the cell nuclei came as a surprise because this dye

usually stains for glycoproteins in the ER. Hence, future investigations by alternative fluorescent dyes and antibody detection of host ER and viral proteins shall discern if the ER intensity increase originated from host cell response, from direct binding of Concanavalin A to CoV-229E viral glycoproteins or from the combination of both. Recently, two independent morphological profiling studies on SARS-CoV-2 infected human cells were presented in BioRxiv. Mirabelli *et al*[259] and Heiser *et al*[260] used artificial intelligence (AI)-driven high-throughput phenomic profiling and identified specific morphological phenotypes in SARS-CoV-2 infected human cells, being in line with our findings with CoV-229E. Clearly, Cell Painting assay opens unexplored avenues for both basic virology and antiviral drug discovery efforts (**Figure 19**).

One objective of the Cell Painting project was to develop a workflow for identification of antiviral compounds. We demonstrated how previously validated antiviral compounds Remdesivir[126,131] and E64d[261] reduced viral infection by antibody staining, and simultaneously reversed the phenotype of infected cells from the "infected" cell signature towards the "non-infected" signature. Remdesivir efficacy was also discovered in the two SARS-CoV-2 morphological profiling studies in BioXriv[259,260], strengthening our approach and results. Treatment with TH3289, TH6744 or TH5487 also indicate a phenotypic rescue, however we observed narrower therapeutic window with the TH-compounds in CoV-229E infection model compared to HAZV or ZIKV models from **Paper I** and **Paper II**, respectively. Differential cytotoxicity profile of these TH-compounds between fibroblast (MRC5) and epithelial (U87 and SW13) cell types could be explained by differences in cell metabolism, compound membrane penetration or other cell type-specific processes. In spite of the narrow therapeutic window in MRC5 cells, TH-compounds shift cellular phenotype towards the "healthy" state, which would have been undetected with evaluating the antiviral activity solely by the antibody-based approach. The antiviral capacity of the remaining tested compounds should be further investigated at different compound concentrations, because our selected doses were most likely too low for Favipiravir, Cathepsin inhibitor L and Camostat and too high for Bafilomycin A. Still, the remarkable phenotypic rescue by Remdesivir and E64d elegantly showcases the power of Cell Painting to enable identification of efficacious antivirals and characterize host responses. To define the scope and universality of virus-induced cellular phenotypes, future Cell Painting studies across virus families and cell types would be insightful. To our knowledge, this is the first protocol that enables simultaneous evaluation of antiviral efficacy by virus-specific antibody staining and of host cells responses by Cell Painting.

Another Cell Painting application is the prediction of compound MoA[197,198,201,254]. Morphological feature clustering of nine selected compounds in the absence of virus infection revealed that structural analogs TH3289, TH6744 and TH5487 grouped together, as expected. Even though the scale of this study is far from sufficient to draw any conclusions about the compound's MoA, it is nonetheless noteworthy how structurally similar compounds cluster together. One possible approach to predict MoA of TH compounds by leveraging image-based methods could be by comparing their morphological profiles with those from accurately annotated reference compounds, for instance by implementing the large existing phenomics

dataset including profiles from over 30'000 compounds[197]. Alternatively, compound morphological profiles can be compared with genetically perturbed cell profiles, such as by RNAi or CRISPR-Cas9[262–264], but this approach is less widely used. These approaches stand on an assumption that compounds with similar MoA induce similar phenotypes and thereby cluster together. Large fraction of drugs are believed to be polypharmacological[265], meaning they simultaneously bind to multiple targets to perform therapeutic activity and predictions based on morphological profiles of polypharmacological compounds have proven to be confounding and challenging[194]. Implementing proteome or transcriptional profiling methods such as TPP[215] or L1000 assay[266], respectively, can readily complement the limitations of image-based methods. Still, Cell Painting comes with relatively low costs, high feasibility and unlike the alternatives, provides a powerful single-cell resolution. The work from this thesis successfully complemented an image-based phenotypic assay with advanced morphological profiling and provided tools for in-depth analysis of host cell responses and rapid therapeutic discovery in epidemic/pandemic setting (**Figure 19**).

Target identification

In **Paper I**, after identifying broad-spectrum antivirals, we followed the next logical question and studied the host cell targets and target pathways of the phenotypic screening hit TH6744. Because we hypothesized a polypharmacological MoA, we chose the state-of-the-art proteome-based and unbiased target identification method TPP, combining the temperature range and concentration range approaches. While OGG1 activity did not seem to drive the antiviral activity of TH3289 and TH6744, instead, our findings from two independent TPP studies suggest that TH6744 broadly affects the components of cellular chaperone pathways. We could not pinpoint towards any obvious protein as the one target candidate, but a group of proteins from ER-related chaperone and co-chaperone networks had the largest differences in thermal stability after TH6744 treatment. DNAJB11, also known as ERdj3, is an ER-resident co-chaperone[267], the most thermally stabilized protein by TH6744 treatment in TPP-TR and previously described to promote Simian Virus 40 capsid assembly[268] and DENV replication[145]. More specifically, DNAJB11 depletion by small hairpin RNA (shRNA) reduced DENV propagation due to its supportive role in vRNA replication and recruitment to DENV replication complexes in the ER[145]. EDEM3, a regulator of ER-associated protein degradation and HYOU1 (also known as ORP150), an ER chaperone[269], were also thermally stabilized by TH6744 and interact with Orf8 protein encoded by SARS-CoV-2 genome[270]. Additionally, HSP70 (encoded by HSPA1A gene), one of the most characterized cellular chaperones was thermally destabilized upon TH6744 treatment in both TPPs and also dose-dependently in the follow-up studies. It is hereby important to mention that thermal destabilization does not equal to protein degradation, but rather intrinsic alterations in protein conformation that render it more sensitive to thermal treatment.

Additionally, TH6744 treatment increased the protein-protein interaction between HAZV NP and HSP70 detected by co-IP. Apart from this, we also observed a consistent thermal stability increase in a subset of other co-chaperones and chaperones located in the ER and consistent

thermal stability decrease of cytosolic chaperones. This observation may be purely coincidental but may also reflect subcellular compartment specific responses to TH6744 treatment. Altogether, TPP revealed a profound thermal stability changes across host cell proteome. However, TPP in cell lysates would be a logical follow-up study to distinguish TH6744 direct targets from indirect downstream effects. Additionally, the role of numerous target candidates remains to be validated, including the understanding of direct and indirect TH6744 targets within the host chaperone network.

Based on the thermal stabilization of co-chaperones and thermal destabilization of HSP70 and other cytosolic chaperones, we propose a MoA where TH6744 disturbs the protein folding machinery. Given that co-chaperones initially bind the substrate protein, guide it to the chaperone to stimulate its adenosine triphosphate (ATP) hydrolysis activity and thereby leave the complex[271,272], we hypothesize that TH6744 directly binds to co-chaperones such as DNAJB11 resulting in increased thermal stability and compromised functionality. TH6744 binding to co-chaperones within the protein folding complex could disturb co-chaperone release from chaperone after ATP hydrolysis and the iterative folding process which leads to thermal destabilization of chaperones such as the HSP70. Our reported increased interaction between HSP70 and HAZV NP supports this MoA by reflecting the increased load of unfolded viral proteins not being properly folded due to the compromised HSP70 capacity. This proposed model is also supported by TH6744 higher potency towards viral progeny production, because the compromised viral protein folding could directly and rapidly hinder the assembly and release of new virions.

Identifying host co-chaperone/chaperones as an antiviral target is not novel, however, our target identification approach by TPP was able to pinpoint highly relevant host pathways as TH6744 targets. Cellular chaperone networks have long been established to support viral replication cycle across families. Taguwa and colleagues reported how diverse set of DNAJ proteins located in distinct subcellular compartments orchestrate the specificity and functionality of HSP70's throughout DENV life cycle[145]. In a more recent study, Taguwa and colleagues defined ZIKV entry, formation of the replication complex in ER and particle production processes dependent on HSP70 and thereby sensitive to HSP70 inhibition[240]. Additionally, host HSP70 interaction with viral proteins have been demonstrated during CCHFV[273], EBOV[274] and Japanese encephalitis virus (JEV)[275] infection, to highlight a few. In addition to HSP70 network, exploring other targets of TH6744 could reveal unexplored pro-viral proteins, presenting one way to investigate host-virus interplay (**Figure 19**). Finally, to connect alternative approaches taken throughout this thesis work to predict the MoA, TPP findings were in line with the Cell Painting study from **Paper III**, appointing ER structures and functions relevant for RNA viruses. Without a doubt, host chaperone network members display importance to viruses across families.

Overall, the plethora of host target candidates were not surprising, because TH6744 and its structural analogs represent screening hits and have not undergone chemical optimization to improve antiviral potency, cellular tolerability or target binding properties. Also, the role of

numerous target candidates remains to be validated including the understanding of direct and indirect TH6744 targets within the host chaperone network. To conclude, we can confidently state that the vast changes within cell proteome thermal stability upon TH6744 treatment suggest a multifactorial host-directed MoA.

Compound mechanism of action

Besides elucidating the host responses, in **Paper II** we demonstrated which ZIKV replication cycle steps are the most vulnerable to TH6744 treatment. Viral kinetics and time-of-addition studies disseminate the main viral replication cycle steps such as viral entry, RNA replication and budding and concurrently facilitate the understanding of compound MoA. ZIKV kinetics revealed that TH6744 does not impede ZIKV vRNA synthesis, but strongly impairs viral progeny release. This was in contrast to Ribavirin treatment that effectively blocked vRNA replication, as expected based on previous studies on ZIKV[116,117,276]. Reduced ZIKV progeny and no reduction in the percentage of infected cells within 24 h treatment suggests TH6744 effect towards late ZIKV replication steps. As a consequence, percentage of ZIKV infected cells reduced at 48 h and 72 h timepoints during TH6744 treatment, reflecting on the reduced secondary infections. The almost immediate reduction of viral progeny release during active replication phase at 24 hpi in the time-of-addition study supports the viral kinetics findings on late life cycle steps. Interestingly, TH6744 also reduced ZIKV entry by compound pre-treatment, in line with a study reporting ZIKV entry hypersensitivity to HSP70 inhibition[240]. Considering our hypothesis involving the host cell chaperone network, we decided to disseminate the ZIKV budding step, but TH6744 role in viral entry shall be further studied. While intra- and extracellular infectious particles reduced to similar extent upon TH6744 treatment during budding, we concluded that TH6744 disturbs ZIKV life cycle after vRNA replication, interfering with either viral protein translation, processing or stability, viral particle maturation process, trafficking or budding into the extracellular environment. To complement the proposed MoA model, we further suggest that rapid reduction of viral progeny release by TH6744 could be mediated by the effect on HSP70 folding capacity. In summary his MoA presents a host-directed approach resulting in defeated virus and healthy host cells.

2.6 CONCLUSION AND FUTURE PERSPECTIVE

Expanding the arsenal of existing antiviral candidates is essential to fight against the ongoing and the next emerging RNA virus epidemic or pandemic. Not less important is understanding how virus interplays with the host during the infection. As multiple strategies exist to feed the pre-clinical antiviral drug discovery, we focus on the phenotypic approach that shines through the whole thesis from drug screening assays to target identification techniques.

Enormous number of repurposing studies are being conducted to battle against COVID-19 and provide grounds for new clinical trials, but only few have harnessed AI or machine-learning resources to assist solving these pharmacological puzzles. It holds true that AI is capable of identifying strong repurposing candidates and even drive the drug design process much faster than human experts exploring the same quantities of candidates experimentally. Even before WHO had declared the COVID-19 pandemic and just as first SARS-CoV-2 cases were reported in Europe, BenevolentAI, an UK-based biotech company identified licenced drug baricitinib as potentially useful host-directed antiviral to treat COVID-19. Eli Lilly, the drug developer responded rapidly, validated the findings in laboratory setting and scheduled clinical trials to treat hospitalized COVID-19 patients. Reaching this drug candidate based on experimental data would have taken weeks or months, but BenevolentAI did it within one week. Further work needs to focus on integrating AI capabilities into early drug discovery and even drug design pipelines to ease exploring the chemical space.

Exploring host-virus interplay is crucial, but the vast information is currently scattered across Pubmed within publications and without proper systematic overview. A unified database similar to Human Protein Atlas resources gathering well annotated and validated virus-host interactions across techniques for relevant human pathogenic viruses would be a gamechanger. Some efforts present promising start such as ViralZone, Viruses.STRING[277] and VirHostNet, but all lack at the comprehensiveness and the degree of integration. This resource would facilitate research and drug discovery in many levels. Applying distinct techniques on the same research question either overlap with or complement the findings from one another. The proposed database would facilitate comparing information from TPP, co-IP, CRISPR-based genetic screens and beyond. At the event of newly emerging virus, such resource would enable mapping the key virus-host interactions and thereby vulnerabilities based on closely related viruses or in other words, where are the druggable interactions?

Finally, to succeed in drug discovery or repurposing for emerging viruses, research capabilities beyond any pandemic or epidemic must be established with dedicated and clear goal to deliver more novel antivirals to the market. It is no surprise that neglected pathogens such as ZIKV, DENV and others fly under the pharmacology companies' radar, due to the sporadic emergence and acute disease presentation. Even more so, academic institutions must enhance their contribution to preparedness. It is more research efforts, dedicated antiviral drug discovery platforms and biosafety infrastructures that result in new antivirals and thereby support our preparedness until the next virus emerges.

3 ACKNOWLEDGEMENTS

Working towards a PhD degree at Karolinska Institutet was challenging but also humbling and inspirational – I would not trade this ride for anything. There have been a lot of people with me during this journey and contributed to this thesis one way or another. I want to take this opportunity to thank you all for your guidance, support and friendship.

First, my supervisor **Ali**, I am grateful that you gave me the opportunity to be part of your team – it has truly been fantastic. You have guided me from the first day with the right balance of supervision and freedom and have been exceptionally supportive to my scientific and career-related decisions. Thank you for your easy-going attitude, creative mind and kindness. Thanks to your help and encouragements I have become an independent researcher with my own ideas.

My co-supervisor **Marjo**, my development as a researcher and team-player have been so steep thanks to your dedicated guidance. I remember our first months working together – fresh MSc graduate and a new postdoc learning to become virologists. Now thinking, I believe we made it. It was even more fun when Aleksandra joined, and the virus team got a real kick-start. Your high demands for quality as well as emphasis on work-life balance have undoubtedly shaped my values as a professional. I have really enjoyed learning from you, and I thank you for guiding me along this challenging yet exciting project.

My co-supervisor **Thomas**, I am very grateful that you welcomed me in your group first as a master student and then as a PhD student and let me experience the multidisciplinary research. Your out-of-the-box way of thinking, positive mindset and passion for science has been a true inspiration!

This thesis work would have not been possible without the brilliant minds of the **Helleday lab crew**, including its present and past members. Thank you: **Ulrika**, for being an empathic and encouraging leader to look up to, our science and career-related discussions guided me through challenging times. **Aleksandra**, for your genuine kindness, wise words ("It always seems impossible until it's done" by N. Mandela) and dedication for our teamwork. Working closely with you inspired me to look for opportunities with open eyes and be hungry for knowledge. It has truly been great sharing this journey with you and I will miss these times. **Maria**, I am very thankful that you chose me as your MSc thesis supervisor and were the best student ever. Besides your excellent skills and ability to discuss ideas, I really enjoyed your company. Thank you for your positive attitude, sense of humor, ambition and for letting me grow as a supervisor. I wish you all the best for your PhD journey in Zürich! All present and previous PhD students in the Helleday lab – **Linda, Anna H., Nick, Saeed, Anna H. N., Petra, Stella, Jemina, Aleksandra, Nadilly, Bishoy** and **Johan** – thank you for your support, input and I have no doubt you all will have a bright future ahead. Special thank you goes to **Lollo, Mari, Flor, Camilla, Kristina, Linn, Sabina and Ashley**, I truly appreciate your willingness to help out, your contribution over the years have been absolutely crucial. Additionally, I value the scientific input and all the help from the rest of the present and past Helleday lab members. Special thanks go to **Patrick, Kumar, Niklas, Torkild, Armando, Ingrid, Eliseé, Maurice, Jordi, Lars, Christina, Adam, Anna H., Linda, Sabin, Andreas, Nina, Sanaz, Karolina, Judith, Nuno, Cynthia, Brent**, **Evert**, **Tobias**, **Olle**, **Åsa**, **Sean** and **Helge**.

My colleagues and the "real virologists" from Ali's group, **Vanessa, Cristiano, Sofia, Mikaela, Samir** and **Liz**. Sincere thank you for your continuous willingness to help without hesitation and to offer input from your profound expertise. Our virology discussions have been very eye-opening and important for my research and personal growth. I will always look up to you ☺.

Thank you, my **SVA team,** especially **Rickard, Lennart, Caroline** and **Lijo** for enabling me to do my research, but most importantly for your support throughout this journey and trusting me to be employed in Uppsala while in reality working in Stockholm. Very special thanks go to **Rickard** for your humble attitude and for everything you taught me.

All of my projects have been possible thanks to our fantastic collaborators – it has been an honor to work with you and learn from you. Firstly, thank you **Rozbeh, Janne** and **Elena** for supporting me over the years, your contribution to my research has been invaluable. **Rozbeh**, we worked together almost from the very beginning until the very end of my PhD studies. You taught me a lot about CETSA and TPP (obviously), but also how to steadily steer through challenging times when experiments fail and almost nothing goes as expected. Thank you for believing in me and I wish you best of success for your research group.

I am so happy for the opportunity to work together with you, **Robin**. Our collaboration began even before my PhD and it became one of the most valuable for our project. The brain organoids are extremely cool and even more remarkable was your dedication to grow and develop hundreds of them for us! Thanks for helping us to demonstrate the possibilities of our antiviral compounds.

My thesis content would not be so coherent without the brilliant ideas and leadership from **Jordi**. We have known each other for years as colleagues and friends – you supported my development as a scientist in the Helleday lab and as a person when you cheered me through the last kilometers of the Trollhättan triathlon. Finally, I could also collaborate with you at the very last stretch of my PhD, it has been a pleasure working with you. **Jonne**, I am glad to have worked so closely with you over the past months. You are a clever young scientist and I have learned a lot from your expertise. Keep up the good work and I wish you all the best for the rest of your PhD and your future career! **Duncan**, I admire your passion for science, and it has been great learning from you and working with you in the BSL-3 with our projects. Additionally, thank you for your efforts in the COVID-19 project **Hanna, Päivi**, **Charlotte**, **Ola**, **Polina**, **Maris** and everyone else involved.

I am fortunate to have many friends (close by and far away) to help take my mind off work and balance my life as a researcher. I am grateful for our small and big memories from the past and those yet to be created. **Karolina, Olivia, Yasmin, David, Henrik, Loan, Georgia** and everyone else, thank you for welcoming me as part of your crew and made my landing in Stockholm (and Vårberg) very smooth and exceptionally fun. **Karolina**, my dear ostentatious friend, please continue being your lovely and ambitious self! My dear colleagues and fellow scientists who became very good friends. Thank you, **Andreas, Sabin, Adam, Sean, Julie, Patrick, Bettina, Linda, Marjo, Nick, Simin, Olga, Anna H.** and everyone else. Thanks for the house-party marathons (oh, how I miss them), adventures in the nature, travelling together, spontaneous summer evening dance parties in Stockholm and the rest of our exciting activities.

I miss hanging out with all of you, but luckily some of you are still around and for those who left Stockholm – hope to see you soon!

Tuleviku teadlased, **Liisi, Helen, Mihkel, Karolina, Carolin, Kadi, Jüri, Kaisa, Timo, Tuuliki, Triin** ja **Siret**. Suur aitäh, et olite TÜ aegadel üks vinge seltskond kellega koos õppida, pidutseda ja Tartu vaimu kogeda.

My german family, **Jara**, **Leonas**, **Susanne**, **Romuald, Elvira, Friedl, Alex** and **Andrea**. Danke, dass ihr mich in eurer Familie willkommen geheißen habt und ich mich immer wie zu Hause fühle.

Thank you, **Monica** for your energy and truly valuable memories that you have helped create from our afternoon teas to my ultimate baby shower surprise. I am excited to see you fearlessly following your dreams - I can't wait to visit you in California.

A fellow mama and a scientist, **Carmen**, jag är glad att kalla dig min vän. Tack för att du inspirerade mig att prata mer svenska och fortsätta lära mig. Vilken positiv energi och glädje du sprider varje gång vi träffas. Jag ser fram emot att spela med dig, Joel och Börge snart!

My fellow expats, **Eleanor** and **Craig**! Your friendship over the past years has been like a breath of fresh air – your adventurous and uncomplicated mindset has brought me a lot of joy and your values in life totally align with mine. I can't wait to plan another midsummer getaway and to attend your wedding!

Linda, my best friend from my PhD studies. We instantly clicked and became like inseparable sisters. How to find words to thank you for wholeheartedly being my caring friend? I miss living in the same city with you and laugh, cry or dance together as often as we want. Thank you for always listening to me with open heart, teaching me how to do proper make-up and guiding me out of darkness for so many times. I truly appreciate your friendship!

Siret, my best friend from university studies. Aitäh, et oled olnud minu kõrval nii inspireeriv alates sellest hetkest kui ma TÜMRI vanas saalis 2010. aasta sügisel sinu kõrvale otsustasin istuda. Ma julgen öelda, et ma võlgnen märkimisväärse osa oma teadlasekarjäärist sinu põhjalikkusele ja uudishimule, mis mulle kuidagimoodi TÜ raamatukogu õppimismaratonide käigus külge jäi. Need ajad kui me koos Tartus ja Stockholmis elasime olid nii-nii vinged, aga õnneks tuleb meil ka long-distance sõprus väga hästi välja ☺. Kindlasti ei tohi siinkohal unustada ka tänu sinu jagatud kaneelisaia/jõhvika-iirisekringli retsepti, mida me üheskoos TÜMRI -80 °C külmikute ruumis kergitasime ja mis on siiani kõrgelt hinnatud! Aitäh, kallis!

Hege, my best friend from primary school. Ma ei oska täpselt öelda kuidas meie pikaaegne sõprus uue hingamise sai, aga ma olen nii tänulik, et saan sinuga nii raskeid kui ka rõõmuhetki jagada. Aitäh armas, et sa oled nii otsekohene, pragmaatiline, sihikindel ja inspireerid mind elu nautima ja uusi kogemusi otsima. Varsti Töölös/Viljandis/Stockis kohtume, arutame investeeringuid, värvime juukseid ja sööme tillikartulit koorekastmega. Ei jaksa enam ära oodata ☺.

My deepest gratitude goes to my parents, **Marge** and **Priit** for their unconditional love and support throughout my whole life. Whatever I do, wherever I decide to go, I know that you will always be there for me. Thank you for raising me into the independent and strong woman I am

today. My dear sister **Miia**, ma olen nii õnnelik, et mul on sinusugune äge õde! Sinuga on super lahe jutustada ja elu üle arutleda ☺ Aitäh, et sa oled nii chill, hea huumorimeelega ja ei võta elu liiga tõsiselt. **Memmeke**, vanaema **Tiina** ja vanaisa **Enn**, aitäh, et olete nii hoolivad, ülivinge ellusuhtumisega, sitked ja siiralt hea südamega inimesed. Teil on sinu südames väga-väga eriline koht.

My own little family – Oli and Jonas. **Oli**, thank you for your endless support and love over the years. You empower my ambitions, make sure I acknowledge my own efforts when in doubt and genuinely respect me for who I am. You hold my hand and guide me when needed and for all that I am eternally grateful. **Jonas**, as kitschy as it sounds, without any specific effort from your 1.5-year-old self, you taught me that happiness depends on ourselves and the way we choose to perceive life. Thank you both for all the memories we have created so far, and I am very excited for the future adventures ahead of us.

4 REFERENCES

1. Clercq, E. & Li, G. Approved Antiviral Drugs over the Past 50 Years. *Clin Microbiol Rev* **29**, 695–747 (2016).

2. Newman, D. J. & Cragg, G. M. Natural Products as Sources of New Drugs over the Nearly Four Decades from 01/1981 to 09/2019. *J. Nat. Prod.* **83**, 770–803 (2020).

3. SIMPSON, D. I. ZIKA VIRUS INFECTION IN MAN. *Trans. R. Soc. Trop. Med. Hyg.* **58**, 335–338 (1964).

4. Guerbois, M. *et al.* Outbreak of Zika Virus Infection, Chiapas State, Mexico, 2015, and First Confirmed Transmission by Aedes aegypti Mosquitoes in the Americas. *J. Infect. Dis.* **214**, 1349–1356 (2016).

5. Wong, P.-S. J., Li, M. I., Chong, C.-S., Ng, L.-C. & Tan, C.-H. Aedes (Stegomyia) albopictus (Skuse): a potential vector of Zika virus in Singapore. *PLoS Negl. Trop. Dis.* **7**, e2348 (2013).

6. Musso, D. *et al.* Potential sexual transmission of Zika virus. *Emerg. Infect. Dis.* (2015).

7. D'Ortenzio, E. *et al.* Evidence of Sexual Transmission of Zika Virus. *New Engl J Med.* **374**, 2195–2198 (2016).

8. Motta, I. J. *et al.* Evidence for Transmission of Zika Virus by Platelet Transfusion. *N. Engl. J. Med.* **375**, 1101–1103 (2016).

9. Blohm, G. M. *et al.* Evidence for Mother-to-Child Transmission of Zika Virus Through Breast Milk. *Clin. Infect. Dis.* **66**, 1120–1121 (2018).

10. Besnard, M., Lastere, S., Teissier, A., VM, C.-L. & Musso, D. Evidence of perinatal transmission of Zika virus, French Polynesia, December 2013 and February 2014. *Euro Surveill.* **19**, 20751 (2014).

11. Driggers, R. W. *et al.* Zika Virus Infection with Prolonged Maternal Viremia and Fetal Brain Abnormalities. *N. Engl. J. Med.* **374**, 2142–2151 (2016).

12. Duffy, M. R. *et al.* Zika Virus Outbreak on Yap Island, Federated States of Micronesia. *N. Engl. J. Med.* **360**, 2536–2543 (2009).

13. Musso, D. *et al.* Zika virus in French Polynesia 2013–14: anatomy of a completed outbreak. *Lancet Infect. Dis.* **18**, e172–e182 (2018).

14. Faria, N. R. *et al.* Zika virus in the Americas: Early epidemiological and genetic findings. *Science (80-.).* **352**, 345–349 (2016).

15. Pan American Health Organization. Epidemiological update. Neurological syndrome, congenital anomalies, and Zika virus infection. (2016).

16. Musso, D. & Gubler, D. J. Zika Virus. *Clin. Microbiol. Rev.* **29**, 487–524 (2016).

17. Musso, D., Nilles, E. J. & Cao-Lormeau, V.-M. Rapid spread of emerging Zika virus in the Pacific area. *Clin. Microbiol. Infect.* **20**, O595-6 (2014).

18. Cao-Lormeau, V.-M. *et al.* Guillain-Barré Syndrome outbreak associated with Zika virus infection in French Polynesia: a case-control study. *Lancet* **387**, 1531–1539 (2016).

19. Oehler, E. *et al.* Zika virus infection complicated by Guillain-Barre syndrome - case report, French Polynesia, December 2013. *Euro Surveill.* **19**, 20720 (2014).

20. Rees, J. H., Thompson, R. D., C, Smeeton, N. C. & Hughes, R. A. Epidemiological study of Guillain-Barré syndrome in south east England. *J. Neurol. Neurosurg. psychiatry* (1998). doi:10.1136/jnnp.64.1.74

21. Wachira, V. K., Peixoto, H. M. & de Oliveira, M. R. F. Systematic review of factors associated with the development of Guillain–Barré syndrome 2007–2017: what has changed? *Trop. Med. Int. Heal.* **24**, 132–142 (2019).

22. Oliveira Melo, A. S. *et al.* Zika virus intrauterine infection causes fetal brain abnormality and microcephaly: Tip of the iceberg? *Ultrasound Obstet. Gynecol.* **47**, 6–7 (2016).

23. Calvet, G. *et al.* Detection and sequencing of Zika virus from amniotic fluid of fetuses with microcephaly in Brazil: a case study. *Lancet Infect Dis* **16**, 653–660 (2016).

24. Mlakar, J. *et al.* Zika Virus Associated with Microcephaly. *N. Engl. J. Med.* **374**, 951–958 (2016).

25. Sarno, M. *et al.* Zika Virus Infection and Stillbirths: A Case of Hydrops Fetalis, Hydranencephaly and Fetal Demise. *PLoS Negl. Trop. Dis.* **10**, e0004517 (2016).

26. Coelho, A. & Crovella, S. Microcephaly Prevalence in Infants Born to Zika Virus-Infected Women: A Systematic Review and Meta-Analysis. *Int J Mol Sci* **18**, 1714 (2017).

27. Brady, O. J. *et al.* The association between Zika virus infection and microcephaly in Brazil 2015-2017: An observational analysis of over 4 million births. *PLoS Med.* **16**, e1002755 (2019).

28. de Melo, A. *et al.* Congenital Zika Virus Infection: Beyond Neonatal Microcephaly. *Jama Neurol* **73**, 1407 (2016).

29. Wheeler, A. C. *et al.* Developmental Outcomes Among Young Children With Congenital Zika Syndrome in Brazil. *JAMA Netw. Open* **3**, e204096 (2020).

30. Zaidi, M. B. *et al.* Non-congenital severe ocular complications of Zika virus infection. *Jmm Case Reports* **5**, (2018).

31. Peloggia, A., Ali, M., Nanda, K. & Bahamondes, L. Zika virus exposure in pregnancy and its association with newborn visual anomalies and hearing loss. *Int J Gynecol Obs.* **143**, 277–281 (2018).

32. Tang, H. *et al.* Zika Virus Infects Human Cortical Neural Progenitors and Attenuates Their Growth. *Cell Stem Cell* **18**, 587–590 (2016).

33. Gabriel, E. *et al.* Recent Zika Virus Isolates Induce Premature Differentiation of Neural Progenitors in Human Brain Organoids. *Cell Stem Cell* **20**, 397-406.e5 (2017).

34. Li, H. *et al.* Zika Virus Infects Neural Progenitors in the Adult Mouse Brain and Alters Proliferation. *Cell Stem Cell* (2016). doi:10.1016/j.stem.2016.08.005

35. Meertens, L. *et al.* Axl Mediates ZIKA Virus Entry in Human Glial Cells and Modulates Innate Immune Responses. *Cell Rep.* **18**, 324–333 (2017).

36. Lum, F.-M. M. *et al.* Zika Virus Infects Human Fetal Brain Microglia and Induces Inflammation. *Clin. Infect. Dis.* **64**, 914–920 (2017).

37. Retallack, H. *et al.* Zika virus cell tropism in the developing human brain and inhibition by azithromycin. *Proc. Natl. Acad. Sci. U.S.A.* **113**, 14408–14413 (2016).

38. Miner, J. J. *et al.* Zika Virus Infection in Mice Causes Panuveitis with Shedding of Virus in Tears. *Cell Rep.* **16**, 3208–3218 (2016).

39. Tan, J. J. L. *et al.* Persistence of Zika virus in conjunctival fluid of convalescence patients. *Sci. Rep.* **7**, 11194 (2017).

40. Mead, P. S. *et al.* Zika Virus Shedding in Semen of Symptomatic Infected Men. *N. Engl. J. Med.* **378**, 1377–1385 (2018).

41. Govero, J. *et al.* Zika virus infection damages the testes in mice. *Nature* (2016). doi:10.1038/nature20556

42. Ma, W. *et al.* Zika Virus Causes Testis Damage and Leads to Male Infertility in Mice. *Cell* **167**, 1511-1524.e10 (2016).

43. Sun, X. *et al.* Transcriptional Changes during Naturally Acquired Zika Virus Infection Render Dendritic Cells Highly Conducive to Viral Replication. *Cell Rep* **21**, 3471–3482 (2017).

44. Hamel, R. *et al.* Biology of Zika Virus Infection in Human Skin Cells. *J Virol* **89**, 8880–8896 (2015).

45. Michlmayr, D., Andrade, P., Gonzalez, K., Balmaseda, A. & Harris, E. CD14(+)CD16(+) monocytes are the main target of Zika virus infection in peripheral blood mononuclear cells in a paediatric study in Nicaragua. *Nat Microbiol* 1 (2017). doi:10.1038/s41564-017-0035-0

46. DICK, G. W. Zika virus. II. Pathogenicity and physical properties. *Trans. R. Soc. Trop. Med. Hyg.* **46**, 521–534 (1952).

47. Sirohi, D. & Kuhn, R. J. Zika Virus Structure, Maturation, and Receptors. *J. Infect. Dis.* **216**, S935–S944 (2017).

48. Mottin, M. *et al.* The A-Z of Zika drug discovery. *Drug Discov. Today* (2018). doi:10.1016/j.drudis.2018.06.014

49. Hamel, R. *et al.* Biology of Zika Virus Infection in Human Skin Cells. *J Virol* **89**, 8880–8896 (2015).

50. Wells, M. F. *et al.* Genetic Ablation of AXL Does Not Protect Human Neural Progenitor Cells and Cerebral Organoids from Zika Virus Infection. *Cell Stem Cell* **19**, 703–708 (2016).

51. Hastings, A. K. *et al.* TAM Receptors Are Not Required for Zika Virus Infection in Mice. *Cell Rep.* **19**, 558–568 (2017).

52. Srivastava, M. *et al.* Chemical proteomics tracks virus entry and uncovers NCAM1 as Zika virus receptor. *Nat. Commun.* **11**, 3896 (2020).

53. Persaud, M., Martinez-Lopez, A., Buffone, C., Porcelli, S. A. & Diaz-Griffero, F. Infection by Zika viruses requires the transmembrane protein AXL, endocytosis and low pH. *Virology* **518**, 301–312 (2018).

54. Allison, S. L. *et al.* Oligomeric rearrangement of tick-borne encephalitis virus envelope proteins induced by an acidic pH. *J. Virol.* **69**, 695–700 (1995).

55. Modis, Y., Ogata, S., Clements, D. & Harrison, S. C. Structure of the dengue virus envelope protein after membrane fusion. *Nature* **427**, 313–319 (2004).

56. Rawle, R. J., Webster, E. R., Jelen, M., Kasson, P. M. & Boxer, S. G. pH Dependence of Zika Membrane Fusion Kinetics Reveals an Off-Pathway State. *ACS Cent. Sci.* **4**, 1503–1510 (2018).

57. Lindenbach, B. D. & Rice, C. M. Molecular biology of flaviviruses. *Adv. Virus Res.* **59**, 23–61 (2003).

58. Cortese, M. *et al.* Ultrastructural Characterization of Zika Virus Replication Factories. *Cell Rep.* **18**, 2113–2123 (2017).

59. Hoenen, A., Liu, W., Kochs, G., Khromykh, A. A. & Mackenzie, J. M. West Nile virus-induced cytoplasmic membrane structures provide partial protection against the interferon-induced antiviral MxA protein. *J. Gen. Virol.* **88**, 3013–3017 (2007).

60. Zhang, X. *et al.* Zika Virus NS2A-Mediated Virion Assembly. *MBio* **10**, (2019).

61. Li, L. *et al.* The flavivirus precursor membrane-envelope protein complex: structure and maturation. *Science (80-.).* **319**, 1830–1834 (2008).

62. Prasad, V. M. *et al.* Structure of the immature Zika virus at 9 Å resolution. *Nat. Struct. Mol. Biol.* **24**, 184–186 (2017).

63. Yu, I.-M. *et al.* Structure of the immature dengue virus at low pH primes proteolytic maturation. *Science* **319**, 1834–7 (2008).

64. Sirohi, D. & Kuhn, R. J. Zika Virus Structure, Maturation, and Receptors. *J. Infect. Dis.* **216**, S935–S944 (2017).

65. Jiang, S., Du, L. & Shi, Z. An emerging coronavirus causing pneumonia outbreak in Wuhan, China: calling for developing therapeutic and prophylactic strategies. *Emerg. Microbes Infect.* **9**, 275–277 (2020).

66. Zhu, N. *et al.* A Novel Coronavirus from Patients with Pneumonia in China, 2019. *N. Engl. J. Med.* **382**, 727–733 (2020).

67. Wu, F. *et al.* A new coronavirus associated with human respiratory disease in China. *Nature* **579**, 265–269 (2020).

68. Zhou, P. *et al.* A pneumonia outbreak associated with a new coronavirus of probable bat origin. *Nature* **579**, 270–273 (2020).

69. Coronaviridae Study Group of the International Committee on Taxonomy of Viruses. The species Severe acute respiratory syndrome-related coronavirus: classifying 2019-nCoV and naming it SARS-CoV-2. *Nat. Microbiol.* **5**, 536–544 (2020).

70. Chan, J. F.-W. *et al.* A familial cluster of pneumonia associated with the 2019 novel coronavirus indicating person-to-person transmission: a study of a family cluster.

Lancet **395**, 514–523 (2020).

71. Chen, N. *et al.* Epidemiological and clinical characteristics of 99 cases of 2019 novel coronavirus pneumonia in Wuhan, China: a descriptive study. *Lancet* **395**, 507–513 (2020).

72. World Health Organization. Coronavirus disease 2019 (COVID-19): situation report, 51. *World Health Organization* (2020). Available at: https://apps.who.int/iris/handle/10665/331475. (Accessed: 20th February 2021)

73. Paraskevis, D. *et al.* Full-genome evolutionary analysis of the novel corona virus (2019-nCoV) rejects the hypothesis of emergence as a result of a recent recombination event. *Infect. Genet. Evol.* **79**, 104212 (2020).

74. Zarocostas, J. WHO team begins COVID-19 origin investigation. *Lancet* **397**, 459 (2021).

75. Meyerowitz, E. A., Richterman, A., Bogoch, I. I., Low, N. & Cevik, M. Towards an accurate and systematic characterisation of persistently asymptomatic infection with SARS-CoV-2. *Lancet. Infect. Dis.* **0**, (2020).

76. The Novel Coronavirus Pneumonia Emergency Response Epidemiology Team. The Epidemiological Characteristics of an Outbreak of 2019 Novel Coronavirus Diseases (COVID-19) — China, 2020. *China CDC Wkly.* **2**, 113–122 (2020).

77. Wang, D. *et al.* Clinical Characteristics of 138 Hospitalized Patients With 2019 Novel Coronavirus–Infected Pneumonia in Wuhan, China. *JAMA* **323**, 1061 (2020).

78. Huang, C. *et al.* Clinical features of patients infected with 2019 novel coronavirus in Wuhan, China. *Lancet* **395**, 497–506 (2020).

79. Giacomelli, A. *et al.* Self-reported Olfactory and Taste Disorders in Patients With Severe Acute Respiratory Coronavirus 2 Infection: A Cross-sectional Study. *Clin. Infect. Dis.* **71**, 889–890 (2020).

80. Sudre, C. H. *et al.* Attributes and predictors of long COVID. *Nat. Med.* 1–6 (2021). doi:10.1038/s41591-021-01292-y

81. Huang, C. *et al.* 6-month consequences of COVID-19 in patients discharged from hospital: a cohort study. *Lancet* **397**, 220–232 (2021).

82. FDA. Coronavirus (COVID-19) Update: FDA Authorizes Monoclonal Antibody for Treatment of COVID-19. (2020). Available at: https://www.fda.gov/news-events/press-announcements/coronavirus-covid-19-update-fda-authorizes-monoclonal-antibody-treatment-covid-19. (Accessed: 13th March 2021)

83. FDA. Coronavirus (COVID-19) Update: FDA Authorizes Monoclonal Antibodies for Treatment of COVID-19. (2020). Available at: https://www.fda.gov/news-events/press-announcements/coronavirus-covid-19-update-fda-authorizes-monoclonal-antibodies-treatment-covid-19. (Accessed: 13th March 2021)

84. Chen, P. *et al.* SARS-CoV-2 Neutralizing Antibody LY-CoV555 in Outpatients with Covid-19. *N. Engl. J. Med.* **384**, 229–237 (2021).

85. Weinreich, D. M. *et al.* REGN-COV2, a Neutralizing Antibody Cocktail, in Outpatients with Covid-19. *N. Engl. J. Med.* **384**, 238–251 (2021).

86. FDA. Coronavirus (COVID-19) Update: FDA Authorizes Monoclonal Antibodies for Treatment of COVID-19. (2021). Available at: https://www.fda.gov/news-events/press-announcements/coronavirus-covid-19-update-fda-authorizes-monoclonal-antibodies-treatment-covid-19-0. (Accessed: 13th March 2021)

87. FDA. FDA's approval of Veklury (remdesivir) for the treatment of COVID-19—The Science of Safety and Effectiveness. (2020). Available at: https://www.fda.gov/drugs/drug-safety-and-availability/fdas-approval-veklury-remdesivir-treatment-covid-19-science-safety-and-effectiveness. (Accessed: 13th March 2021)

88. Liu, D. X., Liang, J. Q. & Fung, T. S. Human Coronavirus-229E, -OC43, -NL63, and -HKU1. in *Encyclopedia of Virology* (Elsevier, 2021). doi:10.1016/B978-0-12-809633-8.21501-X

89. Walsh, E. E., Shin, J. H. & Falsey, A. R. Clinical impact of human coronaviruses 229E and OC43 infection in diverse adult populations. *J. Infect. Dis.* **208**, 1634–42 (2013).

90. Gerna, G. *et al.* Genetic Variability of Human Coronavirus OC43-, 229E-, and NL63-Like Strains and Their Association With Lower Respiratory Tract Infections of Hospitalized Infants and Immunocompromised Patients. *J. Med. Virol.* **78**, 938–949 (2006).

91. Pene, F. *et al.* Coronavirus 229E-related pneumonia in immunocompromised patients. *Clin. Infect. Dis.* **37**, 929–32 (2003).

92. Arbour, N., Day, R., Newcombe, J. & Talbot, P. J. Neuroinvasion by human respiratory coronaviruses. *J. Virol.* **74**, 8913–21 (2000).

93. Arbour, N. *et al.* Persistent infection of human oligodendrocytic and neuroglial cell lines by human coronavirus 229E. *J. Virol.* **73**, 3326–37 (1999).

94. Hawman, D. W. *et al.* A DNA-based vaccine protects against Crimean-Congo haemorrhagic fever virus disease in a Cynomolgus macaque model. *Nat. Microbiol.* **6**, 187–195 (2021).

95. Dowall, S. D. *et al.* Hazara virus infection is lethal for adult type I interferon receptor-knockout mice and may act as a surrogate for infection with the human-pathogenic Crimean–Congo hemorrhagic fever virus. *J. Gen. Virol.* **93**, 560–564 (2012).

96. Monteil, V., Salata, C., Appelberg, S. & Mirazimi, A. Hazara virus and Crimean-Congo Hemorrhagic Fever Virus show a different pattern of entry in fully-polarized Caco-2 cell line. *PLoS Negl. Trop. Dis.* **14**, e0008863 (2020).

97. WHO. Disease outbreak news. Ebola virus disease - Guinea. (2021). Available at: https://www.who.int/csr/don/17-february-2021-ebola-gin/en/.

98. WHO. Disease outbreak news. Ebola virus disease - Democratic Republic of the Congo. *2021* Available at: https://www.who.int/csr/don/10-february-2021-ebola-drc/en/.

99. Ehrhardt, S. A. *et al.* Polyclonal and convergent antibody response to Ebola virus vaccine rVSV-ZEBOV. *Nat. Med.* (2019). doi:10.1038/s41591-019-0602-4

100. Henao-Restrepo, A. M. *et al.* Efficacy and effectiveness of an rVSV-vectored vaccine in preventing Ebola virus disease: final results from the Guinea ring vaccination, open-

label, cluster-randomised trial (Ebola Ça Suffit!). *Lancet* **389**, 505–518 (2017).

101. Milligan, I. D. *et al.* Safety and Immunogenicity of Novel Adenovirus Type 26– and Modified Vaccinia Ankara–Vectored Ebola Vaccines. *JAMA* **315**, 1610 (2016).

102. FDA. FDA Approves First Treatment for Ebola Virus. (2020). Available at: https://www.fda.gov/news-events/press-announcements/fda-approves-first-treatment-ebola-virus. (Accessed: 26th March 2021)

103. FDA. FDA Approves Treatment for Ebola Virus. (2020). Available at: https://www.fda.gov/drugs/drug-safety-and-availability/fda-approves-treatment-ebola-virus. (Accessed: 26th March 2021)

104. Gaudinski, M. R. *et al.* Safety, tolerability, pharmacokinetics, and immunogenicity of the therapeutic monoclonal antibody mAb114 targeting Ebola virus glycoprotein (VRC 608): an open-label phase 1 study. *Lancet* **393**, 889–898 (2019).

105. Ianevski, A., Andersen, P. I., Merits, A., Bjør as, M. & Kainov, D. Expanding the activity spectrum of antiviral agents. *Drug Discov. Today* (2019). doi:10.1016/j.drudis.2019.04.006

106. Bruenn, J. A. A structural and primary sequence comparison of the viral RNA-dependent RNA polymerases. *Nucleic Acids Res.* **31**, 1821–9 (2003).

107. Chaudhuri, S., Symons, J. A. & Deval, J. Innovation and trends in the development and approval of antiviral medicines: 1987–2017 and beyond. *Antiviral Res.* **155**, 76–88 (2018).

108. Bösl, K. *et al.* Common Nodes of Virus-Host Interaction Revealed Through an Integrated Network Analysis. *Front. Immunol.* **10**, 2186 (2019).

109. Streeter, D. G. *et al.* Mechanism of Action of 1-β-D-Ribofuranosyl-1,2,4-Triazole-3-Carboxamide (Virazole), A New Broad-Spectrum Antiviral Agent. *Proc Natl. Acad Sci* **70**, 1174–1178 (1973).

110. Sidwell, R. W. *et al.* Broad-spectrum antiviral activity of Virazole: 1-beta-D-ribofuranosyl-1,2,4-triazole-3-carboxamide. *Science (80-.).* **177**, 705–706 (1972).

111. Fried, M. W. *et al.* Peginterferon alfa-2a plus ribavirin for chronic hepatitis C virus infection. *N. Engl. J. Med.* **347**, 975–982 (2002).

112. Feld, J. J. *et al.* Ribavirin improves early responses to peginterferon through improved interferon signaling. *Gastroenterology* **139**, 154–62.e4 (2010).

113. Bansal, S., Singal, A. K., McGuire, B. M. & Anand, B. S. Impact of all oral anti-hepatitis C virus therapy: A meta-analysis. *World J Hepatol.* **7**, 806–813 (2015).

114. Ascioglu, S., Leblebicioglu, H., Vahaboglu, H. & Chan, K. A. Ribavirin for patients with Crimean-Congo haemorrhagic fever: a systematic review and meta-analysis. *J. Antimicrob. Chemother.* **66**, 1215–1222 (2011).

115. Soares-Weiser, K., Thomas, S., Thomson, G. & Garner, P. Ribavirin for Crimean-Congo hemorrhagic fever: systematic review and meta-analysis. *BMC Infect. Dis.* **10**, 207 (2010).

116. Kim, J.-A., Seong, R.-K., Kumar, M. & Shin, O. Favipiravir and Ribavirin Inhibit Replication of Asian and African Strains of Zika Virus in Different Cell Models.

Viruses **10**, 72 (2018).

117. Kamiyama, N. *et al.* Ribavirin inhibits Zika virus (ZIKV) replication in vitro and suppresses viremia in ZIKV-infected STAT1-deficient mice. *Antiviral Res.* **146**, 1–11 (2017).

118. Dixit, N. M. & Perelson, A. S. The metabolism, pharmacokinetics and mechanisms of antiviral activity of ribavirin against hepatitis C virus. *Cell Mol Life Sci C.* **63**, 832–842 (2006).

119. Todt, D. *et al.* In vivo evidence for ribavirin-induced mutagenesis of the hepatitis E virus genome. *Gut* **65**, 1733–1743 (2016).

120. Vignuzzi, M., Stone, J. K. & Andino, R. Ribavirin and lethal mutagenesis of poliovirus: molecular mechanisms, resistance and biological implications. *Virus Res.* **107**, 173–181 (2005).

121. Markland, W., McQuaid, T. J., Jain, J. & Kwong, A. D. Broad-spectrum antiviral activity of the IMP dehydrogenase inhibitor VX-497: a comparison with ribavirin and demonstration of antiviral additivity with alpha interferon. *Antimicrob. Agents Chemother.* **44**, 859–866 (2000).

122. Tam, R. C. *et al.* Ribavirin polarizes human T cell responses towards a Type 1 cytokine profile. *J. Hepatol.* **30**, 376–382 (1999).

123. Perales, C., Quer, J., Gregori, J., Esteban, J. & Domingo, E. Resistance of Hepatitis C Virus to Inhibitors: Complexity and Clinical Implications. *Viruses* **7**, 5746–5766 (2015).

124. Ibarra, K. D., Jain, M. K. & Pfeiffer, J. K. Host-Based Ribavirin Resistance Influences Hepatitis C Virus Replication and Treatment Response. *J Virol* **85**, 7273–7283 (2011).

125. Sung, H., Chang, M. & Saab, S. Management of Hepatitis C Antiviral Therapy Adverse Effects. *Curr. Hepat. Rep.* **10**, 33–40 (2011).

126. Warren, T. *et al.* Nucleotide Prodrug GS-5734 Is a Broad-Spectrum Filovirus Inhibitor That Provides Complete Therapeutic Protection Against the Development of Ebola Virus Disease (EVD) in Infected Non-human Primates. *Open Forum Infect. Dis.* **2**, (2015).

127. Warren, T. K. *et al.* Therapeutic efficacy of the small molecule GS-5734 against Ebola virus in rhesus monkeys. *Nature* **531**, 381–385 (2016).

128. Lo, M. K. *et al.* GS-5734 and its parent nucleoside analog inhibit Filo-, Pneumo-, and Paramyxoviruses. *Sci. Rep.* **7**, 43395 (2017).

129. Sheahan, T. P. *et al.* Broad-spectrum antiviral GS-5734 inhibits both epidemic and zoonotic coronaviruses. *Sci. Transl. Med.* **9**, (2017).

130. Mulangu, S. *et al.* A Randomized, Controlled Trial of Ebola Virus Disease Therapeutics. *N. Engl. J. Med.* **381**, 2293–2303 (2019).

131. Wang, M. *et al.* Remdesivir and chloroquine effectively inhibit the recently emerged novel coronavirus (2019-nCoV) in vitro. *Cell Res.* **30**, 269–271 (2020).

132. Beigel, J. H. *et al.* Remdesivir for the Treatment of Covid-19 — Final Report. *N. Engl. J. Med.* **383**, 1813–1826 (2020).

133. Spinner, C. D. *et al.* Effect of Remdesivir vs Standard Care on Clinical Status at 11 Days in Patients With Moderate COVID-19. *JAMA* **324**, 1048 (2020).

134. Goldman, J. D. *et al.* Remdesivir for 5 or 10 Days in Patients with Severe Covid-19. *N. Engl. J. Med.* **383**, 1827–1837 (2020).

135. Consortium, W. S. T. Repurposed Antiviral Drugs for Covid-19 — Interim WHO Solidarity Trial Results. *N. Engl. J. Med.* **384**, 497–511 (2021).

136. Furuta, Y. *et al.* Favipiravir (T-705), a novel viral RNA polymerase inhibitor. *Antiviral Res.* **100**, 446–54 (2013).

137. Delang, L., Abdelnabi, R. & Neyts, J. Favipiravir as a potential countermeasure against neglected and emerging RNA viruses. *Antiviral Res.* **153**, 85–94 (2018).

138. Phase 3 Efficacy and Safety Study of Favipiravir for Treatment of Uncomplicated Influenza in Adults. (2015). Available at: https://clinicaltrials.gov/ct2/show/NCT02008344. (Accessed: 29th March 2021)

139. Baranovich, T. *et al.* T-705 (favipiravir) induces lethal mutagenesis in influenza A H1N1 viruses in vitro. *J. Virol.* **87**, 3741–51 (2013).

140. Vanderlinden, E. *et al.* Distinct Effects of T-705 (Favipiravir) and Ribavirin on Influenza Virus Replication and Viral RNA Synthesis. *Antimicrob. Agents Chemother.* **60**, 6679–6691 (2016).

141. Daikoku, T., Yoshida, Y., Okuda, T. & Shiraki, K. Characterization of susceptibility variants of influenza virus grown in the presence of T-705. *J. Pharmacol. Sci.* **126**, 281–4 (2014).

142. Drake, J. W. & Holland, J. J. Mutation rates among RNA viruses. *Proc Natl. Acad Sci* **96**, 13910–13913 (1999).

143. Little, S. J. *et al.* Antiretroviral-drug resistance among patients recently infected with HIV. *N. Engl. J. Med.* **347**, 385–94 (2002).

144. Pichlmair, A. *et al.* Viral immune modulators perturb the human molecular network by common and unique strategies. *Nature* **487**, 486–490 (2012).

145. Taguwa, S. *et al.* Defining Hsp70 Subnetworks in Dengue Virus Replication Reveals Key Vulnerability in Flavivirus Infection. *Cell* **163**, 1108–1123 (2015).

146. Scaturro, P. *et al.* An orthogonal proteomic survey uncovers novel Zika virus host factors. *Nature* 1–5 (2018). doi:10.1038/s41586-018-0484-5

147. Schneider, W. M. *et al.* Genome-Scale Identification of SARS-CoV-2 and Pan-coronavirus Host Factor Networks. *Cell* **184**, 120-132.e14 (2021).

148. Wang, R. *et al.* Genetic Screens Identify Host Factors for SARS-CoV-2 and Common Cold Coronaviruses. *Cell* **184**, 106-119.e14 (2021).

149. Daniloski, Z. *et al.* Identification of Required Host Factors for SARS-CoV-2 Infection in Human Cells. *Cell* **184**, 92-105.e16 (2021).

150. Wei, J. *et al.* Genome-wide CRISPR Screens Reveal Host Factors Critical for SARS-CoV-2 Infection. *Cell* **184**, 76-91.e13 (2021).

151. Tan, G., Song, H., Xu, F. & Cheng, G. When Hepatitis B Virus Meets Interferons. *Front. Microbiol.* **9**, 1611 (2018).

152. Group, T. R. C. Dexamethasone in Hospitalized Patients with Covid-19. *N. Engl. J. Med.* **384**, 693–704 (2021).

153. Schor, S. & Einav, S. Repurposing of Kinase Inhibitors as Broad-Spectrum Antiviral Drugs. *DNA Cell Biol.* **37**, 63–69 (2017).

154. Bekerman, E. *et al.* Anticancer kinase inhibitors impair intracellular viral trafficking and exert broad-spectrum antiviral effects. *J. Clin. Invest.* **127**, 1338–1352 (2017).

155. Mazzon, M. & Mercer, J. Lipid interactions during virus entry and infection. *Cell. Microbiol.* **16**, 1493–502 (2014).

156. Martínez-Gutierrez, M., Castellanos, J. E. & Gallego-Gómez, J. C. Statins reduce dengue virus production via decreased virion assembly. *Intervirology* **54**, 202–16 (2011).

157. Zhu, Q. *et al.* Statin therapy improves response to interferon alfa and ribavirin in chronic hepatitis C: a systematic review and meta-analysis. *Antiviral Res.* **98**, 373–9 (2013).

158. Giguère, J.-F. & Tremblay, M. J. Statin compounds reduce human immunodeficiency virus type 1 replication by preventing the interaction between virion-associated host intercellular adhesion molecule 1 and its natural cell surface ligand LFA-1. *J. Virol.* **78**, 12062–5 (2004).

159. Delang, L. *et al.* Statins potentiate the in vitro anti-hepatitis C virus activity of selective hepatitis C virus inhibitors and delay or prevent resistance development. *Hepatology* **50**, 6–16 (2009).

160. Frausto, S. D., Lee, E. & Tang, H. Cyclophilins as modulators of viral replication. *Viruses* **5**, 1684–701 (2013).

161. Hopkins, S. *et al.* The cyclophilin inhibitor SCY-635 suppresses viral replication and induces endogenous interferons in patients with chronic HCV genotype 1 infection. *J. Hepatol.* **57**, 47–54 (2012).

162. Flisiak, R. *et al.* The cyclophilin inhibitor Debio 025 combined with PEG IFNalpha2a significantly reduces viral load in treatment-naïve hepatitis C patients. *Hepatology* **49**, 1460–8 (2009).

163. Geller, R., Taguwa, S. & Frydman, J. Broad action of Hsp90 as a host chaperone required for viral replication. *Biochim. Biophys. Acta - Mol. Cell Res.* **1823**, 698–706 (2012).

164. Wan, Q., Song, D., Li, H. & He, M. Stress proteins: the biological functions in virus infection, present and challenges for target-based antiviral drug development. *Signal Transduct. Target. Ther.* **5**, 125 (2020).

165. Moffat, J. G., Vincent, F., Lee, J. A., Eder, J. & Prunotto, M. Opportunities and challenges in phenotypic drug discovery: An industry perspective. *Nat. Rev. Drug Discov.* **16**, 531–543 (2017).

166. Swinney, D. C. & Anthony, J. How were new medicines discovered? *Nat Rev Drug*

Discov **10**, 507 (2011).

167. Berdichevsky, Y. *et al.* A novel high throughput screening assay for HCV NS3 serine protease inhibitors. *J. Virol. Methods* **107**, 245–55 (2003).

168. Sáez-Álvarez, Y., Arias, A., del Águila, C. & Agudo, R. Development of a fluorescence-based method for the rapid determination of Zika virus polymerase activity and the screening of antiviral drugs. *Sci. Rep.* **9**, 5397 (2019).

169. Basu, A., Mills, D. M. & Bowlin, T. L. High-throughput screening of viral entry inhibitors using pseudotyped virus. *Curr. Protoc. Pharmacol.* **Chapter 13**, Unit 13B.3 (2010).

170. Salata, C. *et al.* Ebola Virus Entry: From Molecular Characterization to Drug Discovery. *Viruses* **11**, (2019).

171. Tao, W., Gan, T., Guo, M., Xu, Y. & Zhong, J. Novel Stable Ebola Virus Minigenome Replicon Reveals Remarkable Stability of the Viral Genome. *J. Virol.* **91**, (2017).

172. Patkar, C. G., Larsen, M., Owston, M., Smith, J. L. & Kuhn, R. J. Identification of inhibitors of yellow fever virus replication using a replicon-based high-throughput assay. *Antimicrob. Agents Chemother.* **53**, 4103–14 (2009).

173. Kotaki, T., Xie, X., Shi, P.-Y. & Kameoka, M. A PCR amplicon-based SARS-CoV-2 replicon for antiviral evaluation. *Sci. Rep.* **11**, 2229 (2021).

174. Xie, X. *et al.* Inhibition of dengue virus by targeting viral NS4B protein. *J. Virol.* **85**, 11183–95 (2011).

175. Phan, N. *et al.* A simple high-throughput approach identifies actionable drug sensitivities in patient-derived tumor organoids. *Commun. Biol.* **2**, 78 (2019).

176. Brodin, B. A. *et al.* Drug sensitivity testing on patient-derived sarcoma cells predicts patient response to treatment and identifies c-Sarc inhibitors as active drugs for translocation sarcomas. *Br. J. Cancer* **120**, 435–443 (2019).

177. Saeed, K. *et al.* Comprehensive Drug Testing of Patient-derived Conditionally Reprogrammed Cells from Castration-resistant Prostate Cancer. *Eur. Urol.* **71**, 319–327 (2017).

178. Hild, M. & Jaffe, A. B. Production of 3-D Airway Organoids From Primary Human Airway Basal Cells and Their Use in High-Throughput Screening. *Curr. Protoc. Stem Cell Biol.* **37**, IE.9.1-IE.9.15 (2016).

179. Renner, H. *et al.* A fully automated high-throughput workflow for 3D-based chemical screening in human midbrain organoids. *Elife* **9**, (2020).

180. Pudelko, L. *et al.* An orthotopic glioblastoma animal model suitable for high-throughput screenings. *Neuro. Oncol.* **20**, 1475–1484 (2018).

181. Zhang, Z.-R. *et al.* A cell-based large-scale screening of natural compounds for inhibitors of SARS-CoV-2. *Signal Transduct. Target. Ther.* **5**, 218 (2020).

182. Xu, M. *et al.* Identification of small-molecule inhibitors of Zika virus infection and induced neural cell death via a drug repurposing screen. *Nat. Med.* **22**, 1101–1107 (2016).

183. Schmidtke, M., Schnittler, U., Jahn, B., Dahse, H. & Stelzner, A. A rapid assay for evaluation of antiviral activity against coxsackie virus B3, influenza virus A, and herpes simplex virus type 1. *J. Virol. Methods* **95**, 133–43 (2001).

184. Wagner, B. K. & Schreiber, S. L. The Power of Sophisticated Phenotypic Screening and Modern Mechanism-of-Action Methods. *Cell Chem. Biol.* **23**, 3–9 (2016).

185. Kaur, P. *et al.* Inhibition of chikungunya virus replication by harringtonine, a novel antiviral that suppresses viral protein expression. *Antimicrob. Agents Chemother.* **57**, 155–67 (2013).

186. Bernatchez, J. A. *et al.* Development and Validation of a Phenotypic High-Content Imaging Assay for Assessing the Antiviral Activity of Small-Molecule Inhibitors Targeting Zika Virus. *Antimicrob. Agents Chemother.* **62**, (2018).

187. Zhou, T. *et al.* High-Content Screening in hPSC-Neural Progenitors Identifies Drug Candidates that Inhibit Zika Virus Infection in Fetal-like Organoids and Adult Brain. *Cell Stem Cell* (2017). doi:10.1016/j.stem.2017.06.017

188. Postnikova, E. *et al.* Testing therapeutics in cell-based assays: Factors that influence the apparent potency of drugs. *PLoS One* **13**, e0194880 (2018).

189. Riva, L. *et al.* Discovery of SARS-CoV-2 antiviral drugs through large-scale compound repurposing. *Nature* **586**, 113–119 (2020).

190. Caicedo, J. C., Singh, S. & Carpenter, A. E. Applications in image-based profiling of perturbations. *Curr. Opin. Biotechnol.* **39**, 134–142 (2016).

191. Bray, M.-A. *et al.* Cell Painting, a high-content image-based assay for morphological profiling using multiplexed fluorescent dyes. *Nat. Protoc.* (2016). doi:10.1038/nprot.2016.105

192. Carpenter, A. E. *et al.* CellProfiler: image analysis software for identifying and quantifying cell phenotypes. *Genome Biol.* **7**, R100 (2006).

193. McQuin, C. *et al.* CellProfiler 3.0: Next-generation image processing for biology. *PLOS Biol.* **16**, e2005970 (2018).

194. Chandrasekaran, S. N., Ceulemans, H., Boyd, J. D. & Carpenter, A. E. Image-based profiling for drug discovery: due for a machine-learning upgrade? *Nat. Rev. Drug Discov.* **20**, 145–159 (2021).

195. Woehrmann, M. H. *et al.* Large-scale cytological profiling for functional analysis of bioactive compounds. *Mol. Biosyst.* **9**, 2604 (2013).

196. Christoforow, A. *et al.* Design, Synthesis, and Phenotypic Profiling of Pyrano-Furo-Pyridone Pseudo Natural Products. *Angew. Chemie Int. Ed.* **58**, 14715–14723 (2019).

197. Bray, M.-A. *et al.* A dataset of images and morphological profiles of 30 000 small-molecule treatments using the Cell Painting assay. **6**, 1–5 (2017).

198. Way, G. P. *et al.* Predicting cell health phenotypes using image-based morphology profiling. *Mol. Biol. Cell* E20-12–0784 (2021). doi:10.1091/mbc.E20-12-0784

199. Slack, M. D., Martinez, E. D., Wu, L. F. & Altschuler, S. J. Characterizing heterogeneous cellular responses to perturbations. *Proc. Natl. Acad. Sci.* (2008).

200. Reisen, F. *et al.* Linking phenotypes and modes of action through high-content screen fingerprints. *Assay Drug Dev. Technol.* **13**, 415–27 (2015).

201. Laraia, L. *et al.* Image-Based Morphological Profiling Identifies a Lysosomotropic, Iron-Sequestering Autophagy Inhibitor. *Angew. Chemie Int. Ed.* **59**, 5721–5729 (2020).

202. Cataldo, A. M. *et al.* Abnormalities in mitochondrial structure in cells from patients with bipolar disorder. *Am. J. Pathol.* **177**, 575–85 (2010).

203. Blanchet, L. *et al.* Quantifying small molecule phenotypic effects using mitochondrial morpho-functional fingerprinting and machine learning. *Sci. Rep.* **5**, 8035 (2015).

204. Hung, C. L.-K. *et al.* A patient-derived cellular model for Huntington's disease reveals phenotypes at clinically relevant CAG lengths. *Mol. Biol. Cell* **29**, 2809–2820 (2018).

205. Schiff, L. *et al.* Deep learning and automated Cell Painting reveal Parkinson's disease-specific signatures in primary patient fibroblasts. *BioXriv* (2020). doi:10.1101/2020.11.13.380576

206. Rietdijk, J. *et al.* A rapid phenomics workflow for the in vitro identification of antiviral drugs. *BioXriv* (2021). doi:10.1101/2021.01.13.423947

207. Mechanism matters. *Nat. Med.* **16**, 347–347 (2010).

208. Overington, J. P., Bissan, A.-L. & Hopkins, A. L. How many drug targets are there? *Nat Rev Drug Discov* **5**, 993–996 (2006).

209. Neggers, J. E. *et al.* Target identification of small molecules using large-scale CRISPR-Cas mutagenesis scanning of essential genes. *Nat. Commun.* **9**, 502 (2018).

210. Bantscheff, M. *et al.* Quantitative chemical proteomics reveals mechanisms of action of clinical ABL kinase inhibitors. *Nat. Biotechnol.* **25**, 1035–44 (2007).

211. Niesen, F. H., Berglund, H. & Vedadi, M. The use of differential scanning fluorimetry to detect ligand interactions that promote protein stability. *Nat. Protoc.* **2**, 2212–2221 (2007).

212. Martinez Molina, D. *et al.* Monitoring drug target engagement in cells and tissues using the cellular thermal shift assay. *Science (80-.).* **341**, 84–87 (2013).

213. Jafari, R. *et al.* The cellular thermal shift assay for evaluating drug target interactions in cells. *Nat. Protoc.* **9**, 2100–2122 (2014).

214. Almqvist, H. *et al.* CETSA screening identifies known and novel thymidylate synthase inhibitors and slow intracellular activation of 5-fluorouracil. *Nat. Commun.* **7**, 11040 (2016).

215. Savitski, M. M. *et al.* Tracking cancer drugs in living cells by thermal profiling of the proteome. *Science (80-.).* **346**, 1–33 (2014).

216. Franken, H. *et al.* Thermal proteome profiling for unbiased identification of direct and indirect drug targets using multiplexed quantitative mass spectrometry. *Nat. Protoc.* **10**, 1567–1593 (2015).

217. Herneisen, A. L. *et al.* Identifying the Target of an Antiparasitic Compound in *Toxoplasma* Using Thermal Proteome Profiling. *ACS Chem. Biol.* **15**, 1801–1807

(2020).

218. Becher, I. *et al.* Thermal profiling reveals phenylalanine hydroxylase as an off-target of panobinostat. *Nat. Chem. Biol.* **12**, 908–910 (2016).

219. Reinhard, F. B. M. *et al.* Thermal proteome profiling monitors ligand interactions with cellular membrane proteins. *Nat. Methods* **12**, 1129–1131 (2015).

220. Kalxdorf, M. *et al.* Cell surface thermal proteome profiling tracks perturbations and drug targets on the plasma membrane. *Nat. Methods* **18**, 84–91 (2021).

221. Huang, J. X. *et al.* High throughput discovery of functional protein modifications by Hotspot Thermal Profiling. *Nat. Methods* **16**, 894–901 (2019).

222. Potel, C. M. *et al.* Impact of phosphorylation on thermal stability of proteins. *BioRxiv* (2020). doi:10.1101/2020.01.14.903849

223. Smith, I. R. *et al.* Identification of phosphosites that alter protein thermal stability. *BioRxiv* (2020). doi:10.1101/2020.01.14.904300

224. Tan, C. S. H. *et al.* Thermal proximity coaggregation for system-wide profiling of protein complex dynamics in cells. *Science* **359**, 1170–1177 (2018).

225. Mateus, A. *et al.* Thermal proteome profiling in bacteria: probing protein state in vivo. *Mol. Syst. Biol.* **14**, e8242 (2018).

226. Becher, I. *et al.* Pervasive Protein Thermal Stability Variation during the Cell Cycle. *Cell* **173**, 1495-1507.e18 (2018).

227. Sridharan, S. *et al.* Proteome-wide solubility and thermal stability profiling reveals distinct regulatory roles for ATP. *Nat. Commun.* **10**, 1155 (2019).

228. Selkrig, J. *et al.* SARS-CoV-2 infection remodels the host protein thermal stability landscape. *Mol. Syst. Biol.* **17**, e10188 (2021).

229. Hashimoto, Y., Sheng, X., Murray-Nerger, L. A. & Cristea, I. M. Temporal dynamics of protein complex formation and dissociation during human cytomegalovirus infection. *Nat. Commun.* **11**, 806 (2020).

230. Gullberg, R. C., Steel, J. J., Moon, S. L., Soltani, E. & Geiss, B. J. Oxidative stress influences positive strand RNA virus genome synthesis and capping. *Virology* **475**, 219–229 (2015).

231. Ivanov, A. V *et al.* Oxidative Stress during HIV Infection: Mechanisms and Consequences. **2016**, 1–18 (2016).

232. Camini, F. C., da Silva Caetano, C. C., Almeida, L. T. & de Brito Magalhães, C. L. Implications of oxidative stress on viral pathogenesis. *Arch. Virol.* **162**, 907–917 (2017).

233. Valyi-Nagy, T. & Dermody, T. S. Role of oxidative damage in the pathogenesis of viral infections of the nervous system. *Histol. Histopathol.* **20**, 957–67 (2005).

234. Gad, H. *et al.* MTH1 inhibition eradicates cancer by preventing sanitation of the dNTP pool. *Nature* **508**, 215–221 (2014).

235. Visnes, T. *et al.* Small-molecule inhibitor of OGG1 suppresses proinflammatory gene

expression and inflammation. *Science (80-.).* **362**, 834–839 (2018).

236. Zhang, J.-H., Chung, T. D. Y. & Oldenburg, K. R. A Simple Statistical Parameter for Use in Evaluation and Validation of High Throughput Screening Assays. *J. Biomol. Screen.* **4**, 67–73 (1999).

237. Radicella, J. P., Dherin, C., Desmaze, C., Fox, M. S. & Boiteux, S. Cloning and characterization of hOGG1, a human homolog of the OGG1 gene of Saccharomyces cerevisiae. *Proc. Natl. Acad. Sci. U. S. A.* **94**, 8010–5 (1997).

238. Klungland, A. & Bjelland, S. Oxidative damage to purines in DNA: role of mammalian Ogg1. *DNA Repair (Amst).* **6**, 481–8 (2007).

239. Rosenquist, T. A., Zharkov, D. O. & Grollman, A. P. Cloning and characterization of a mammalian 8-oxoguanine DNA glycosylase. *Proc. Natl. Acad. Sci. U. S. A.* **94**, 7429–34 (1997).

240. Taguwa, S. *et al.* Zika Virus Dependence on Host Hsp70 Provides a Protective Strategy against Infection and Disease. *Cell Rep* **26**, 906-920.e3 (2019).

241. Howe, M. K. *et al.* An inducible heat shock protein 70 small molecule inhibitor demonstrates anti-dengue virus activity, validating Hsp70 as a host antiviral target. *Antiviral Res.* **130**, 81–92 (2016).

242. Qian, X. *et al.* Brain-Region-Specific Organoids Using Mini-bioreactors for Modeling ZIKV Exposure. *Cell* **165**, 1238–1254 (2016).

243. Watanabe, M. *et al.* Self-Organized Cerebral Organoids with Human-Specific Features Predict Effective Drugs to Combat Zika Virus Infection. *Cell Rep.* **21**, 517–532 (2017).

244. Kamiyama, N. *et al.* Ribavirin inhibits Zika virus (ZIKV) replication in vitro and suppresses viremia in ZIKV-infected STAT1-deficient mice. *Antivir Res* **146**, 1–11 (2017).

245. Oestereich, L. *et al.* Evaluation of antiviral efficacy of ribavirin, arbidol, and T-705 (favipiravir) in a mouse model for Crimean-Congo hemorrhagic fever. *PLoS Negl Trop Dis* **8**, e2804 (2014).

246. Hung, I. F.-N. *et al.* Triple combination of interferon beta-1b, lopinavir-ritonavir, and ribavirin in the treatment of patients admitted to hospital with COVID-19: an open-label, randomised, phase 2 trial. *Lancet* **395**, 1695–1704 (2020).

247. Gabriel, E. *et al.* Recent Zika Virus Isolates Induce Premature Differentiation of Neural Progenitors in Human Brain Organoids. *Cell Stem Cell* **20**, 397-406.e5 (2017).

248. Yin, Y., Xu, Y., Ou, Z., Yang, X. & Liu, H. An antiviral drug screening system for enterovirus 71 based on an improved plaque assay: A potential high-throughput method. *J. Med. Virol.* **91**, 1440–1447 (2019).

249. Lee, E. M., Titus, S. A., Xu, M., Tang, H. & Zheng, W. High-Throughput Zika Viral Titer Assay for Rapid Screening of Antiviral Drugs. *Assay Drug Dev. Technol.* **17**, 128–139 (2019).

250. Zhou, T. *et al.* High-Content Screening in hPSC-Neural Progenitors Identifies Drug Candidates that Inhibit Zika Virus Infection in Fetal-like Organoids and Adult Brain.

Cell Stem Cell **21**, 274-283.e5 (2017).

251. Barrows, N. J. *et al.* A Screen of FDA-Approved Drugs for Inhibitors of Zika Virus Infection. *Cell Host Microbe* **20**, 259–270 (2016).

252. Ouyang, W., Mueller, F., Hjelmare, M., Lundberg, E. & Zimmer, C. ImJoy: an open-source computational platform for the deep learning era. *Nat. Methods* **16**, 1199–1200 (2019).

253. Nyffeler, J. *et al.* Bioactivity screening of environmental chemicals using imaging-based high-throughput phenotypic profiling. *Toxicol. Appl. Pharmacol.* **389**, 114876 (2020).

254. Cox, M. J. *et al.* Tales of 1,008 small molecules: phenomic profiling through live-cell imaging in a panel of reporter cell lines. *Sci. Rep.* **10**, 13262 (2020).

255. Zhang, Q., Li, J., Peng, S., Zhang, Y. & Qiao, Y. Rosmarinic Acid as a Candidate in a Phenotypic Profiling Cardio-/Cytotoxicity Cell Model Induced by Doxorubicin. *Molecules* **25**, 836 (2020).

256. Calafat, J. & Hageman, P. C. Binding of Concanavalin A to the Envelope of Two Murine RNA Tumour Viruses. *J. Gen. Virol.* **14**, 103–106 (1972).

257. Perez, L., Estepa, A. & Coll, J. M. Purification of the glycoprotein G from viral haemorrhagic septicaemia virus, a fish rhabdovirus, by lectin affinity chromatography. *J. Virol. Methods* **76**, 1–8 (1998).

258. Pashov, A. *et al.* Concanavalin A binding to HIV envelope protein is less sensitive to mutations in glycosylation sites than monoclonal antibody 2G12. *Glycobiology* **15**, 994–1001 (2005).

259. Mirabelli, C. *et al.* Morphological Cell Profiling of SARS-CoV-2 Infection Identifies Drug Repurposing 1 Candidates for COVID-19. *BioRxiv* (2020). doi:10.1101/2020.05.27.117184

260. Heiser, K. *et al.* Title: Identification of potential treatments for COVID-19 through artificial intelligence-enabled phenomic analysis of human cells infected with SARS-CoV-2. *BioXriv* (2020). doi:10.1101/2020.04.21.054387

261. Hoffmann, M. *et al.* SARS-CoV-2 Cell Entry Depends on ACE2 and TMPRSS2 and Is Blocked by a Clinically Proven Protease Inhibitor. *Cell* **181**, 271-280.e8 (2020).

262. Eggert, U. S. *et al.* Parallel chemical genetic and genome-wide RNAi screens identify cytokinesis inhibitors and targets. *PLoS Biol.* **2**, e379 (2004).

263. Ohnuki, S., Oka, S., Nogami, S. & Ohya, Y. High-Content, Image-Based Screening for Drug Targets in Yeast. *PLoS One* **5**, e10177 (2010).

264. Breinig, M., Klein, F. A., Huber, W. & Boutros, M. A chemical-genetic interaction map of small molecules using high-throughput imaging in cancer cells. *Mol. Syst. Biol.* **11**, 846 (2015).

265. Proschak, E., Stark, H. & Merk, D. Polypharmacology by Design: A Medicinal Chemist's Perspective on Multitargeting Compounds. *J. Med. Chem.* **62**, 420–444 (2019).

266. Subramanian, A. *et al.* A Next Generation Connectivity Map: L1000 Platform and the

First 1,000,000 Profiles. *Cell* **171**, 1437-1452.e17 (2017).

267. Kampinga, H. H. & Craig, E. A. The HSP70 chaperone machinery: J proteins as drivers of functional specificity. *Nat. Rev. Mol. Cell Biol.* **11**, 579–592 (2010).

268. Goodwin, E. C. *et al.* BiP and multiple DNAJ molecular chaperones in the endoplasmic reticulum are required for efficient simian virus 40 infection. *MBio* **2**, e00101-11 (2011).

269. Bando, Y. *et al.* 150-kDa oxygen-regulated protein (ORP150) functions as a novel molecular chaperone in MDCK cells. *Am. J. Physiol. Cell Physiol.* **278**, C1172-82 (2000).

270. Gordon, D. E. *et al.* A SARS-CoV-2 protein interaction map reveals targets for drug repurposing. *Nature* **583**, 459–468 (2020).

271. Laufen, T. *et al.* Mechanism of regulation of hsp70 chaperones by DnaJ cochaperones. *Proc. Natl. Acad. Sci. U. S. A.* **96**, 5452–7 (1999).

272. Szabo, A. *et al.* The ATP hydrolysis-dependent reaction cycle of the Escherichia coli Hsp70 system DnaK, DnaJ, and GrpE. *Proc. Natl. Acad. Sci. U. S. A.* **91**, 10345–9 (1994).

273. Surtees, R. *et al.* Heat Shock Protein 70 Family Members Interact with Crimean-Congo Hemorrhagic Fever Virus and Hazara Virus Nucleocapsid Proteins and Perform a Functional Role in the Nairovirus Replication Cycle. *J. Virol.* **90**, 9305–9316 (2016).

274. Isabel, G.-D. *et al.* Elucidation of the Cellular Interactome of Ebola Virus Nucleoprotein and Identification of Therapeutic Targets. *J. Proteome Res.* **15**, 4290–4303 (2016).

275. Ye, J. *et al.* Heat shock protein 70 is associated with replicase complex of Japanese encephalitis virus and positively regulates viral genome replication. *PLoS One* **8**, e75188 (2013).

276. Zmurko, J. *et al.* The Viral Polymerase Inhibitor 7-Deaza-2'-C-Methyladenosine Is a Potent Inhibitor of In Vitro Zika Virus Replication and Delays Disease Progression in a Robust Mouse Infection Model. *PLoS Negl. Trop. Dis.* **10**, e0004695 (2016).

277. Cook, H., Doncheva, N., Szklarczyk, D., von Mering, C. & Jensen, L. Viruses.STRING: A Virus-Host Protein-Protein Interaction Database. *Viruses* **10**, 519 (2018).